Università degli Studi di Sassari

PhD course in Agricultural Sciences

Department of Agricultural Sciences

Agrometeorology and ecophysiology of agriculture and forest ecosystem

---

Water resource use and management scenarios in Mediterranean environments in relation to climate change, food security and multisector conflict mitigation (NEXUS)

Andrea BORGO

Supervisors: Dr. Marta Debolini and Prof. Serena Marras

Course Coordinator: Prof. Severino ZARA

XXXVIII Cycle

Academic Year 2022 - 2023

Declaration of Authorship

I hereby declare that this thesis is an original work and represents the culmination of my doctoral studies in Agricultural Sciences at the University of Sassari. This work has not been previously submitted, in whole or in part, for any other degree or qualification. All sources consulted, including published and unpublished materials, have been duly cited and acknowledged.

Andrea Borgo, 01/04/2026

Abstract

Mediterranean countries are facing increasing water scarcity, as climate change and water-intensive human activities reduce the availability of water resources, with major implications for productive sectors and ecosystem sustainability. Although several frameworks have been developed to promote optimal water allocations and mitigate sectoral conflicts, their practical implementation remains fragmented. In addition, data scarcity further limits the application of advanced management tools. This thesis aims to develop and apply a set of modelling tools to support multiscale water resource management in the Mediterranean region. This includes both the spatial dimension (from farm to regional scale), and the temporal dimension (from real-time to multi-year forecast). These tools prioritize accessibility through simplified modeling structures and minimal data requirements, enabling direct accessibility to farmers and water managers.

The thesis is structured into four studies. The first examines future irrigation water demand under different climate change scenarios, including an analysis on the effects of rising atmospheric CO_2 concentrations on crop evapotranspiration. The study shows that the effect of CO_2 will moderate the growth of irrigation demand, maintaining it below 8% rather than 12-18% without CO2 effect. The second study introduces ACQUAOUNT-Farm, an IoT platform for real-time irrigation management. The platform is designed to farmers, suggesting optimal irrigation recommendations to minimize water withdrawals. ACQUAOUNT-Farm was tested on four farms in Tunisia, revealing potential water savings of 60-80% for citrus and potato crops. The third study explores the potential of satellite imagery for crop classification through the IOTA^2 automatic processing chain, providing up-to-date information on cropping patterns at the regional scale. Ultimately, the fourth study develops and applies ACQUAOUNT-DST, an integrated decision support tool for basin-scale water management, evaluating trade-offs between farm scale water optimization and regional management strategies, under changing climatic and socio-economic conditions. The DST combines hydrological modelling with a set of socio-economic and environmental indicators, translating water stress risk into decision-relevant metrics for governance strategies.

By integrating analyses across different operational scales, this thesis aims to strengthen the connections among the different operational scales of water management, supporting the development of a more coordinated framework and contributing to the identification of shared metrics. Moreover, by providing tools that are easily accessible and require limited data, this work offers practical support for the implementation of strategies in real-world contexts, contributing to more effective governance and decision making.

Acknowledgements

My acknowledgments first go to Marta, Antonio and Serena, my principal supervisors of this thesis. From my first arrival in Sardinia, they welcomed and assisted me, allowing me to grow not only professionally, but also as a person, creating a constructive and motivating work environment and giving me the confidence of having trusted reference point. Over these years, they have entrusted me with various responsibilities that have contributed significantly to my growth. They have fulfilled my greatest dream, that of being able to travel, by giving me the opportunity to participate in numerous conferences, seminars, and project meetings throughout Europe and North Africa.

A great thank you goes to Vincent and his welcome at CESBIO in France. I thank him for everything he taught me in the field of remote sensing and for the two wonderful periods spent in Toulouse, despite the unforeseen difficulties related to authorizations from the Ministry of Defense.

A big thank you to Kamel Fathia for their hospitality at the IRA Institute. They showed me what true hospitality really means, making me feel at home in another continent and continuously supporting me in the development of the ACQUAOUNT-Farm model. I am also grateful for the opportunity to get to know this beautiful country called Tunisia.

My gratitude also goes to all the CMCC researchers with whom I had the opportunity to collaborate, particularly Annamaria, Lisa, and Elisa, for the numerous meetings and video calls while developing the Decision Support Tool during the ACQUAOUNT project. It was a wonderful opportunity for growth and collaboration.

My gratitude goes to prof. Andrzej Walega as well, for my last Erasmus experience of the PhD at URK University. We did not know each other before, no shared projects, no formal supervision or any other collaborations before. However, he didn’t hesitate to welcome me in his department, actually in his office. He offered me all his time and expertise in hydrology to support me in the adaptation of the ACQUAOUNT-DST in Polish environments. “My office is your office” he constantly said. He was one of the strongest life coaches that I’ve ever met, making me believe in my potential as a water researcher and encouraging me to pursue in this field of research.

A thank you to my family, who supported me throughout my journey, believing together with me in the dream of this doctorate. And finally, a big thank you to Ewa, my fiancée. She believed in this doctorate even more than I did; she knew that I could do it. She constantly supported me in every moment; from the most

stressful ones to the successes, she was there, next to me. She followed me on many of my PhD travels, and she gave me the self-esteem necessary to express my full potential.

Conference presentations, submissions and publications

Publications and submissions

Chapter 2 submission

Borgo, A., Aslam, M.F., Spano, D. et al. Evaluating the effects of climate change and CO_2 fertilization on the irrigation demand assessment in South-West France. Irrig. Sci. (submitted: 11/2025)

Chapter 3 submission

Borgo, A., Elmokh, F., Nagaz, K. et al. ACQUAOUNT-Farm: an IoT-based real-time platform for optimizing daily irrigation under water-scarcity. Comput. Electron. Agric. (submitted: 05/2026)

Other submissions and publications within the PhD

Aslam, M.F., Masia, S., Spano, D. et al. (2025). Modelling crop water demand under climate change: the case of Sardinia region. Irrig Sci. https://doi.org/10.1007/s00271-025-01027-8

Aslam, M. F., Borgo, A., Masia, S., et al.(2026). Modelling the influence of atmospheric CO_2 on irrigation demand in vineyards of the Sardinia region. BIO Web of Conferences, 235, 03003. https://doi.org/10.1051/bioconf/202623503003

Villani, L., Piemontese, L., Castelli, G., Borgo, A. (2026). Neglecting plant physiology: Systematic overestimation of drought projections. Environmental Research: Climate, 5(2), 022001. https://doi.org/10.1088/2752-5295/ae583c

Conference presentations

Borgo, A., Debolini, M., Rianna, G. & Mereu, S. (2025). Advancing digital solutions for sustainable irrigation water management in Mediterranean agriculture. Oral presentation at the XIX World Water Congress – Water in a Changing World: Innovation and Adaptation, International Water Resources Association (IWRA), Marrakesh, Morocco, December 1–5, 2025.

Delpiazzo, E., Mazzoni, A., Napolitano, L., Borgo, A., Rianna, G., Trabucco, A., Debolini, M., Mereu, S. (2025). Futures for Water Resource Management in Sardinia. Oral presentation at the Mediterranean Geosciences Union (MedGU), Athens, Greece, November 10–12, 2025.

Borgo, A., Debolini, M., Rianna, G. & Mereu, S. (2025). Toward digital twin for sustainable irrigation water management in Mediterranean agriculture. Oral presentation at the XIII World Congress of the European Water Resources Association (EWRA) – New challenges in understanding and managing water-related risks in a changing environment, Palermo, Italy, June 24–28, 2025.

Borgo, A., Debolini, M., Rianna, G. & Mereu, S. (2025). Integrated digital solutions for sustainable farm-scale water allocation in Mediterranean environments. Oral presentation at the EGU General Assembly 2025, European Geosciences Union, Vienna, Austria, April 27 – May 2, 2025. Abstract EGU25-9410. https://doi.org/10.5194/egusphere-egu25-9410

Borgo, A., Trabucco, A., Aslam, M.F., Masia, S., Spano, D., Debolini, M. (2024). Assessment of crop water needs and its sustainability based on future climate scenarios: the Aude Department (South-West France). Oral presentation at the EGU General Assembly 2024, European Geosciences Union, Vienna, Austria, April 14–19, 2024. Abstract EGU24-20336. https://doi.org/10.5194/egusphere-egu24-20336

Borgo, A., Masia, S., Spano, D., Mereu, V., Debolini, M., Snyder, R.L. & Trabucco, A. (2023). Assessment of crop water demand and its sustainability based on future projections. The case of the Aude Department (France). Oral presentation at the 9th International Conference on Meteorology and Climatology of the Mediterranean (MetMed 2023), University of Genoa / AISAM / ACAM, Genoa, Italy, May 22–24, 2023.

Borgo, A., Masia, S., Spano, D., Mereu, V., Debolini, M., Snyder, R.L. & Trabucco, A. (2022). Assessment of crop water use and its sustainability based on future projections, Aude Department (South-West France). Poster presentation at the 10th Annual Conference of the Italian Society for Climate Sciences (SISC2022): Governing the Future, SISC – Italian Society for Climate Sciences, Rome, Italy, October 19–21, 2022.

Table of Contents

Chapter 1. General introduction

The challenges of water resources in the Mediterranean

The Mediterranean basin is one of the regions where climate change and water scarcity are expected to represent one of the most critical challenges of the twenty-first century. Climate change is affecting this region particularly intensely, to the extent that the Mediterranean is widely recognized as a climate change hotspot (Ferragina & Canitano, 2014; Turco et al., 2015). Average temperatures are rising rapidly, while effective precipitation, that is, the portion of rainfall that can be stored and used as a manageable water resource, is declining (IPCC, 2023; MedECC, 2020). Rainfall patterns are becoming increasingly irregular, with fewer but more extreme events, resulting in alternating episodes of severe droughts and intense floods (MedECC, 2020). These dynamics directly reduce the availability and reliability of water resources across sectors. As water becomes scarce and more variable, competition among users intensifies, particularly between agriculture, urban demand, and ecosystems (Adamovic et al., 2019). This growing pressure has already led, and is likely to further lead, to the overexploitation of water resources, causing environmental degradation or scarcity in many areas (Lionello et al., 2014; Santos Pereira et al., 2009).

Agriculture is the sector most dependent on water availability. According to the United Nations, it accounts for approximately 70% of global freshwater withdrawals for human activities (FAO, 2017). In water-stressed regions such as the Mediterranean, this high demand makes agricultural systems particularly vulnerable and central to the sustainability challenge.

To monitor and assess water use sustainability, several indicators have been developed over the past decades. One widely adopted metric is the Water Exploitation Index (WEI) (Braca et al., 2023; Casadei et al., 2020), which measures the ratio between total water withdrawals and available renewable water resources in a given region. The WEI has been used extensively to evaluate water stress levels across Mediterranean countries, revealing that many of them exceed the commonly accepted water stress threshold of 0.4. In some Mediterranean countries, values even surpass 0.8 or 0.9, indicating extremely high levels of water stress. Under such conditions, persistent overexploitation increases the fragility of the entire socio-ecological system (Adamovic et al., 2019; Carmona-Moreno et al., 2021). Human activities become less resilient to recurring drought events, while ecosystems suffer from reduced environmental flows and declining ecological integrity. In this context, ensuring sustainable and integrated water management is not only an environmental necessity but also a prerequisite for long-term regional stability.

Existing approaches for solving interlinkages of water use among sectors

Over the past decades, several efforts have been undertaken to promote a more integrated and sustainable management of water resources. Among the most prominent initiatives, in the '90s the United Nations has advanced the concept of Integrated Water Resources Management (IWRM), a framework aimed at coordinating water use across sectors while ensuring environmental sustainability and equitable allocation (Grigg, 2008; GWP, 2000). IWRM emphasizes the need to move beyond sectoral approaches and to explicitly recognize the water requirements of ecosystems alongside agricultural, urban, and industrial demands. Afterward, the Water–Energy–Food-Ecosystem (WEFE) Nexus framework has gained increasing attention within the scientific and policy communities, especially after the Bonn Conference of 2011 (Al-Saidi & Elagib, 2017; Eriksson et al., 2025; Purwanto et al., 2021). While IWRM remains more water-centric, the WEFE Nexus highlights the interdependences between water, food production, energy systems, and ecosystems. In this regard, the Nexus approach seeks to identify trade-offs and synergies across sectors, promoting more coherent and balanced resource governance (Bazilian et al., 2011; Endo et al., 2017; Hoff, 2011). As a result, research on integrated water management and nexus-based approaches has expanded significantly in recent years.

Limitations and research gaps

Although IWRM and WEFE Nexus has become a widely promoted framework for sustainable water governance, their concepts remain more theorical than practical, and ambiguous, with no universally accepted definition (Allouche et al., 2015; Biswas, 2004; Mooren et al., 2025). In relation to the IWRM, Biswas (2004) reported that "*while at a first glance, the concept of IWRM looks attractive, a deeper analysis brings out many problems, both in concept and implementation, especially for meso- to macro-scale projects*" and "*in the real world, the concept will be exceedingly difficult to be made operational*". Even if this statement was formulated more than 20 years ago, several others reported similar comments across these years, highlighting the lack of emphasis on practical implementations and coordination problems among institutions (Gallegos et al., 2026; Grigg, 2024). Also the WEFE Nexus have been highly criticized due to its largely theoretical nature and the scarcity of empirical applications, despite its growing body of literature (Li et al., 2025; Purwanto et al., 2021).

Indeed, the practical implementation of these principles is limited and mostly fragmented. In many regions, water management continues to be predominantly sectoral, lacking a holistic perspective on cross-sectoral interconnections and cumulative impacts (Liu et al., 2017; Rasul & Sharma, 2016; Seidou et al., 2020).

Where integration efforts do exist, they are often limited to specific case studies or pilot regions and are not systematically embedded in governance structures (Lucca et al., 2023). Moreover, water management practices are frequently reactive rather than preventive (Kampragou et al., 2011; Wilhite & Pulwarty, 2017). Interventions are commonly triggered by extreme events such as severe droughts or floods, while proactive strategies aimed at anticipating and mitigating water scarcity risks remain underdeveloped (Urquijo-Reguera et al., 2022). This reactive orientation reduces the system's capacity to adapt to long-term climatic trends and increasing variability.

A further challenge lies in the lacking dialogue between the water managers operating at different scales, in particular the spatial and temporal levels (Hamidov & Helming, 2020; McGrane et al., 2019; Mersha, 2021). For instance, innovations at the farm level, such as improvements in irrigation efficiency, are often not coordinated with basin-level allocation policies (e.g., water pricing). At the same time, short-term operational decisions, such as daily or seasonal water allocation and irrigation scheduling, are rarely aligned with long-term projections that assess how water availability may evolve over decades under different climate change scenarios. Without bridging these spatial and temporal scales, these misalignments weaken the effectiveness of individual water management and governance interventions (Abulibdeh & Zaidan, 2020).

In the world of research, the scientific community has developed a wide range of models and analytical approaches to tackle these challenges. These include statistical or process-based models that simulate the interlinkages of the WEFE Nexus and climate change (Gao et al., 2024; Yates et al., 2005), hydrologic and crop growth models (Hammouch et al., 2024; Siad et al., 2019), and remote sensing–based classification algorithms capable of mapping land use and crop distribution (Hammouch et al., 2024; Tarate et al., 2024). Collectively, these tools have significantly enhanced our ability to predict the impacts of climate change on agricultural and water systems and to monitor how landscapes evolve and adapt over time.

Despite their effectiveness, many of these approaches remain isolated and their implications limited (Siad et al., 2019). Process-based models often focus either on long-term dynamics under changing climatic conditions, or on short-term irrigation management purposes. At the same time, regional scale instruments aim to regulate water allocation across multiple stakeholders within a basin, yet without a solid understanding of the physical processes governing sectoral water demand. Yet these different modeling efforts are rarely integrated into a coherent framework. Also at the scientific level, there is a lack of methodological continuity between scales (Hamidov & Helming, 2020; Wang et al., 2026). Long-term assessments of crop water demand are seldom directly connected to short-term irrigation scheduling tools in a harmonic framework. Likewise, local efficiency improvements are not always embedded within basin-scale allocation strategies.

Data scarcity

In many Mediterranean environments, particularly in countries outside the European Union, datasets containing sufficient and reliable information for different water-related applications remain scarce or fragmented (Zubel & Apprioual, 2020). In such contexts, accessing the necessary data often requires on-site data collection or informal consultations with local stakeholders. This represents a significant limitation for the implementation of integrated, multi-approach pipelines for sustainable water management. Depending on their complexity, many existing models require large amounts of input data for proper implementation (Koch et al., 2025). When the required datasets are unavailable, these models may either be impossible to apply or may require large preliminary costs associated with data acquisition, which are often unsustainable for many research and operational applications (Kayatz et al., 2024). For this reason, there is an increasing need for tools that rely on minimal and easily accessible input data, thereby facilitating their application across Mediterranean regions, including non-expert users. Considering the urgent challenges posed by water scarcity, the widespread adoption of simplified models and frameworks aimed at optimizing water use may ultimately prove more impactful than the application of highly precise yet complex modelling approaches. Indeed, simple tools are generally more accessible and more likely to be adopted for real-world applications.

Objectives of the thesis

Taking all these factors into account, there is an urgent need to identify the strategies to translate IWRM and WEFE Nexus into operational frameworks for real-world applications. Keeping this purpose in mind, the objective of this thesis consists in the development and application of modelling approaches to support multiscale water resource management in the Mediterranean region, to optimize allocations among sectors. Multiscale refers to both spatial and temporal dimensions, linking field-level processes to regional dynamics and bridging short-term (weekly) operational predictions with long-term (decadal) climate-driven projections. Some of the applications used in this research build upon approaches previously developed in literature, while others have been developed and validated specifically within this thesis. These tools are conceived to be simple, with few input variables and clear outputs, to make them accessible to a wider range of non-expert users across the Mediterranean.

As agriculture is the main water consumer in most Mediterranean contexts, while urban use, hydropower production, and industrial processes account for a relatively limited share of water consumption, the IWRM and WEFE Nexus frameworks must place the agricultural sector at the core of their interventions. For this reason, this thesis does not explicitly address all the aspects of the Nexus; instead, it focuses on those effective solutions that can maximize savings and trade-offs in agriculture, to reduce the overall intensity of water exploitation within a basin or region.

The thesis is structured into four main chapters, each operating at a distinct combination of spatial and temporal scales; Figure 1 shows this combination for each model, together with their potential range of applicability.

More specifically, Chapter 2 investigates future irrigation water demand for multiple crops in the Aude basin in southwestern France, assessing how irrigation requirements may evolve under different climate change scenarios. Attention is given to the potential effects of rising atmospheric CO_2 concentrations on crop evapotranspiration and, consequently, on irrigation demand. This chapter sets the base to understanding which strategies should then be considered to cope with these combined effects. The analysis is conducted on the regional scale and explores long-term trajectories up to the end of the century. The study adopts SIMETAW (Simulation of Evapotranspiration of Applied Water), a daily crop–soil–water balance model used to estimate ET0, ETc, ETa, and net applied water (NAc) at the point scale (Mancosu et al., 2016). Among the four tools, SIMETAW is the most versatile across different scales.

Chapter 3 introduces ACQUAOUNT-Farm, a real-time IoT digital platform designed to support farmers by recommending optimal irrigation scheduling. By relying on a physically based representation of crop water requirements, the tool supports irrigation decisions grounded in quantitative estimates rather than subjective judgment. The tool was developed within the ACQUAOUNT project and made operational across farms in four Mediterranean pilots (Sardinia, Jordan, Lebanon, Tunisia). In this thesis, ACQUAOUNT-Farm was tested across four farms in Medenine (South Tunisia). Differently than SIMETAW, ACQUAOUNT-Farm is specifically designed to work in real-time and at the local scale, as it depends on the information from sensors installed in the field.

To enable a more accurate assessment of irrigation demand at the regional scale, Chapter 4 explores the potential of satellite imagery for crop classification by applying the IOTA² processing chain in Sardinia. This approach maps agricultural areas and crop distributions using remote sensing data, providing timely information on cropping patterns. The method addresses common limitations associated with agricultural land-use data availability, particularly the lack of up-to-date information, and offers a fast, transferable and data-efficient framework that relies primarily on remotely sensed observations rather than ground-based surveys. IOTA^2 is highly flexible and can be applied at virtually any spatial scale, since it primarily relies on the availability and distribution of reference data for model training, whereas satellite time series are available worldwide.

Finally, Chapter 5 develops and applies ACQUAOUNT-DST, a decision-support tool for basin-scale water management. The tool evaluates alternative climate and water management scenarios by quantifying trade-offs between agricultural productivity and strategies for water use efficiency. The tool presents a modular architecture, connecting the hydrological, climate and sectoral demand components with a set of socioeconomic and environmental indicators, to translate water stress risk into decision-relevant metrics. Due to its design, ACQUAOUNT-DST is specifically targeting the basin scale, still, the range of the forecast can span from the short (1-10 years) to the long term (40+ years).

Taken together, the tools developed in this thesis provide an integrated framework that bridges scales and sectors typically addressed in isolation. This integration is grounded in the simplicity and accessibility of the tools, designed for end-users without specialized expertise, enabling their practical application across Mediterranean water systems. By studying these interconnected scales simultaneously, the framework reveals the real trade-offs that emerge in water management, allowing decision-makers to identify solutions that benefit multiple sectors and stakeholders rather than optimizing for single domains.

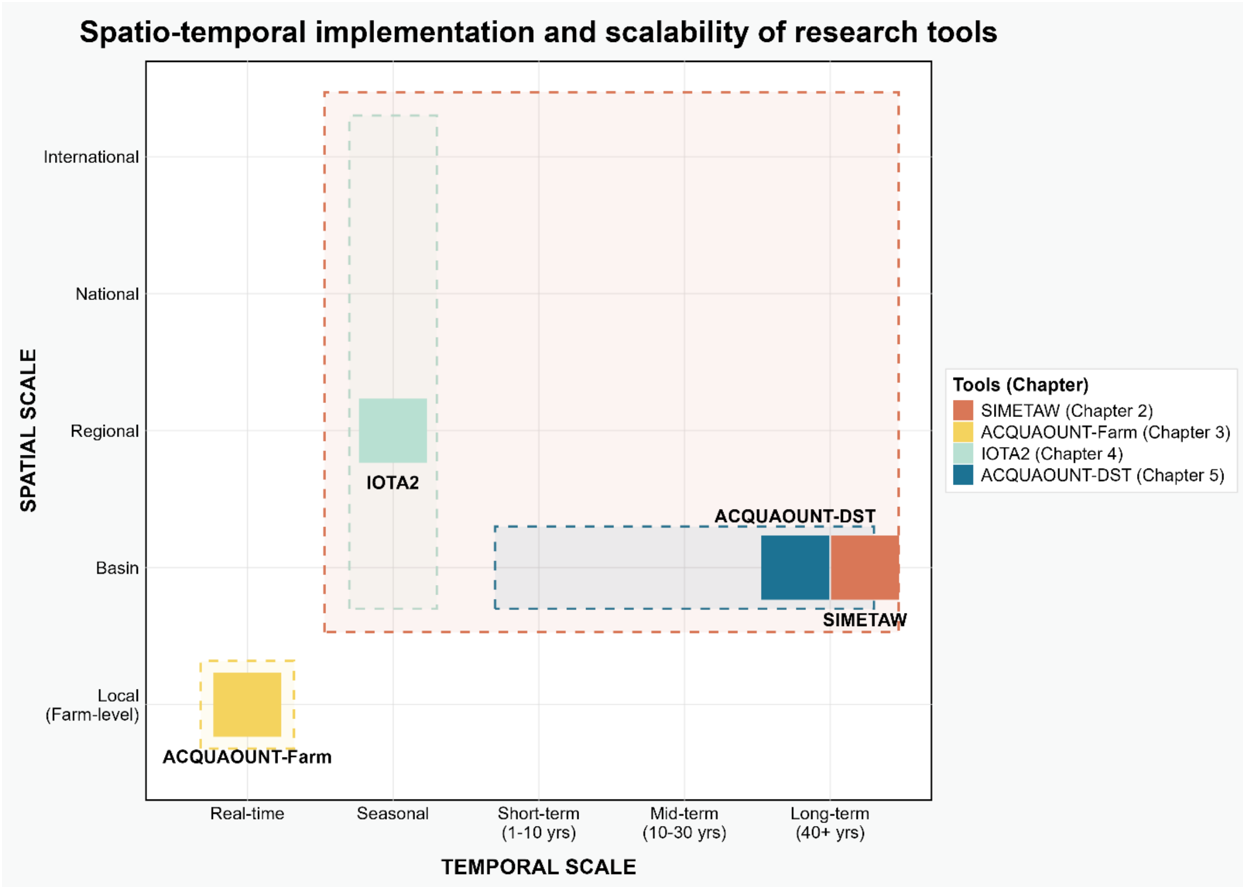

Figure 1: spatio-temporal implementation and scalability of the research tools developed during the PhD project. The solid rectangles represent the current implementation within the PhD project, while dashed lines represent the scalability range of these tools across the spatial and temporal scales

References

Abulibdeh, A., & Zaidan, E. (2020). Managing the water-energy-food nexus on an integrated geographical scale. *Environmental Development*, *33*, 100498. https://doi.org/10.1016/j.envdev.2020.100498

Adamovic, M., Al-Zubari, W., Amani, A., Ameztoy Aramendi, I., Bacigalupi, C., Barchiesi, S., Bisselink, B., Bodis, K., Bouraoui, F., Caucci, S., Dalton, J., De Roo, A., Dudu, H., Dupont, C., El Kharraz, J., Embid, A., Farajalla, N., & Fernandez Blanco Carra, G. (2019). *Position Paper on Water, Energy, Food and Ecosystems (WEFE) Nexus and Sustainable Development Goals (SDGS)*. https://doi.org/10.2760/5295

Allouche, J., Middleton, C., & Gyawali, D. (2015). *Technical Veil, Hidden Politics: Interrogating the Power Linkages behind the Nexus*. *8*(1), 610–626.

Al-Saidi, M., & Elagib, N. A. (2017). Towards understanding the integrative approach of the water, energy and food nexus. *Science of The Total Environment*, *574*, 1131–1139. https://doi.org/10.1016/j.scitotenv.2016.09.046

Bazilian, M., Rogner, H., Howells, M., Hermann, S., Arent, D., Gielen, D., Steduto, P., Mueller, A., Komor, P., Tol, R. S. J., & Yumkella, K. K. (2011). Considering the energy, water and food nexus: Towards an integrated modelling approach. *Energy Policy*, *39*(12), 7896–7906. https://doi.org/10.1016/j.enpol.2011.09.039

Biswas, A. K. (2004). Integrated Water Resources Management: A Reassessment: A Water Forum Contribution. *Water International*, *29*(2), 248–256. https://doi.org/10.1080/02508060408691775

Braca, G., Lastoria, B., Mariani, S., Piva, F., & Tropeano, R. (2023). *WEI+ WATER EXPLOITATION INDEX PLUS*. https://indicatoriambientali.isprambiente.it/it/risorse-idriche-e-bilancio/wei-water-exploitation-index-plus

Carmona-Moreno, C., Crestaz, E., Cimmarrusti, Y., Farinosi, F., Biedler, M., Amani, A., Mishra, A., & Carmona-Gutierrez, A. (2021). *Implementing the Water–Energy–Food–Ecosystems Nexus and Achieving the Sustainable Development Goals*. United Nations Educational, Scientific and Cultural Organization (UNESCO). ISBN 978-92-3100473-5

Casadei, S., Peppoloni, F., & Pierleoni, A. (2020). A new approach to calculate the water exploitation index (WEI+). *Water (Switzerland)*, *12*(11), 1–16. https://doi.org/10.3390/w12113227

Endo, A., Tsurita, I., Burnett, K., & Orencio, P. M. (2017). A review of the current state of research on the water, energy, and food nexus. *Journal of Hydrology: Regional Studies*, *11*, 20–30. https://doi.org/10.1016/j.ejrh.2015.11.010

Eriksson, N., Avellán, T., Teutschbein, C., & Blicharska, M. (2025). Towards a common understanding of water-energy-food nexus research: A view of the European nexus community and beyond. *Science of The Total Environment*, *967*, 178775. https://doi.org/10.1016/j.scitotenv.2025.178775

FAO. (2017). *Water for Sustainable Food and Agriculture*. www.fao.org/publications

Ferragina, E., & Canitano, G. (2014). Water and Food Security in the Arab Countries: National and Regional Implications. *Global Environment*, *7*(2), 326–351. https://doi.org/10.3197/ge.2014.070204

Gallegos, A., Grigg, N. S., & Llano, W. (2026). Enablers and Obstacles in Integrated Water Resources Management (IWRM) Implementation and Their Contributions to Sustainable Territorial Development. *Land*, *15*(2), 270. https://doi.org/10.3390/land15020270

Gao, D., Chen, A. S., & Memon, F. A. (2024). A Systematic Review of Methods for Investigating Climate Change Impacts on Water-Energy-Food Nexus. *Water Resources Management*, *38*(1), 1–43. https://doi.org/10.1007/s11269-023-03659-x

Grigg, N. S. (2008). Integrated water resources management: Balancing views and improving practice. *Water International*, *33*(3), 279–292. https://doi.org/10.1080/02508060802272820

Grigg, N. S. (2024). Framework and Function of Integrated Water Resources Management in Support of Sustainable Development. *Sustainability*, *16*(13), 5441. https://doi.org/10.3390/su16135441

GWP. (2000). *Integrated water resources management*. Global water partnership.

Hamidov, A., & Helming, K. (2020). Sustainability Considerations in Water–Energy–Food Nexus Research in Irrigated Agriculture. *Sustainability*, *12*(15), 6274. https://doi.org/10.3390/su12156274

Hammouch, H., El-Yacoubi, M. A., Qin, H., & Berbia, H. (2024). A Systematic Review and Meta-Analysis of Intelligent Irrigation Systems. *IEEE Access*, *12*, 128285–128304. https://doi.org/10.1109/ACCESS.2024.3421322

Hoff, H. (2011). *Understanding the Nexus. Background Paper for the Bonn2011 Conference: The Water, Energy and Food Security Nexus*. Stockholm Environment Institute.

IPCC. (2023). *IPCC, 2023: Summary for Policymakers. In: Climate Change 2023: Synthesis Report. Contribution of Working Groups I, II and III to the Sixth Assessment Report of the Intergovernmental Panel on Climate Change*. https://www.unep.org/resources/report/climate-change-2023-synthesis-report

Kampragou, E., Apostolaki, S., Manoli, E., Froebrich, J., & Assimacopoulos, D. (2011). Towards the harmonization of water-related policies for managing drought risks across the EU. *Environmental Science & Policy*, *14*(7), 815–824. https://doi.org/10.1016/j.envsci.2011.04.001

Kayatz, B., Baroni, G., Hillier, J., Lüdtke, S., Freese, D., & Wattenbach, M. (2024). Supporting decision-making in agricultural water management under data scarcity using global datasets – chances, limits and potential improvements. *Agricultural Water Management*, *296*, 108803. https://doi.org/10.1016/j.agwat.2024.108803

Koch, H., Yangouliba, G. I., & Liersch, S. (2025). From Data Scarcity to Solutions: Hydrological and Water Management Modeling in a Highly Managed River Basin. *Water*, *17*(6), 823. https://doi.org/10.3390/w17060823

Li, W., Ward, P. J., & Van Wesenbeeck, L. (2025). A critical review of quantifying water-energy-food nexus interactions. *Renewable and Sustainable Energy Reviews*, *211*, 115280. https://doi.org/10.1016/j.rser.2024.115280

Lionello, P., Abrantes, F., Gacic, M., Planton, S., Trigo, R., & Ulbrich, U. (2014). The climate of the Mediterranean region: Research progress and climate change impacts. *Regional Environmental Change*, *14*(5), 1679–1684. https://doi.org/10.1007/s10113-014-0666-0

Liu, J., Yang, H., Cudennec, C., Gain, A. K., Hoff, H., Lawford, R., Qi, J., Strasser, L. D., Yillia, P. T., & Zheng, C. (2017). Challenges in operationalizing the water–energy–food nexus. *Hydrological Sciences Journal*, *62*(11), 1714–1720. https://doi.org/10.1080/02626667.2017.1353695

Lucca, E., El Jeitany, J., Castelli, G., Pacetti, T., Bresci, E., Nardi, F., & Caporali, E. (2023). A review of water-energy-food-ecosystems Nexus research in the Mediterranean: Evolution, gaps and applications. *Environmental Research Letters*, *18*(8), 083001. https://doi.org/10.1088/1748-9326/ace375

McGrane, S. J., Acuto, M., Artioli, F., Chen, P., Comber, R., Cottee, J., Farr-Wharton, G., Green, N., Helfgott, A., Larcom, S., McCann, J. A., O'Reilly, P., Salmoral, G., Scott, M., Todman, L. C., Van Gevelt, T., & Yan, X. (2019). Scaling the nexus: Towards integrated frameworks for analysing water, energy and food. *The Geographical Journal*, *185*(4), 419–431. https://doi.org/10.1111/geoj.12256

MedECC. (2020). *Current situation and risks for the future First Mediterranean Assessment Report* (p. 632). https://zenodo.org/record/4768833

Mersha, A. N. (2021). *Integrated Water Resources Management: A Systems Perspective of Water Governance and Hydrological Conditions: Integrated Water Resources Management* (1ª ed.). CRC Press. https://doi.org/10.1201/9781003231035

Mooren, C. E., Munaretto, S., La Jeunesse, I., Sievers, E., Hegger, D. L. T., Driessen, P. P. J., Hüesker, F., Cirelli, C., Canovas, I., Mounir, K., & Madrigal, J. G. (2025). Water–energy–food–ecosystem nexus: How to frame and how to govern. *Sustainability Science*, *20*(6), 2313–2334. https://doi.org/10.1007/s11625-025-01691-x

Purwanto, A., Sušnik, J., Suryadi, F. X., & De Fraiture, C. (2021). Water-Energy-Food Nexus: Critical Review, Practical Applications, and Prospects for Future Research. *Sustainability*, *13*(4), 1919. https://doi.org/10.3390/su13041919

Rasul, G., & Sharma, B. (2016). The nexus approach to water–energy–food security: An option for adaptation to climate change. *Climate Policy*, *16*(6), 682–702. https://doi.org/10.1080/14693062.2015.1029865

Santos Pereira, L., Cordery, I., & Iacovides, I. (2009). Coping with Water Scarcity. Addressing the Challenges. In L. Santos Pereira, I. Cordery, & I. Iacovides, *Coping with Water Scarcity* (pp. 1–6). Springer Netherlands. https://doi.org/10.1007/978-1-4020-9579-5_1

Seidou, O., Maiga, F., Ringler, C., Kalcic, S., & Ferrini, L. (2020). Challenges and Opportunities in the Operationalization of the Water-Environment-Energy-Food (WE^2 F) Nexus: Case Study of the Upper Niger Basin and Inner Niger Delta, West Africa. *E3S Web of Conferences*, *183*, 02001. https://doi.org/10.1051/e3sconf/202018302001

Siad, S. M., Iacobellis, V., Zdruli, P., Gioia, A., Stavi, I., & Hoogenboom, G. (2019). A review of coupled hydrologic and crop growth models. *Agricultural Water Management*, *224*, 105746. https://doi.org/10.1016/j.agwat.2019.105746

Tarate, S. B., Patel, N. R., Danodia, A., Pokhariyal, S., & Parida, B. R. (2024). Geospatial Technology for Sustainable Agricultural Water Management in India—A Systematic Review. *Geomatics*, *4*(2), 91–123. https://doi.org/10.3390/geomatics4020006

Turco, M., Palazzi, E., Von Hardenberg, J., & Provenzale, A. (2015). Observed climate change hotspots. *Geophysical Research Letters*, *42*(9), 3521–3528. https://doi.org/10.1002/2015GL063891

Urquijo-Reguera, J., Gómez-Villarino, M. T., Pereira, D., & De Stefano, L. (2022). An Assessment Framework to Analyze Drought Management Plans: The Case of Spain. *Agronomy*, *12*(4), 970. https://doi.org/10.3390/agronomy12040970

Wang, K., Onodera, S., Saito, M., & Nang, Y. W. (2026). Advancing Physical Realism in Hydrological Modelling: Selection and Integration — A Review and Synthesis. *Water Resources Management*, *40*(5), 181. https://doi.org/10.1007/s11269-026-04534-1

Wilhite, D. A., & Pulwarty, R. S. (2017). *Drought and Water Crises: Integrating Science, Management, and Policy* (D. Wilhite & R. S. Pulwarty, A c. Di; 2ª ed.). CRC Press. https://doi.org/10.1201/b22009

Yates, D., Sieber, J., Purkey, D., & Huber-Lee, A. (2005). WEAP21—A Demand-, Priority-, and Preference-Driven Water Planning Model: Part 1: Model Characteristics. *Water International*, *30*(4), 487–500. https://doi.org/10.1080/02508060508691893

Zubel, K., & Apprioual, A. (2020). *Agriculture and Food Security in Climate Sensitive Areas in the Mediterranean*. IEMed. https://www.iemed.org/publication/agriculture-and-food-security-in-climate-sensitive-areas-in-the-mediterranean/

Chapter 2. Evaluating the effects of climate change and CO_2 fertilization on the irrigation demand assessment in South-West France

Authors: ANDREA BORGO[a,c], Muhammad Faizan Aslam[a,c], Donatella Spano[a,c], Sara Masia[b,c], Antonio Trabucco[a,c], Nina Graveline[d], Marta Debolini[c]

(a) Department of Agriculture, University of Sassari, Viale Italia, 39a, 07100 Sassari, Italy

(b) Land and Water Management Department, IHE Delft Institute for Water Education, Westvest 7, 2611 AX Delft, The Netherlands

(c) CMCC Foundation – Euro-Mediterranean Centre on Climate Change, Italy

(d) INRAE, UMR Innovation, Montpellier, France

Email corresponding author: andrea.borgo@cmcc.it

Abstract

An accurate assessment of irrigation demand, and their dynamics linked to climate change, is essential to foresee impacts of water abstractions and unsustainable overexploitation over ecosystems. Moreover, quantifying the effect of CO_2 fertilization in soil water balance models is necessary to get accurate projections of irrigation demand (Net Application, *NAc*) change under future climate conditions. This work investigates future changes of *NAc* in the Aude basin, in South-West France, to assess the amount of irrigation water required by the local crops (wine grape mainly) in the current conditions and according to future climate change scenarios and CO_2 fertilization approaches. This project relies on SIMETAW, a soil water balance model that computes the daily crop actual evapotranspiration (*ETa*) and *NAc*, given climate, soil, crop and irrigation management conditions. The study relies on high-resolution dynamically downscaled climate CMIP5 data, considering period 1976 – 2065 and RCPs 2.6, 4.5 and 8.5 for emission scenarios. Results show that including CO_2 fertilization within the modelling framework induces a modest increase of *NAc* among crops between the historical period and 2050 (3-6%, under RCP 8.5 and 4.5, respectively), with wine grapes reducing its demand (-2.5%, under RCP 8.5). Without CO_2 fertilization, *NAc* will significantly grow, exceeding 13% increase under RCP 8.5. These findings highlight the role of CO_2 fertilization in partially offsetting the effects of rising temperatures on vegetation water demand.

Without including CO_2 fertilization in the model, instead, the increase of *NAc* could place additional pressure on freshwater resources, emphasising the need for adaptive strategies in water use in agriculture.

Introduction

Climate change is one of the greatest challenges of 21st century. The anthropic greenhouse gas emissions in the atmosphere are increasing the instability of Earth's climate, which will likely worsen in the next decades. A changing climate not only leads to rising air temperatures but also alters the hydrological cycle, resulting in more intense precipitation events and an increased frequency of prolonged droughts in many regions of the world (IPCC, 2023b). Climate change is expected to have a non-uniform impact across the world, generating the so-called "climate change hotspots" (Turco et al., 2015b), i.e., areas characterised by stronger change of the mean, variability and extremes of seasonal temperature and precipitation. The Mediterranean has been identified as one of these hotspots (Ferragina & Canitano, 2014b), and it is an area where water resources are already scarce and unevenly distributed along its territory (MedECC, 2020b). Furthermore, the rising demand for water driven by population and economic growth in some areas of the Mediterranean will intensify its scarcity (Adamovic et al., 2019b).

Among all economic sectors, agriculture accounts for the highest freshwater consumption, approximately 70% of global water usage (FAO, 2017b), rising to around 80% in the Mediterranean region (Ferragina & Canitano, 2014b). On a national average, France does not experience chronic water scarcity, however, there are several regions which are already exposed to water-related scarcity (European Environment Agency, 2015; SDES, 2021). Given the intensification and expansion of irrigated agriculture to sustain food security (MedECC, 2020b), along with increasingly arid conditions projected for the Mediterranean due to climate change (Cramer et al., 2018a), crop water modelling tools are essential. They help to assess current and future irrigation demands under various emissions scenarios and evaluate the sustainability of irrigated agriculture under different crop management strategies (Masia et al., 2021a). A wide range of crop models is available to simulate irrigation demand (or Net Application, *NAc*) at both local and regional scales. Some are calibrated for individual crops (C. A. Jones & Kiniry, 1986), while others support multiple crops (J. W. Jones et al., 2003; McCown et al., 1995; Sharpley & Williams, 1990; Smith, 1992; van Diepen et al., 1989). Certain models can also be applied to various crop rotations regimes (Nendel, 2014). The need for models able to estimate the interactions between soil, water, crop, irrigation systems and climate at different temporal and spatial scales is increasing, considering the urgency following water scarcity. Moreover, there is still uncertainty related to the magnitude of the CO2 fertilization effect on crop evapotranspiration, enhancing the challenge in the assessment of future crop water use under climate change. Reference Evapotranspiration (*ET0*) is often estimated adopting the widely used Penman-Monteith (PM) equation (R. G. Allen et al., 1998a, 2006; Monteith, 1965), which has been formulated at a fixed level of CO_2 concentration (372 ppm). However, with climate change, atmospheric CO_2 is expected to rise up to 400-550 ppm by 2050, even exceeding 900 ppm by 2100 under RCP 8.5 (IPCC, 2013). Several studies reveal that increased atmospheric CO_2 enhances photosynthetic rates and reduces stomatal conductance due to partial stomata closure (L. H. Allen, 1990; Drake et al., 1997; Field et al., 1995). Therefore, an increase of canopy resistance can affect the estimation of *ET0*. This effect has been modelled in different studies (Kruijt et al., 2008; Stockle et al., 1992; Yang et al., 2019) and field experiments have been conducted, such as the Free-Air CO_2 Enrichment Experiments (Long et al., 2004), which monitored plant response to elevated CO_2 concentrations in the open air. However, few guidelines exist about the relation between CO_2 and *ET0* and its consequences on modelling results (Lemaitre-Basset et al., 2022) and not all the modelling exercises take it into account this effect on their estimation . In this context, the present study aims at investigating future variations of *NAc* of different crop systems, comparing the difference in the estimation with and without the effect of CO_2 fertilization in crop evapotranspiration. The analysis is applied to the case study of the Aude river basin, located in South-West France, which is a region strongly dedicated to wine grapes cultivation, and is also one of the driest and warmest regions of France (Chambres d'agriculture Occitanie, 2018; Direction Régionale de l'Alimentation, 2018). It has already faced strong climate variations which impacted local water resources (Lespinas et al., 2010). In the frame of the existing literature, the present study proposes a novel methodology for deriving operationally relevant estimates of Net Application (NAc) for the region's dominant crops. Methodologically, the work extends the standard Penman–Monteith approach by introducing an empirically based CO2-adjusted canopy resistance (Snyder et al., 2011) and propagates that adjustment through a full water-balance framework implemented at regional scale, in order to give information that can be used as starting point for possible future policies. The findings of this study demonstrate that incorporating CO_2 fertilization significantly impacts the magnitude and ranking of scenario impacts (e.g., an increase in irrigation demand under RCP4.5 relative to RCP8.5 in certain instances), underscoring the significance for water planners of accounting for CO_2 effects when projecting future agricultural water requirements. These contributions serve to bridge the existing gap between process-level CO2 response experiments and decision-support tools that are currently utilised for basin water management.

Materials and Methods

Case study description

The Aude basin (Figure 1) is located in South-West France, within the Occitanie region. The department spans over 139 km^2 and hosts a population of 370 thousand people (in 2017) (Chambres d'agriculture Occitanie, 2018). South-West Occitanie is one of the warmest and driest regions in France, with an average temperature of 23.7 °C in summer and a winter of 8.1 °C. Average yearly precipitation around 670 mm (Lezignan−Corbieres) (Météo-France, 2025). Nevertheless, climate change is increasing both the number and duration of dry periods, causing an early decline in soil water reserves (Cambrea et al., 2020). In addition, the growing crop water use due to expansion of irrigated areas is contributing to the overexploitation of both surface and groundwater resources, thus requiring additional efforts to improve irrigation efficiency and to identify strategies to support agricultural production (Fader et al., 2015; Masia et al., 2018).

Historically, agriculture in the Aude has focused on wine grapes, with 67800 hectares of vineyards spread over the Corbières and Minervois massifs, on the plains of Narbonne and Carcassonne. These vineyards represent 61% of the value of agricultural production in 2019 (Chambres d'agriculture Occitanie, 2018). In addition to vineyards, the region holds cultivation of cereals, forage crops, vegetables and fruits. Total agricultural land covers almost 110 thousand ha, of which 20 thousand ha are irrigated (18% of total cultivated land) and almost 90% of irrigated surface is devoted to wine grapes.

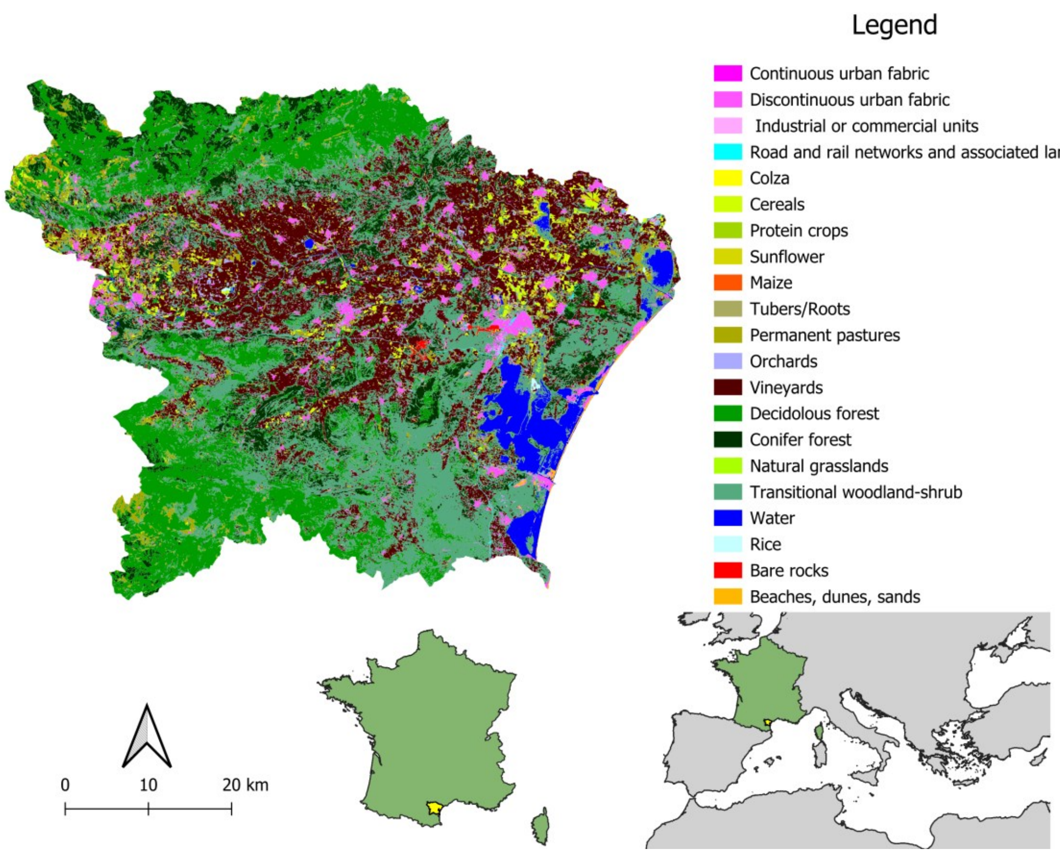

Figure 1: Land Use (LU) map of Aude basin, according to the Occupation de Sols (OSO) Nomenclature (Theia, 2018b)

The study analyses the period 1976-2065, under the emission scenarios RCP 2.6 (active mitigation), RCP 4.5 (moderate mitigation) and RCP 8.5 (no mitigation). The estimation of *ET0* is adjusted to incorporate the effects of CO_2 fertilization, following the indications of (Snyder et al., 2011), who identified a linear relationship between stomatal conductance and changes in CO_2 concentration, based on FACE experiments. The daily water budget is obtained from the use of the Simulation of Evapotranspiration of Applied Water model (Masia et al., 2021a), a model designed as a decision support tool for system management, which processes different geospatial climate and environmental data, allowing simulations at the regional level. The model is calibrated for multiple cropping systems and is capable of simulating *ET0*, crop-specific evapotranspiration (*ETc*), actual evapotranspiration (*ETa*) and *NAc*, under varying irrigation management conditions. The advantage of this model is the reduced number of input parameters required, which makes it ideal for iterating the processes over the basin. In this work, the outputs of SIMETAW_GIS are then coupled with the irrigated surfaces provided by the agricultural census of 2020 (Agreste, 2020), to have clear picture of the evolution of irrigation volumes for each crop, under the different CO_2 fertilization options

Modelling of crop water needs

The Simulation of Evapotranspiration of Applied Water (SIMETAW model), a daily crop-soil-water balance model, is used in this work to estimate *ET0*, *ETc*, *ETa* and *NAc* at the single-point level (Mancosu et al., 2016). The performance of SIMETAW have been validated for several relevant crops in Mediterranean environments (Aslam et al., 2025; Kimball et al., 2023; Masia et al., 2021a; Montazar et al., 2016; Orang et al., 2013). This study utilizes the version of SIMETAW integrated into a GIS spatial platform under R (SIMETAW_GIS), to apply the estimation of crop water consumption and irrigation demand from single-point to grid-level. *ET0* represents the evapotranspiration from a well-watered, 12 cm-tall reference grass surface, with known aerodynamic and canopy resistances. For this reference grass, *ET0* (mm/day) is influenced only by climatic parameters and is calculated using the standardized FAO Penman-Monteith (PM) equation (R. G. Allen et al., 1998a, 2006; Monteith, 1965):

$$ET0 = \frac{0.408\Delta\,(Rn - G) + \gamma \frac{900}{T + 273}\, u_2\,(es - ea)}{\Delta + \gamma\,(1 + 0.34\, u_2)} \tag{1}$$

Where Rn is the net radiation at the crop surface (MJ/m^2/day), G the soil heat flux density (MJ/m^2/day), γ the psychometric constant (kPa/°C), T is the mean daily air temperature at two meters height (°C), u_2 is the two-meter wind speed (m/s), es and ea are the saturation and actual vapor pressure (kPa) and Δ is the slope of the vapor pressure curve (kPa/°C), considering a fixed CO_2 concentration (372 ppm). In this work, CO_2 concentration is allowed to change over time, rising from 372 to 550 ppm, i.e. the projected CO_2 concentration in 2050 under RCP 8.5 (Büchner & Reyer, 2017), thus reducing plant stomatal conductance from 10 mm/s to 8 mm/s (Mancosu et al., 2016; Snyder et al., 2011). Assuming linear relationship up to 550 ppm, the canopy resistance (r_c, m/s) can be formulated as a function of CO_2 concentration (ppm), following the guidelines of (Snyder et al., 2011):

$$r_c = \frac{1000}{1.44\,(14.18 - 0.0112\ \mathrm{CO_2})} \tag{2}$$

r_c can be then introduced in equation (1), by substituting the component 0.34 u_2 with the relation:

$$\frac{r_c}{r_a} = \frac{70}{208/u_2} \approx 0.34\, u_2 \tag{3}$$

Where r_a (m/s) is the aerodynamic resistance to sensible and latent heat transfer.

One of the key features of SIMETAW is the possibility of adjustment of the crop coefficient k_c (-) in the mid-season ($k_{c,mid}$) according to the local climate as:

$$k_{c,mid} = k_{c,tab} + 0.261(\mathrm{ET0} - 7.3)(k_{c,tab} - 1) \tag{4}$$

Where $k_{c,tab}$ is the tabular k_c value expected with $ET0 \approx 7.3$ mm/day (Guerra et al., 2015).

NAc (mm) is the total required irrigation input that contributes to crop evapotranspiration over a season, calculated as

$$NA_c = ET_{c,cum} - C_{cum} - \mathrm{P}_{eff,cum} - \Delta\mathrm{SW} \tag{5}$$

Where $ET_{c,cum}$ (mm) is the cumulative crop evapotranspiration over the season, C_{cum} (mm) is the cumulative seepage, P_{eff} (mm) is the cumulative effective rainfall, and ΔSW (mm) is the difference between initial and final soil water storage in the root zone over the season. The model runs on a daily scale, computing the daily soil water depletion (SWD_i, mm) across the root zone. The root zone is estimated following the FAO guidelines (Allen et al., 1990), evolving according to the crop's phenological phases. The balance of SWD_i is expressed by the equation:

$$\mathrm{SWD}_i = \mathrm{SWD}_{i-1} + \mathrm{ET}_{c,i} + \mathrm{P}_{cp,i} + \mathrm{C}_i - \mathrm{DP}_i - \mathrm{R}_{off,i} + \mathrm{NA}_{c,i} \tag{6}$$

Where SWD_{i-1} is the soil water depletion of the previous day, $ET_{c,i}$ is the crop evapotranspiration of the current day, P_i (mm) is the current day precipitation, C_i (mm) is the capillary rise or seepage, DP_i (mm) is the percolation below the root layer, $R_{off,i}$ (mm) is the runoff of the current day and $NAc_{,i}$ is the depth of irrigation applied on the current day. By calculating the daily *SWD* the model identifies when it exceeds the manageable allowable depletion (*MAD*, mm), which is the amount of water that can be depleted before the plant experiences water stress. This threshold allows the model to optimize the irrigation scheduling throughout the season. SIMETAW can assess crop water requirements for different irrigation methods (gravity, sprinkler, micro-sprinkler and drip), each characterized by different application rates, distribution uniformity, and operational times.

Input data

Climate data

SIMETAW_GIS requires climate data to calculate *ET0*, which drives the daily soil water balance. Daily climate variables are acquired from several Euro-Cordex projections, using dynamic downscaling of Global Circulation Models (GCMs) with Regional Climate Models (RCMs), and stored in the Copernicus Climate Data Store (Copernicus Climate Change Service, 2022). The simulations have been realized between January and June 2023, and we decided to use CMIP5 as at that time these were the only simulations integrating bias correction The complete list of global and regional climate models used in this simulation is provided in Table 4 (in the Annex), while the units for each variable are found in Table 5 (Annex). The variables are collected at a spatial resolution of 0.11 degrees (approximately 11 km), covering both historical (1976-2005) and future (2006-2065) time periods, under RCP 2.6, 4.5 and 8.5 scenarios, which represent different greenhouse gas emission pathways.

Soil and crop data

For the computation of daily soil water budget SIMETAW_GIS model requires Soil Depth (*SD*) and the Available Water Capacity (*AWC*) as soil input data, along with elevation values to determine atmospheric pressure for the Penman-Monteith *ET0* calculation. The *SD* raster is sourced from the Food and Agriculture Organization (FAO, 2012), *AWC* from Hengl and Gupta (2019), and the elevation map from the United States Geological Survey (United States Geological Survey, 2022). Regarding crops, the selection is based on those with the greatest regional significance. Crop surface area estimates are collected from the local agricultural census of 2020, which reports both rainfed and irrigated areas by crop for each municipality in the basin. Therefore, the study focuses on the following crops, as reported in Table 1: vineyards (17692 ha, 89% of the Total Irrigated Area, TIA), forage crops (531 ha, 3% TIA), peach (representative crops for fruits, 542 ha, 3% TIA), tomato (representative crops for vegetables, 387 ha, 2% TIA), olives (298 ha, 2% of TIA), and durum wheat (80 ha, 0.4% TIA). Overall, these selected crops account for nearly 92% of the total irrigated utilized Agricultural Area (UAA) in the region. Values of k_c inflections through growing season (i.e., the k_c values of initial, mid-term and final stage of the season), as well as the rooting depths for all considered crops are derived from the values tabulated on paper FAO-56 (R. G. Allen et al., 1998a).

Irrigation management data

The adoption of SIMETAW_GIS is linked to its ability to assess crop water requirements based on various irrigation methods (gravity, sprinkler, micro-sprinkler and drip) each characterized by distinct application rates, distribution uniformity and operational times. Crop water needs are simulated under both rainfed and irrigated conditions, with specific irrigation methods assigned to crops. In particular, following the indications received by local farmers and farm associations, we considered drip irrigation for olives, peach, tomato and wine grapes, while sprinkler irrigation is used for improved pasture and wheat.

By default, the irrigated scenario involves replenishing soil water content to field capacity, preventing water stress and ensuring maximum yield. However, for wine grapes, a deficit irrigation strategy is applied to prioritize grain quality of in addition to yield. Based on input from local farmers participating in the project, irrigation for wine grapes is maintained at 70% of total daily requirements from bud break to flowering, and at 20% from flowering to harvest. A realistic estimate of irrigation demand in the basin therefore requires evaluating deficit irrigation specifically for wine grapes, which account for approximately 90% of the irrigated area of the basin.

The planting (or budburst) and harvesting dates of each crop are acquired from TEMPO (Maury et al., 2023), a French network of observatories focused on the phenology of the entire living kingdom. This platform provides dates for the key phenological phases of selected crop species or subspecies, specific to locations throughout France and across different years. For this study, data from the South-East part of the Occitanie region are selected and then averaged to obtain a single value (Table 1).

Table 1: list of crops used in the simulation, with their total and irrigated surfaces, main phenological events (planting/budbreak date, harvesting date) and irrigation methods. Peach and Tomato are the representative crops of Fruits and Vegetables, respectively

Crop	Total surface (ha)	Irrigated surface (ha)	Planting date/Bud break (dd/mm)	Harvesting date (dd/mm)	Irrigation method
Improved Pasture	29936	531	01/01	31/12	Sprinkler
Olives	868	298	20/02	01/10	Drip
Peach (rep. *Fruits*)	693	542	23/03	08/08	Drip
Tomato (rep. *Vegetables*)	460	387	02/06	07/09	Drip
Wheat	3307	80	24/11	31/05	Sprinkler
Wine Grape	65070	17692	22/03	05/09	Drip

Resampling results

Climate data projections have a spatial resolution of 0.11 degrees (approximately 11 km at the equator), while the soil map has a resolution of 250 m. Rather than resampling and running SIMETAW_GIS model simulation at the finer resolution of AWC raster, which would be computationally inefficient, the models is run at the resolution of the climate data projections, combined with 5 fixed levels of AWC, specifically 108, 230, 260, 284, 400 mm, representing the range of AWC values in the basin. In a second step, each cell of the AWC raster is assigned the value from the SIMETAW_GIS output that corresponds to the closest AWC level (e.g., if the AWC in position i, j corresponds to 225 mm, then the assigned ETai,j corresponds to the ETa value from the SIMETAW_GIS run at 230 mm of available water capacity).

Statistical tests and trend significance

In this study, statistically significant differences among results are evaluated using Student's t-test, implemented with the R package *t.test*, with a confidence l interval of 0.95. Statistically significant trends are assessed using the *no_trend* R function, which applies a Sieve Bootstrap Based Test for the null hypothesis of no trend, versus the alternative hypothesis of a linear trend (Student's t-test), with a 0.95 confidence interval.

Results

Reference Evapotranspiration

Figure 2 shows the pattern of *ET0* in the Aude basin during the period 1976-2065, based on RCP2.6, RCP4.5 and RCP8.5 for future projections (2006 onward), using both the standard PM equation with constant CO_2 (*CO_2const*) and the PM equation adjusted to incorporate the fertilization effect of increasing atmospheric CO_2 (*CO_2fert)*. Historical data (1976-2005) are paired with future projections (2006-2065). The figure reports the annual ensemble mean along with the annual maximum and minimum values from the five GCM-RCM climate models (Table 4), to account for variability across projections. Figure2.d shows the *ET0* trend obtained under *CO_2fert* approach, where the three future scenarios exhibit very similar patterns throughout the entire simulation period. Comparing historical and future values through their 30-year time averages (also called Climate Normals, CL), *ET0* is 1155 mm/y for the historical period (CL around 1990), while it becomes 1181, 1179 and 1176 mm/y under RCP2.6, RCP4.5 and RCP8.5, respectively for future CL around 2020; and 1186, 1188 and 1165 mm/y in 2050. These results show that between historical conditions and those projected for 2050, *ET0* exhibits a rather flat trend, with an increase of about 2.5-3% for RCP 2.6 and RCP 4.5 and less than <1% for RCP 8.5. A completely different pattern is observed under *CO_2const* approach (Figure 2.*e*), where *ET0* increases proportionally with rising mean temperature in the basin (Figure2.*a*). Similar to mean temperature, a consistent trend is expected under the three RCPs up to 2040 approximately, after which results diverge, coherently with diverging CO_2 projections (Figure2.*c*). Under this approach, *ET0* in 2050 is expected to increase by about 2% for RCP2.6 and 6% for RCP4.5, relative to the historical period, with the trend for RCP2.6 stabilizing by mid-century. *ET0* under RCP 8.5, however, is expected to increase by more than 12% by 2050, with a continuous rising trend throughout the entire period.

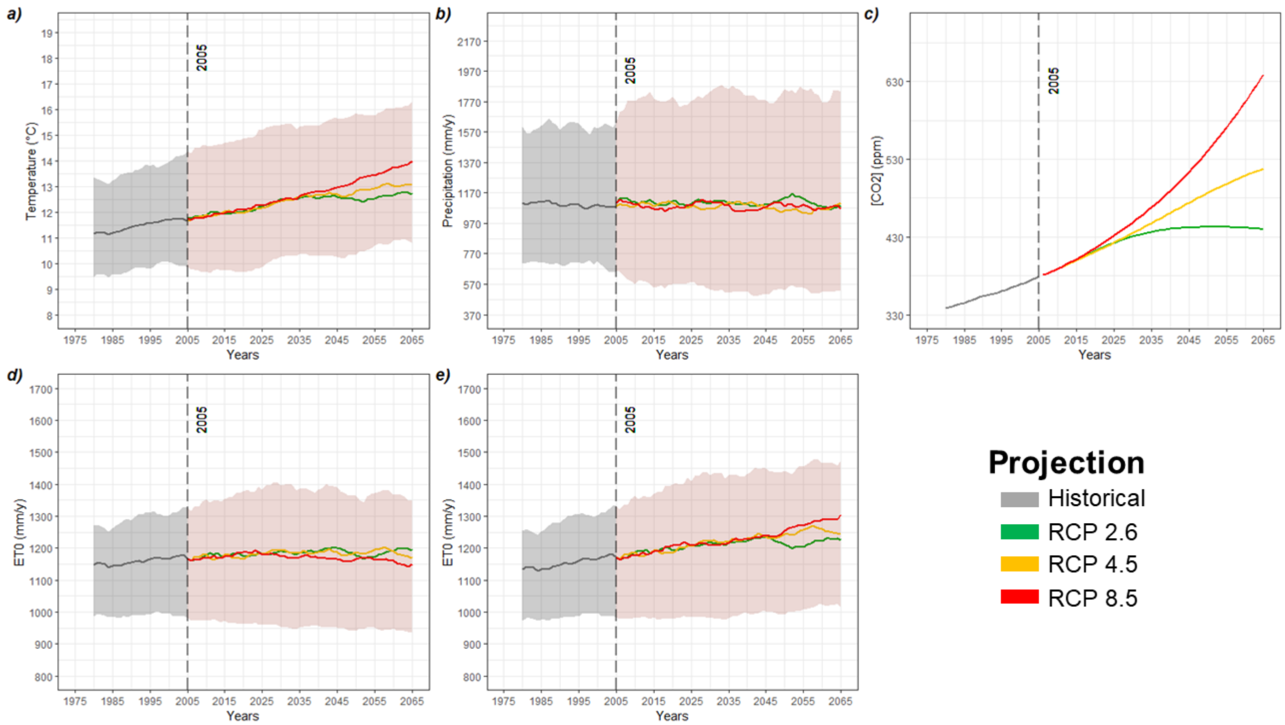

Figure 2: time series of climate variables in Aude basin, for the period 1976-2065 under RCPs 2.6, 4.5 and 8.5 scenarios. a) Evolution of mean temperature (°C). b) Evolution of total yearly precipitation (in mm/y). c) Evolution of CO_2 concentration under the three RCPs (in ppm). d) ET0 calculated with PM-equation corrected to account CO_2 fertilization. e) ET0 obtained with PM-equation assuming constant CO_2 concentration (CO_2=372 ppm). To simplify visualization, time series in panels a, b, d and e are smoothed with a 10-year running average

Actual evapotranspiration and net application with CO_2 fertilization

Comparing the differences in the estimation of *NAc* of each crop, Figure 3 shows that improved pasture is the crop with the greatest irrigation demand (NAc_{1990} = 560 mm/y). Although this crop is not usually irrigated to field capacity conditions, this high value of irrigation demand is explained by the duration of its growing period, which spans the entire year. Regarding climate change trends, results do not indicate a clear evolution of *NAc* for most crops, except for olive and peach crops, which show a very mild increase between 1990 and 2050. Specifically, *NAc* for olive changes from 440 mm/y in 1990 to 450-470 mm/y in 2050, while peach increases from 275 mm/y in 1990 to 300-315 mm/y in 2050. At the same time, *NAc* in the other crops exhibits no clear trend throughout the period. The *NAc* changes between 1990 and 2050 exceeds 10% only for peach, under RCP 2.6 and 4.5 (see Table 2). Specifically, improved pasture, olive, peach and tomato are expected to increase by about 4 – 10%, while the change for wheat and wine grape is less pronounced smaller (-3 - +3%). There is not a significant divergence in results between the different climate scenarios.

Overall, Table 2 shows that RCP 4.5 results in the greatest irrigation demand increase for all the crops, approximately 1 – 4 % higher than results under RCP 2.6 and RCP 8.5, due to the balance between temperature, precipitation and CO_2 concentration changes.

The share of irrigation demand over actual evapotranspiration is depicted in Figure 4, which partitions the *ETa* of each crop into its *NAc* and ETa_{prec} components, that is. the contributions of irrigation and precipitation to evapotranspiration, respectively. As in Figure 3, no consistent variation of *ETa* is observed between the historical and future periods, nor among the climate scenarios, although peach, olive, tomato and improved pasture show a mild increase. However, Figure 4 highlights differences between crops in terms of crop water requirements, with improved pasture exhibiting the highest evapotranspiration demand (approximately 970 mm/y). It also quantifies the contribution of irrigation relative to total water requirements. In this case, tomato is the crop with the highest percentage of irrigation water (> 78%), even though its *ETa* is comparable to most crops (i.e., peach, wheat and wine grape). This is explained by its growing period (from June to September), which is the time of the year with the lowest precipitation share, thus the remaining demand is replenished by irrigation.

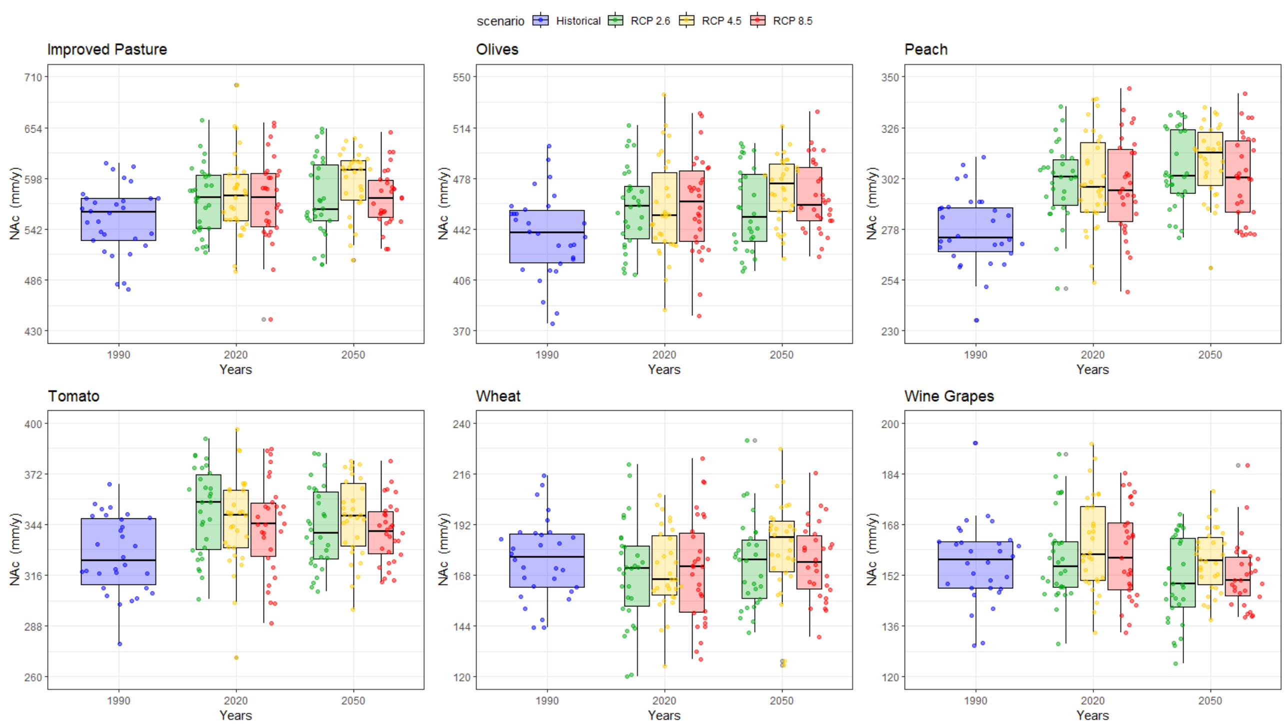

Figure 3: Net Application (NAc) trends of the 6 main crops among the 30-year time average around 1990, 2020, 2050, under the emission scenarios RCP 2.6, 4.5 and 8.5.

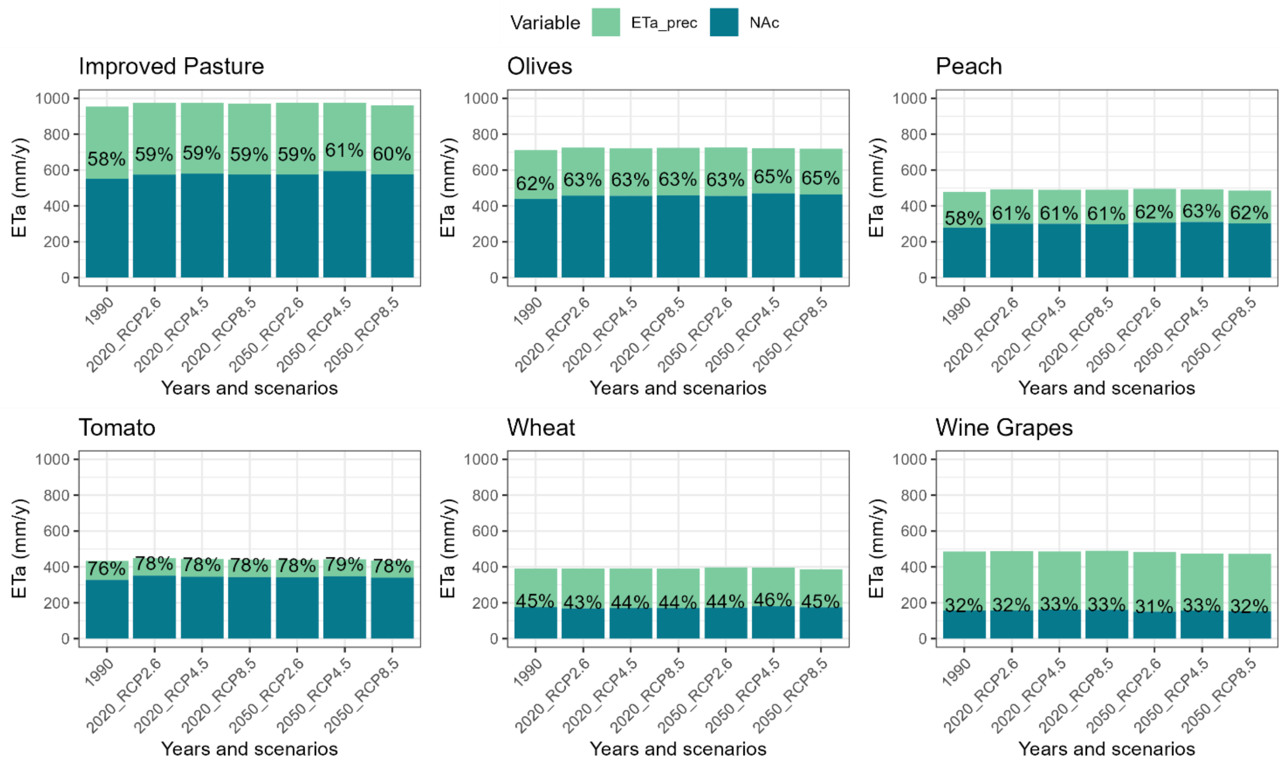

Figure 4: Actual Evapotranspiration (ETa) trends of the 6 main crops among the 30-year time average of 1990, 2020, 2050, under the emission scenarios RCP 2.6, 4.5 and 8.5. ETa is partitioned into the irrigation component (NAc) and the rainfall component (ETa_{prec}). The number above each bar represents the percentage of NAc over ETa

Table 2: rate of change of Net Application (NAc) of the 6 crops between historical and 2050, with (CO2fert) and without (CO2const) the CO_2 fertilization effect. Results expressed in %

	CO_2fert			CO_2const		
Crop	**RCP 2.6**	**RCP 4.5**	**RCP 8.5**	**RCP 2.6**	**RCP 4.5**	**RCP 8.5**
Improved Pasture	+4.0	+7.5	+4.4	+7.6	+13.7	+14.0
Olive	+4.1	+7.3	+6.0	+7.1	+12.1	+12.7
Peach	+10.2	+11.6	+8.8	+12.3	+16.6	+17.0
Tomato	+4.5	+6.2	+3.9	+8.2	+12.0	+13.1
Wheat	-1.4	+3.0	-0.7	+7.2	+15.8	+18.6
Wine Grape	-3.6	+0.5	-2.5	+1.0	+5.4	+3.2

Comparison of results with and without CO_2 fertilization effect

The boxplots in Figure 5 highlight the differences of SIMETAW_GIS outputs under the two fertilization approaches. Under *CO_2const* approach, *ETa* is expected to grow consistently for all crops and across all RCPs, with a more pronounced increase under RCP 8.5. Under *CO_2fert* approach, instead, the *ETa* increase is moderate for all crops. Considering the variations between 1990 and 2050, the *ETa* of Aude's crops (excluding wine grape) under the *CO_2const* approach is projected to increase by about 4-6 % under RCP 2.6, 5-8% under RCP 4.5 and 6-9% under RCP 8.5, while under *CO_2fert* variations remain overall between -1 and +3% change. This provides evidence that CO2 fertilization has a mitigating effect on the climate change-driven increase in crop water demand. Focusing on crops individually, tomato and wheat are those with the steepest increases in evapotranspiration under *CO_2const* (8% and 8.6% increase respectively, under the RCP8.5 scenario), and almost no change under *CO_2fert* (-1 – +0.5%). Improved pasture, olive and peach also exhibit increases under *CO_2const*, although less pronounced than for the previous crops (6 – 7% under RCP8.5), while wine grape do not show any notable upward trend in evapotranspiration (<1% increase).

Table 3 compares the mean *NAc* values of years 1990, 2020 and 2050 for the 6 crops, under the *CO_2fert* and *CO_2const* approaches and RCPs 2.6, 4.5 and 8.5. In the *Trend Significance* column, the p-values resulting from the trend tests are reported, while the *t-test* section shows the p-values from the Student's t-test, which compares the mean values obtained with the two fertilization approaches for each year and RCP. From the table, under RCP 2.6 no significant trend is expected (apart from the decreasing trend for wine grape, $p<0.05$) under both approaches. Under RCP 4.5 and 8.5, and with the *CO_2const*, the trend is highly significant for all crops (except wine grape), while under *CO_2fert* there is no significant trend, again with the exception of wine grape, which shows a significant decreasing trend across the years. Regarding the differences in values obtained with the two fertilization approaches, no significant differences are observed under RCPs 2.6 and 4.5, whereas under RCP 8.5 the difference becomes statistically significant for all crops.

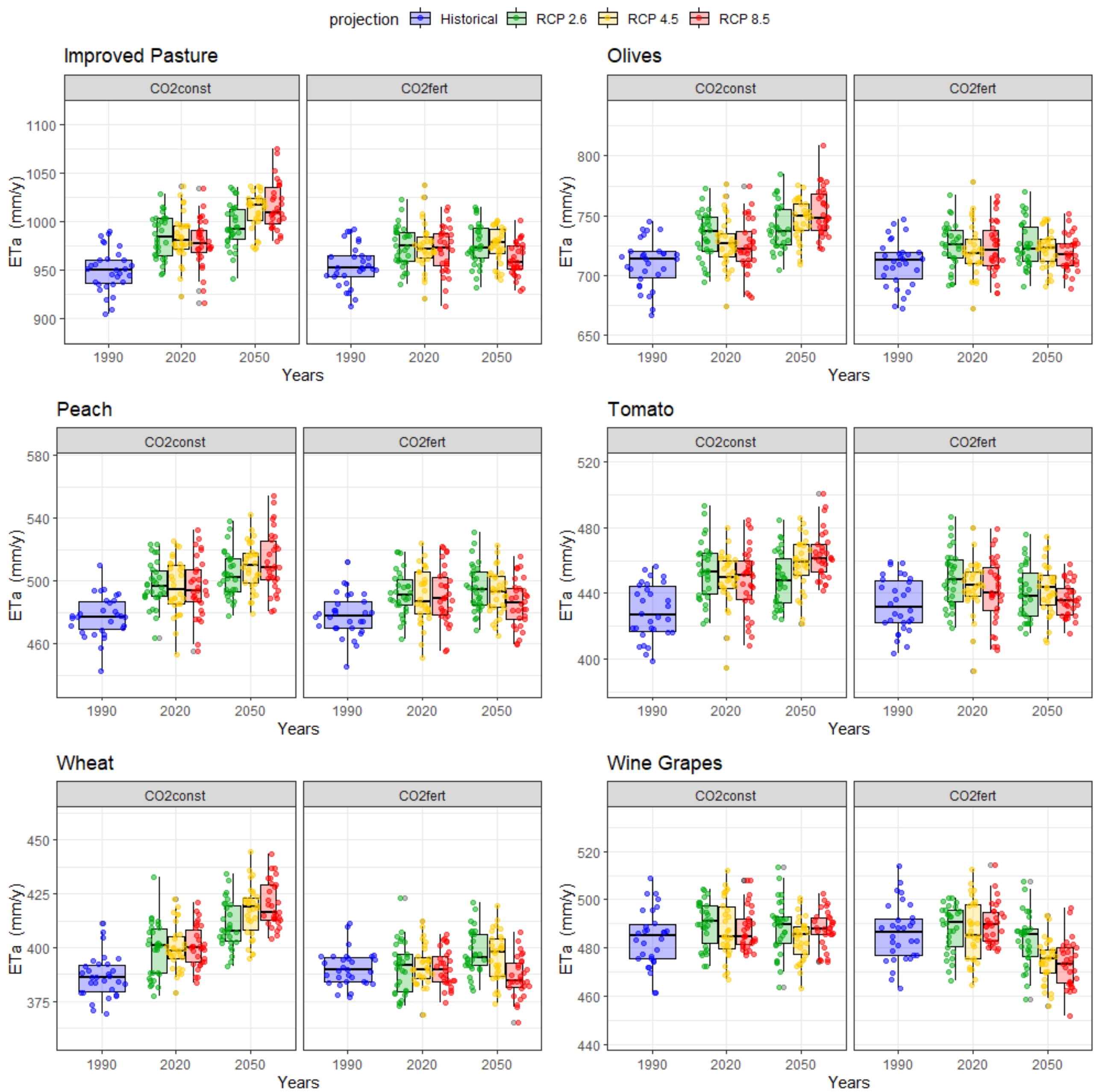

Figure 5: comparison of the evolution of Actual Evapotranspiration (ETa) of the 6 crops among the 30 years' time average of 1990, 2020, 2050, according to the 3 emission scenarios RCP 2.6, 4.5 and 8.5, with (CO2fert) and without (CO_2const) CO_2 fertilization effect.

Table 3: comparison of the evolution of Net Application (NAc) of the 6 crops among the 30 years' time average of 1990, 2020, 2050, according to the three climate simulations RCP 2.6, 4.5 and 8.5, with and without CO_2 fertilization effect. Trend

significance section tests the presence of significant trends across the period, while t-test investigates statistical difference between NAc obtained with the two approaches.

crop	**Approach**	**Historical**	**RCP 2.6**	**RCP 2.6**	**RCP 2.6**	**RCP 4.5**	**RCP 4.5**	**RCP 4.5**	**RCP 8.5**	**RCP 8.5**	**RCP 8.5**
	-	1990	2020	2050	Trend significance	2020	2050	Trend significance	2020	2050	Trend significance
Improved Pasture	CO_2fert	553	574	575	0.754	580	594	0.171	575	577	0.779
	CO_2const	548	580	590	0.529	586	624	**<.001*****	579	625	**<.001*****
	t-test	0.647	0.520	0.585		0.752	0.184		**0.003****	**<.001*****	
Olive	CO_2fert	438	457	456	0.677	456	470	0.095	459	464	0.285
	CO_2const	437	463	468	0.598	460	490	**<.001*****	458	492	**<.001*****
	t-test	0.894	0.443	0.650		0.906	0.105		**0.003****	**<.001*****	
Peach	CO_2fert	278	301	306	0.197	300	310	0.053	299	302	0.156
	CO_2const	277	305	311	0.057	307	323	**<.001*****	307	325	**<.001*****
	t-test	0.904	0.422	0.286		0.189	0.239		**0.006****	**<.001*****	
Tomato	CO_2fert	327	351	342	0.078	345	348	0.685	343	340	0.785
	CO_2const	323	355	349	0.312	350	362	**0.029***	351	365	**0.002****
	t-test	0.416	0.571	0.475		0.225	0.211		**0.019***	**<.001*****	
Wheat	CO_2fert	176	169	173	0.332	171	181	0.072	171	175	0.772
	CO_2const	172	176	184	0.085	178	199	**<.001*****	180	204	**<.001*****
	t-test	0.447	0.253	0.136		0.158	0.046		**0.003****	**<.001*****	
Wine grape	CO_2fert	156	158	150	**0.005**	162	157	0.153	160	152	**0.036***
	CO_2const	154	159	156	0.119	161	162	0.734	157	159	0.234
	t-test	0.564	0.788	0.838		0.420	0.134		**0.036***	**0.026***	

Significance: * $p<0.05$ ** $p<0.01$ *** $p<0.001$

Discussion

The present study provides basin-scale, crop-specific projections of irrigation demand for a Mediterranean climate hotspot (Aude), offering directly usable evidence for local water governance and adaptation planning. The application of SIMETAW_GIS, a pragmatic model requiring a limited number of inputs, facilitates the delivery of operational decision-support outputs that can be seamlessly integrated into irrigation planning and farmer practices. This includes the development of realistic deficit-irrigation strategies for vineyards. The analysis addresses a substantial practical uncertainty by quantifying how the inclusion or exclusion of CO2 fertilisation alters projected irrigation demand. This methodological issue has been increasingly emphasised in recent literature, with direct implications for assessing whether future irrigation requirements may intensify pressure on regional water resources. The obtained *ET0* projections can be compared with the results of (Lemaitre-Basset et al., 2022), who examined different methodologies for assessing the impact of CO_2 fertilization on ET0 estimation in France, particularly the approaches of (Stockle et al., 1992), (Kruijt et al., 2008) and (Yang et al., 2019), under RCP 4.5 and 8.5 for the period 1970-2100. According to (Lemaitre-Basset et al., 2022), *ET0* estimated without CO_2 fertilization (CO_2const) shows a greater increase than *ET0* estimated using the other three approaches (ΔET0 = +11% and +21% by the end of the century compared with period 1970-1999, under RCP 4.5 and 8.5, respectively). Under RCP 4.5, the approach of Stockle et al. (1992) forecasts a milder increase ($\Delta ET0$ = +5% by the end of the century), while the approaches of Kruijt et al. and Yang et al. produce similar, nearly constant increases, slightly greater than the values from Stockle et al. (1992). Under RCP 8.5, *ET0* from Stockle et al. (1992) is projected to decrease by the end of the century ($\Delta ET0$ = -3%) after peaking in 2070, whereas the other two formulations result in intermediate positive changes. This work estimates *ET0* using the approach proposed by (Snyder et al., 2011), projecting a growth between the historical period and 2050 of about 2.5-2.8%, under RCP 2.6 and 4.5, respectively, while under RCP 8.5 the increase remains below 1%. These results are in-line with those of Stockle et al. (2011), considering that the present study limits future projections to 2050 to be consistent with the conditions of the FACE experiments (Long et al., 2004), which tested plant responses to elevated CO_2 levels (550-600 ppm, approximately the projected CO2 concentration in 2050 under RCP 8.5).

Regarding irrigation demand, modest changes between historical and future periods ($\Delta NAc_{1990\text{-}2050} < 10\%$) are expected, with variations depending on the crop. Notably, RCP 8.5 does not correspond to the greatest increases; RCP 4.5 appears to produce the largest variations. Under RCP 8.5, CO_2 growth almost totally offsets the effects of temperature and precipitation changes, leading to a flat trend (or even a decrease) in future *NAc* projections. Comparable *NAc* values under CO_2const approach are reported by (Rodríguez Díaz et al., 2007a), who estimated average irrigation demand increases of about 16-19%, depending on the climate scenario and crop. (Fader et al., 2016), who studied the future irrigation demand under different CO2 fertilization approaches, estimates an average increase of about 4% under a low-emission scenario combined with strong CO_2 fertilization. This aligns with the values reported in Table 2, where the average NAc increase for the six crops between the historical period and 2050 is estimated to be around 3% under RCP 2.6 and CO_2fert. Similar findings are reported by Saadi et al. (2015) and Tanasijevic et al. (2014).

Regarding wine grape crop, the practice of deficit irrigation influences *ETa* and *NAc* trends, diverging from the trends of the other crops. Under CO_2fert, *ETa* and *NAc* show a mainly decreasing trend over time, while other crops exhibit relatively stable trends. This is because deficit irrigation induces water stress, reducing its evapotranspiration capacity. Since the partial irrigation coefficients remain constant over the years, total annual *ETa* declines in response to rising temperatures and decreasing precipitation rates.

Selecting a single approach to adjust canopy resistance (r_c) with rising CO_2 is challenging due to limitations in existing models. The formulation of (Snyder et al., 2011) is based on FACE experiments, which cannot support simulations to the end of the century, as stomatal resistance cannot grow indefinitely, plants still require gas exchange even in strongly CO_2-enriched environment. The approach of (Yang et al., 2019) fits *ETa* from climate models to an empirical model, but may require regional adjustments to improve accuracy, as suggested by (Lemaitre-Basset et al., 2022). Furthermore, canopy resistance responses to elevated CO_2 are not uniform vegetation types; they vary according to functional groups (C3 vs. C4 crops) and environmental conditions (Ainsworth & Rogers, 2007). Using a simple equation to adjust *ET0* for CO_2 overlooks complex surface-atmosphere feedback, leaving uncertainty in future *ETa* trends, which vary across studies and are influenced by factors as humidity changes and stomatal responses. This work at regional level is particularly interesting because it gives insight into possible adaptation strategies and future policies for water management. However, some uncertainties are associated with the estimation. In particular, the growing season was assumed to remain constant in the future, but we know that this is a quite relevant assumption for assessing crop water consumption. At the same time, very few models already integrate phenological modeling with water needs assessment, and these are mostly crop models (e.g., crop model STICS, from Brisson et al., 2003)) which requires relevant amount of input data. Moreover, we considered water management at farm scale as homogeneous in the study area, in terms of irrigation and efficiency.

In the near future, water scarcity issues in the Mediterranean are expected to intensify, leading to reduced crop productivity and exacerbating intersectoral conflicts over water use due to the combined effects of increasing droughts and socio-economic trends (MedECC, 2020b). In Southern Europe, non-irrigated agriculture is likely to decrease by nearly 50% by 2050, potentially causing crop abandonment in some regions (EEA, 2019). While CO_2 fertilization may advantage crop production and water use efficiency (e.g., enhanced photosynthetic rates and reduced evapotranspiration), these benefits are likely to be overcome by climate-induced challenges, such as increased long-term droughts, more severe precipitation events, shifts in crop phenology and increased risk of pests and diseases due to warmer temperatures (MedECC, 2020b). Moreover, elevated atmospheric CO_2 concentrations has been associated with a decline in crop nutritional quality (Grays, 2022; Kidane et al., 2025; Panozzo et al., 2014).

Addressing these challenges begins with raising awareness of irrigation demand assessment and quantifying water consumption in the agricultural sector, giving support to governance and policy formulations that tackle adaptation to water scarcity. Furthermore, expanding research on the effects of CO_2 on plant growth can enable more realistic assessments of its impacts in relation to the other effects of climate change, helping to clarify whether CO2 fertilization can effectively constitute an offset to climate change.

Conclusion

This study provides a comprehensive assessment of irrigation management in the Aude basin under different climate change scenarios, using the SIMETAW_GIS model to evaluate the impacts on the six major crops of the region. Results reveal that future irrigation demands are highly dependent on whether CO_2 fertilization effects are considered. When the effect of increased atmospheric CO_2 is included, the rise in irrigation demand is relatively modest, with increases between 3-10% from 1990 to 2050, depending on the crop, under full irrigation conditions. This result is associated to the influence of CO_2 in reducing plant evapotranspiration through increased canopy resistance. On the other hand, without including CO_2 fertilization, expected increases in irrigation demand are significantly higher, reaching up to 18% for wheat under the RCP 8.5 scenario.

Wine grape, the dominant irrigated crop, exhibits a different trend. The practice of deficit irrigation, aimed at improving grape quality, combined with CO_2 fertilization, leads to a decrease in water requirements over time, due to its reduction of evapotranspiration caused by water stress and possible side effects on yield and quality. Without CO_2 fertilization, irrigation demand for wine grape remains stable over the years, without a clear trend. This suggests that adjusting deficit irrigation to meet water savings with sustainable crop yield could be an effective adaptation measure to address future water scarcity. In contrast, other crops, such as improved pasture, olive, and peach, show slight increases in *ETa* and *NAc*, particularly under RCP 4.5, where CO_2 fertilization effects are less pronounced.

These findings underscore the importance of improving the understanding of CO_2 fertilization effect in relation to crop evapotranspiration, to refine the assessment of irrigation demand change under future climate projections. In this regard, this study adds information to support adaptation strategies in agricultural water management, by considering the uncertainty of climate change forecasts. A clearer understanding of future irrigation demand can support informed governance interventions to mitigate water scarcity in Mediterranean environments. In fact, the study reinforces that climate-driven water scarcity in Mediterranean regions will remain a critical challenge, even when CO_2 fertilization partially offsets rising evaporative demand. Improving the estimation of CO2 effect in water crop demand integrating socio-economic pathways into future assessments will be essential for developing robust adaptation strategies.

The results presented here offer a quantitative basis for guiding water governance and agricultural management in the Aude basin and similar Mediterranean environments as they navigate the transition toward more climate-resilient irrigation systems.

Declarations

Research funding

This work was supported by the TALANOA-WATER project funded under the Grant Agreement number: [2023] [TALANOA-WATER] [Call 2020 Section 1 Water IA] of the PRIMA program. The work was developed within the Ph.D program in Agrometeorology and Ecophysiology of Agricultural and Forestry Ecosystems at the University of Sassari in collaboration with INRAE of Montpellier, France.

References

Adamovic, M., Al-Zubari, W., Amani, A., Ameztoy Aramendi, I., Bacigalupi, C., Barchiesi, S., Bisselink, B., Bodis, K., Bouraoui, F., Caucci, S., Dalton, J., De Roo, A., Dudu, H., Dupont, C., El Kharraz, J., Embid, A., Farajalla, N., & Fernandez Blanco Carra, G. (2019). Position Paper on Water, Energy, Food and Ecosystems (WEFE) Nexus and Sustainable Development Goals (SDGS). https://doi.org/10.2760/5295

Agreste. (2020). Recensement agricole 2020. https://vizagreste.agriculture.gouv.fr/#/indicateur/11/2020

Ainsworth, E. A., & Rogers, A. (2007). The response of photosynthesis and stomatal conductance to rising [CO 2]: Mechanisms and environmental interactions. Plant, Cell and Environment, 30(3), 258–270. https://doi.org/10.1111/j.1365-3040.2007.01641.x

Allen, L. H. (1990). Plant Responses to Rising Carbon Dioxide and Potential Interactions with Air Pollutants. Journal of Environmental Quality. https://doi.org/10.2134/jeq1990.00472425001900010002x

Allen, R. G., Pereira, L. S., Raes, D., & Smith, M. (1998). FAO Irrigation and Drainage Paper No. 56—Crop Evapotranspiration (Fascicolo 56). FAO - Food and Agriculture Organization of the United Nations.

Allen, R. G., Pruitt, W. O., Wright, J. L., Howell, T. A., Ventura, F., Snyder, R., Itenfisu, D., Steduto, P., Berengena, J., Yrisarry, J. B., Smith, M., Pereira, L. S., Raes, D., Perrier, A., Alves, I., Walter, I., & Elliott, R. (2006). A recommendation on standardized surface resistance for hourly calculation of reference ETo by the FAO56 Penman-Monteith method. Agricultural Water Management, 81(1–2), 1–22. https://doi.org/10.1016/j.agwat.2005.03.007

Aslam, M. F., Masia, S., Spano, D., Mereu, V., Debolini, M., Snyder, R. L., Borgo, A., & Trabucco, A. (2025). Modelling crop water demand under climate change: The case of Sardinia region. Irrigation Science. https://doi.org/10.1007/s00271-025-01027-8

Brisson, N., Gary, C., Justes, E., Roche, R., Mary, B., Ripoche, D., Zimmer, D., Sierra, J., Bertuzzi, P., Burger, P., Bussière, F., Cabidoche, Y. M., Cellier, P., Debaeke, P., Gaudillère, J. P., Hénault, C., Maraux, F., Seguin, B., & Sinoquet, H. (2003). An overview of the crop model stics. European Journal of Agronomy, 18(3–4), 309–332. https://doi.org/10.1016/S1161-0301(02)00110-7

Büchner, M., & Reyer, C. P. O. (2017). ISIMIP2b CO2 input data (v1.0). ISIMIP Repository. https://doi.org/10.48364/ISIMIP.943362

Cambrea, L., Lafon, C., & Mayoux, L. (2020). Vine irrigation in the former Languedoc-Roussillon region: Production potential maintained through water savings (pp. 28–33). Sciences Eaux & Territoires.

Chambres d'agriculture Occitanie. (2018). L'agriculture, Aude, en bref.

Copernicus Climate Change Service, C. D. S. (2022). CORDEX regional climate model data on single levels. Copernicus Climate Change Service (C3S) Climate Data Store (CDS). https://doi.org/10.24381/cds.bc91edc3

Cramer, W., Guiot, J., Fader, M., Garrabou, J., Gattuso, J. P., Iglesias, A., Lange, M. A., Lionello, P., Llasat, M. C., Paz, S., Peñuelas, J., Snoussi, M., Toreti, A., Tsimplis, M. N., & Xoplaki, E. (2018). Climate change and interconnected risks to sustainable development in the Mediterranean. Nature Climate Change, 8(11), 972–980. https://doi.org/10.1038/s41558-018-0299-2

Direction Régionale de l'Alimentation, de l'Agriculture et de la F. (2018). Aude (11). Prefét de la region Occitanie.

Drake, B. G., Gonzàlez-Meler, M. A., & Long, S. P. (1997). More efficient plants: A Consequence of Rising Atmospheric CO2? Annual Review of Plant Biology, 48(July 1997), 609–639. https://doi.org/10.1146/annurev.arplant.48.1.609

EEA. (2019). Climate change threatens future of farming in Europe. European Environment Agency. https://www.eea.europa.eu/highlights/climate-change-threatens-future-of

European Environment Agency. (2015). Mediterranean Sea region briefing—The European environment—State and outlook 2015 (pp. 1–6). https://www.eea.europa.eu/soer-2015/countries/black-sea

Fader, M., Shi, S., Von Bloh, W., Bondeau, A., & Cramer, W. (2015). Mediterranean irrigation under climate change: More efficient irrigation needed to compensate increases in irrigation water requirements. Hydrology and Earth System Sciences Discussions, 12(8), 8459–8504. https://doi.org/10.5194/hessd-12-8459-2015

Fader, M., Shi, S., Von Bloh, W., Bondeau, A., & Cramer, W. (2016). Mediterranean irrigation under climate change: More efficient irrigation needed to compensate for increases in irrigation water requirements. Hydrology and Earth System Sciences, 20(2), 953–973. https://doi.org/10.5194/hess-20-953-2016

FAO. (2012). FAO GeoNetwork. Food and Agriculture Organization of the United Nation (FAO). https://data.apps.fao.org/map/catalog/srv/eng/catalog.search#/search?any=soil depth

FAO. (2017). Water for Sustainable Food and Agriculture. www.fao.org/publications

Ferragina, E., & Canitano, G. (2014). Water and Food Security in the Arab Countries: National and Regional Implications. Global Environment, 7(2), 326–351. https://doi.org/10.3197/ge.2014.070204

Field, C. B., Jackson, R. B., & Mooney, H. A. (1995). Stomatal responses to increased CO2: Implications from the plant to the global scale. Plant, Cell & Environment, 18(10), 1214–1225. https://doi.org/10.1111/j.1365-3040.1995.tb00630.x

Grays, L. (2022). Changing crops in a changing climate: The impact of rising CO2 levels on the nutritional quality of crops. Farming Connect. https://businesswales.gov.wales/farmingconnect/news-and-events/technical-articles/changing-crops-changing-climate-impact-rising-co2-levels-nutritional-quality-crops

Guerra, E., Ventura, F., Spano, D., & Snyder, R. L. (2015). Correcting Midseason Crop Coefficients for Climate. Journal of Irrigation and Drainage Engineering, 141(6). https://doi.org/10.1061/(asce)ir.1943-4774.0000839

IPCC. (2013). Climate Change 2013—The Physical Science Basis. In Stocker TF, Qin D, Plattner GK, TignorM, Allen SK, Boschung J, Nauels A, Xia Y, Bex V, Midgley PM (eds) Climate change 2013: The physical science basis. Contribution of Working Group I to the Fifth Assessment Report of the Intergovernmental Panel on Clima (Vol. 43, Fascicolo 4, pp. 22–23). Cambridge University Press. https://doi.org/10.1515/ci-2021-0407

IPCC. (2023). IPCC, 2023: Summary for Policymakers. In: Climate Change 2023: Synthesis Report. Contribution of Working Groups I, II and III to the Sixth Assessment Report of the Intergovernmental Panel on Climate Change. https://www.unep.org/resources/report/climate-change-2023-synthesis-report

Jones, C. A., & Kiniry, J. (1986). CERES-Maize: A Simulation Model of Maize Growth and Development (Texas A&M Univ. Press, A c. Di). College Station.

Jones, J. W., Hoogenboom, G., Porter, C. H., Boote, K. J., Batchelor, W. D., Hunt, L. A., Wilkens, P. W., Singh, U., Gijsman, A. J., & Ritchie, J. T. (2003). The DSSAT cropping system model (Vol. 18).

Kidane, B., Urugo, M. M., Hirpha, H. H., Paulos, T., Hundea, W., & Tessema, F. (2025). Nutritional challenges of staple crops due to increasing atmospheric carbon dioxide levels: Case of Sub-Saharan Africa. Journal of Agriculture and Food Research, 19(November 2024), 101592. https://doi.org/10.1016/j.jafr.2024.101592

Kimball, B. A., Thorp, K. R., Boote, K. J., Stockle, C., Suyker, A. E., Evett, S. R., Brauer, D. K., Coyle, G. G., Copeland, K. S., Marek, G. W., Colaizzi, P. D., Acutis, M., Alimagham, S., Archontoulis, S., Babacar, F., Barcza, Z., Basso, B., Bertuzzi, P., Constantin, J., … Zhou, W. (2023). Simulation of evapotranspiration and yield of maize: An Inter-comparison among 41 maize models. Agricultural and Forest Meteorology, 333(February). https://doi.org/10.1016/j.agrformet.2023.109396

Kruijt, B., Witte, J. P. M., Jacobs, C. M. J., & Kroon, T. (2008). Effects of rising atmospheric CO2 on evapotranspiration and soil moisture: A practical approach for the Netherlands. Journal of Hydrology, 349(3–4), 257–267. https://doi.org/10.1016/j.jhydrol.2007.10.052

Lemaitre-Basset, T., Oudin, L., & Thirel, G. (2022). Evapotranspiration in hydrological models under rising CO2: A jump into the unknown. Climatic Change, 172(3–4), 1–19. https://doi.org/10.1007/s10584-022-03384-1

Lespinas, F., Ludwig, W., & Heussner, S. (2010). Impact of recent climate change on the hydrology of coastal mediterranean rivers in Southern France. Climatic Change, 99(3–4), 425–456. https://doi.org/10.1007/s10584-009-9668-1

Long, S. P., Ainsworth, E. A., Rogers, A., & Ort, D. R. (2004). Rising Atmospheric Carbon Dioxide: Plants FACE the future. Annual Review of Plant Biology, 55, 591–628. https://doi.org/10.1146/annurev.arplant.55.031903.141610

Mancosu, N., Spano, D., Orang, M., Sarreshteh, S., & Snyder, R. L. (2016). SIMETAW#—A model for agricultural water demand planning. Water Resources Management, 30(2), 541–557. https://doi.org/10.1007/s11269-015-1176-7

Masia, S., Sušnik, J., Marras, S., Mereu, S., Spano, D., & Trabucco, A. (2018). Assessment of irrigated agriculture vulnerability under climate change in Southern Italy. Water, 10(2), 1–19. https://doi.org/10.3390/w10020209

Masia, S., Trabucco, A., Spano, D., Snyder, R. L., Sušnik, J., & Marras, S. (2021). A modelling platform for climate change impact on local and regional crop water requirements. Agricultural Water Management, 255(June). https://doi.org/10.1016/j.agwat.2021.107005

Maury, O., Quidoz, M.-C., Garcia de Cortazar Atauri, I., Chuine, I., & El Hasnaoui, Mohamed Tromel, L. (2023). Portail de données phénologiques du réseau TEMPO / TEMPO Data Portal. Recherche Data Gouv, V1. https://doi.org/10.57745/NQ9HRV

McCown, R. L., Hammer, G. L., Hargreaves, G. N. G., Holzworth, D., & Huth, N. I. (1995). APSIM: an agricultural production system simulation model for operational research. Mathematics and Computers in Simulation, 39(3–4), 225–231. https://doi.org/10.1016/0378-4754(95)00063-2

MedECC. (2020). Current situation and risks for the future First Mediterranean Assessment Report (p. 632). https://zenodo.org/record/4768833

Météo-France. (2025). Station Météo-France commune de Lézignan-Corbières)—Fiche climatologique—Période 1991-2020.

Montazar, A., Rejmanek, H., Tindula, G., Little, C., Shapland, T., Anderson, F., Inglese, G., Mutters, R., Linquist, B., Greer, C. A., Hill, J., & Snyder, R. L. (2016). Crop Coefficient Curve for Paddy Rice from Residual Energy Balance Calculations. Journal of Irrigation and Drainage Engineering, 143(2), 1–14. https://doi.org/10.1061/(asce)ir.1943-4774.0001117

Monteith, J. L. (1965). Evaporation and Environment. XIXth Symposium of the Society for Experimental Biology. Swansea, 19(2393175), 205–234.

Nendel, C. (2014). MONICA : A Simulation Model for Nitrogen and Carbon Dynamics in Agro-MONICA : A Simulation Model for Nitrogen and Carbon Dynamics in Agro-Ecosystems. October 2013. https://doi.org/10.1007/978-3-319-01017-5

Orang, M. N., Snyder, R. L., Shu, G., Hart, Q. J., Sarreshteh, S., Falk, M., Beaudette, D., Hayes, S., & Eching, S. (2013). California Simulation of Evapotranspiration of Applied Water and Agricultural Energy Use in California. Journal of Integrative Agriculture, 12(8), 1371–1388. https://doi.org/10.1016/S2095-3119(13)60742-X

Panozzo, J. F., Walker, C. K., Partington, D. L., Neumann, N. C., Tausz, M., Seneweera, S., & Fitzgerald, G. J. (2014). Elevated carbon dioxide changes grain protein concentration and composition and compromises baking quality. A FACE study. Journal of Cereal Science, 60(3), 461–470. https://doi.org/10.1016/j.jcs.2014.08.011

Rodríguez Díaz, J. A., Weatherhead, E. K., Knox, J. W., & Camacho, E. (2007). Climate change impacts on irrigation water requirements in the Guadalquivir river basin in Spain. Regional Environmental Change, 7(3), 149–159. https://doi.org/10.1007/s10113-007-0035-3

SDES. (2021). Bilan environnemental de la France Édition 2021 (p. 128). Le service des données et études statistiques (SDES). www.statistiques.developpement-durable.gouv.fr

Sharpley, A. N., & Williams, J. R. (1990). EPIC: The erosion-productivity impact calculator. U.S. Department of Agriculture Technical Bulletin, 1768, 235.

Smith, M. (1992). CROPWAT : a computer program for irrigation planning and management. Food and Agriculture Organization (FAO).

Snyder, R. L., Moratiel, R., Song, Z., Swelam, A., Jomaa, I., & Shapland, T. (2011). Evapotranspiration response to climate change. Acta Horticulturae, 922, 91–98. https://doi.org/10.17660/ActaHortic.2011.922.11

Stockle, C. O., Dyke, P. D., Williams, J. R., Jones, A. C., & Rosenberg, N. J. (1992). A method for estimating the direct and climatic effects of rising atmospheric carbon dioxide on growth and yield of crops: Part II—Sensitivity analysis at three sites in the Midwestern USA. Agricultural Systems, 38(3), 239–256.

Theia. (2018). Occupation des sols (OSO). https://www.theia-land.fr/ceslist/ces-occupation-des-sols/

Turco, M., Palazzi, E., Von Hardenberg, J., & Provenzale, A. (2015). Observed climate change hotspots. Geophysical Research Letters, 42(9), 3521–3528. https://doi.org/10.1002/2015GL063891

United States Geological Survey. (2022). Earth Explorer. USGS. https://earthexplorer.usgs.gov/

van Diepen, C. A., Wolf, J., van Keulen, H., & Rappoldt, C. (1989). WOFOST: a simulation model of crop production. Soil Use and Management, 5(1), 16–24. https://doi.org/10.1111/j.1475-2743.1989.tb00755.x

Yang, Y., Roderick, M. L., Zhang, S., McVicar, T. R., & Donohue, R. J. (2019). Hydrologic implications of vegetation response to elevated CO2 in climate projections. Nature Climate Change, 9(1), 44–48. https://doi.org/10.1038/s41558-018-0361-0

Annex

Table 4: list of Global Circulation Models (GCMs) and Regional Climate Models (RCMs) used for climate data acquisition

Global Climate model	Regional climate model
NCC-NorESM1-M (Norway)	GERIC-REM02015 (Germany)
MPI-M-MPI-ESM-LR (Germany)	SMHI-RCA4 (Sweden)
CNRM-CERFACS-CNRM-CM5 (France)	KNMI-RACM022E (Netherlands)
CNRM-CERFACS-CNRM-CM5 (France)	CNRM-ALADIN63 (France)
NCC-NorESM1-M (Norway)	SMHI-RCA4 (Sweden)

Table 5: summary table of input variables for SIMETAW_GIS model

Variable	Units	Resolution	Source
2 m air temperature	K	0.11°x0.11°	Copernicus Climate Change Service, 2019
Mean precipitation flux	$kg/m^2/s$	0.11°x0.11°	Copernicus Climate Change Service, 2019
2 m relative humidity	%	0.11°x0.11°	Copernicus Climate Change Service, 2019
Surface solar radiation downwards	W/m^2	0.11°x0.11°	Copernicus Climate Change Service, 2019
Surface thermal radiation downward	W/m^2	0.11°x0.11°	Copernicus Climate Change Service, 2019
10 m Wind Speed	m/s	0.11°x0.11°	Copernicus Climate Change Service, 2019
Soil depth	m	0.11°x0.11°	*FAO*, 2012
Available Water Capacity	mm_{water} /m_{soil}[1]	250 m	Hengl & Gupta, 2019
Elevation	m	0.11°x0.11°	*EarthExplorer*, n.d.
Crop surface	ha	Municipal scale	
Growing season	dd/mm	/	Maury et al., 2023

Chapter 3. ACQUAOUNT-Farm: an IoT-based real-time platform for optimizing daily irrigation under water-scarcity

Andrea Borgo[a,b], Fathia Elmokh[c], Kameleddine Nagaz[c], Simone Mereu[b,d], Guido Rianna[b], Gennaro Sequino[b], Francesco Martini[e], Josep Pijuan Parra[f], Mauro Lo Cascio[a], Serena Marras[a,b], Antonio Trabucco[b], Marta Debolini[b]

(a) Department of Agriculture, University of Sassari, Viale Italia, 39a, 07100 Sassari, Italy
(b) CMCC Foundation – Euro-Mediterranean Centre on Climate Change, Italy
(c) Institut des Régions Arides, Medenine, Tunisia
(d) Institute of BioEconomy, Italian National Research Council, Italy
(e) Abinsula srl, Viale Umberto I, 42, 07100 Sassari, Italy
(f) Eurecat, Centre Tecnològic de Catalunya, Unit of Applied Artificial Intelligence, Lleida, Spain

Email corresponding author: a.borgo@studenti.uniss.it

Highlights

- IoT platform providing optimal irrigation scheduling
- User-friendly IoT dashboard with interoperable real-time sensors
- Weekly forecasts of full and deficit irrigation needs based on FAO equations
- Calibrated in South Tunisia for citrus orchards and potato fields (2024–2025)
- Potential water savings of 60% in citrus and 80% in autumn potato fields

Keywords

Precision agriculture; Irrigation scheduling; Mediterranean; Water saving; Water scarcity

Abstract

Efficient water management is critical in modern agriculture due to unsustainable depletion of water resources, intensified by climate change. Digital technologies such as IoT offer opportunities to optimize water use through precise, real-time assessment of water requirements. This study presents ACQUAOUNT-Farm, a real-time platform designed to assist farmers in irrigation planning across Mediterranean environments. The tool integrates on-site IoT sensors (soil moisture, water flow, weather) with a physically based model following the FAO-56 dual crop coefficient approach, embedded within a user-friendly interface. The platform requires minimal input data, providing soil moisture monitoring and scheduling capabilities suitable for non-expert users. ACQUAOUNT-Farm updates daily, reconstructing hourly soil moisture and irrigation needs up to one week ahead and generating an irrigation calendar based on crop-specific water stress thresholds. ACQUAOUNT-Farm was tested on four farms in southern Tunisia for citrus and potato crops (2024-2025). Simulated and observed soil moisture showed good agreement for three out of four farms ($R^2 \approx 0.65$, RMSE ≈ 0.022 m^3 m^{-3}, MAD ≈ 0.016 m^3 m^{-3}), with differences below sensor accuracy (0.03 m^3 m^{-3}) up to four days in three farms and up to two days in one farm, confirming the model's forecasting ability. Compared to farmers' practices, ACQUAOUNT-Farm indicated water savings of 63–65% for one citrus field and 80–84% for autumn potato, while spring potato showed 17–33% savings. In one citrus field, the model confirmed the farmer's deficit irrigation strategy. These results suggest that ACQUAOUNT-Farm has the potential to support farmers in Mediterranean regions in reducing water withdrawals.

Introduction

Increasing competition for water among sectors, hastened by climate change and population growth, is driving water scarcity and degradation in Mediterranean environments (Lionello et al., 2014; MedECC, 2020a; Santos Pereira et al., 2009). In the Mediterranean, climate change is expected to increase evapotranspiration rates due to rising temperatures while reducing precipitation amounts, resulting in increased irrigation demand in agriculture (Cramer et al., 2018b; IPCC, 2023a; Saadi et al., 2015). On a global average, agriculture currently accounts for approximately 70% of freshwater withdrawals (FAO, 2017a), and in some Mediterranean countries, this share can exceed 80% (Ferragina & Canitano, 2014a). However, future increases in food demand and crop evapotranspiration driven by climate change are expected to force a shift of many agricultural areas from rainfed to irrigated (Malek & Verburg, 2018), in addition to increases in irrigation rates.

The digitalization of the agricultural sector offers a significant opportunity to enhance water management practices and improve irrigation efficiency. By leveraging advanced technologies, such as Internet of Things (IoT), sensors and data analytics (Fernandes De Oliveira et al., 2021; Noun et al., 2022), farmers can monitor soil moisture in real-time, optimize irrigation schedules, and reduce water losses (Morchid et al., 2025). Applying these tools can lead to more sustainable agriculture, by aligning water applications with effective crop water requirements, ultimately improving water productivity and climate resilience (Ali et al., 2025; El Mokh et al., 2024).

Recent years have seen a growing body of work on sensor-based decision support systems (DSS) for precision irrigation, yet the field remains fragmented across substantially different approaches. Some models focus on the integration of IoT sensor networks with physically based soil water balance models. For instance, Hydro-Tech (Todorovic et al., 2016) and SWIM2 (Hendrickx et al. 2026) are DSS which combine FAO-56 evapotranspiration modelling with real-time sensor data and short-term weather forecasting for multi-crop farm management. A second strand leverages purely data-driven and multi-index approaches: for instance, Crop2Cloud (Nsoh et al., 2025) is a platform that combines volumetric water content sensors, canopy temperature measurements, and fuzzy-logic rules to generate real-time irrigation recommendations based on multiple water stress indices. A third line of research considers the use of remote sensing data, alone or assimilated into irrigation models (Bellvert et al., 2023; Nasim & Khurram, 2025). Despite these advancements, critical gaps remain. Most of these platforms require extensive parameterization and technical expertise that limit their direct adoption by farmers. Data-driven tools such as Crop2Cloud do not explicitly represent the soil–water–plant continuum, reducing their interpretability and transferability across sites. Moreover, the majority of existing platforms have been developed and validated in temperate contexts, with limited testing under the arid and semi-arid conditions prevalent across the Mediterranean basin, where water scarcity is more prominent. Finally, other existing platforms are designed for single crops (Granados-Olivas et al., 2026; Zia et al., 2021).

Against this background, the study introduces ACQUAOUNT-Farm, a real-time, sensor-based platform which combines IoT-based monitoring and control, interoperability through the Web of Things (WoT) platform, and dynamic modelling combined with data analytics to optimize water use in Mediterranean agriculture. ACQUAOUNT-Farm is specifically targeted to farmers, thus requiring only a minimal set of readily accessible inputs. The platform updates daily and provides updates on soil moisture conditions, crop-specific irrigation requirements for a collection of diverse crops, and a set of irrigation recommendations, namely “Early” (no water stress), “Late” (moderate water stress) and “Limit” (severe water stress). These outputs are conceived to allow farmers to have a full overview of the state of water resources in the field and to dynamically plan the irrigation, balancing effective crop water needs and water availability. In this context, ACQUAOUNT-Farm is proposed as a bridging tool between scientific research and real-world applications, building upon the standardized FAO-56 methodology (R. G. Allen et al., 1998b) and adapting it to real-time, sensor-based operational use. To evaluate its performance, ACQUAOUNT-Farm has been tested in four farms in southern Tunisia under arid conditions, with both annual (potato) and perennial (citrus) crops. The model's irrigation recommendations are compared against the farmers' actual irrigation practices, with the aim of assessing the model's reliability and quantifying the potential for water savings.

Materials and methods

ACQUAOUNT-Farm is executed daily (at 5 a.m) and updates the corresponding outputs in the platform. Each execution considers a two-week period, returning the evolution of the full irrigation demand (Irr_{full}), deficit irrigation (Irr_{def}), and soil moisture (*SM*). The time frame of each execution is structured on an iterative soil water balance, which includes one week preceding the instant of the execution *i* and one week of forecast after i. The past week soil-water balance is updated based on the soil moisture field sensors, while future dynamics are obtained from a self-updating soil water balance. Reproducing the soil water balance over the past week is required by the model to calibrate its parameters and refine predictions. Based on scenarios of optimal irrigation (“Early”), moderate (“Late”), and high (“Limit”) water stress, the model schedules irrigation events for both full and deficit irrigation strategies. Inputs are divided into four categories, namely weather, soil, crop and irrigation data, sourced from on-site sensors, weather-forecast APIs, FAO tables, and user input.

Input data

Climate data

Climate inputs include hourly temperature (*T*, °C), relative humidity (*RH*, %), solar radiation (*SWrad*, W m^{-2}), precipitation (*P*, mm), and wind speed (u_2, m s^{-1}). Historical records are collected at hourly scale from on-site weather stations located near the farm. For weather predictions, the model relies on weather forecast APIs, taken from the OpenMeteo website (Open-Meteo, 2025), which provides open-source forecasts for multiple meteorological models at a given location.

Soil data

To provide an easily obtainable set of data for soil characterization, the model requires the percentages of sand, silt and clay (P_{sand}, P_{silt}, P_{clay}, respectively, %), the saturated hydraulic conductivity (*Ks*, cm s^{-1}), the bulk density (Pb, kg m^{-3}) and the organic-matter content (P_{om}, %). Water-retention parameters (WRPs), that is the soil water content at saturation (θ_{sat}), field capacity (θ_{fc}) and the wilting point (θ_{wp}), are also needed and are expressed in volumetric water content (m^3 m^{-3}). These variables are considered a reasonable trade-off for effective soil characterization, without relying on more complex parameters and they can be inferred from other measurements or downloaded from global datasets if measured values are not available.

In addition to model parameters, two *SM* probes (Delta OHM probes HD3910.1, two-electrodes version) are installed in each field to monitor the evolution of *SM* at three depths, specifically 15, 30 and 45 cm. The sensor accuracy is declared to be 0.03 m^3 m^{-3} when *SM* range is between 0 and 0.5 m^3 m^{-3} and soil temperature is at 23 °C (Delta OHM, 2021).

Crop data

Crop parameters and their irrigation thresholds are listed together in a separate file. Crop coefficient (k_c) thresholds $k_{c,in}$, $k_{c,mid}$ and $k_{c,end}$; phenological-stage durations; depletion factor (*DF*); minimum and maximum root depths RD_{min}, RD_{max}, m); and crop height (h, m) are taken from FAO guidelines, while irrigation deficit thresholds are provided by local stakeholders. Users are asked to enter planting dates and optionally harvesting dates of the selected crop directly on the platform.

Irrigation data

ACQUAOUNT-Farm requires an hourly irrigation flow dataset (in m^3 h^{-1}), recorded by the water meter installed in the irrigation system. The model also requires characterization of the entire irrigation system, including the irrigation method (sprinkler, drip or subsurface). For sprinkler systems, the number of emitters and the sprinkler flow rate (s_{rate}, m^3 s^{-1}) are specified. For drip systems, the emitter flow rate (d_{rate}, m^3 s^{-1}), emitter spacing (d_{sp}, m), total length of the drip lines (w, m) and, if subsurface, the dripper depth (d_{sp}, m) are provided.

Model description

Water Retention Parameter Estimation

Accurate soil water retention parameters are critical for determining available water capacity and for driving the soil-water balance. To guarantee flexibility in its use, ACQUAOUNT-Farm either allows the user to define the WRPs directly or estimates them from a set of pedotransfer functions (PTFs), based on four independently developed methods (Table 3). Each PTF predicts θ_{sat}, θ_{fc}, and θ_{wp} based on soil texture (sand, silt, clay fractions), bulk density, and organic matter content. The ensemble mean of the four methods is computed for each retention parameter. If the deviation between the user-provided retention parameter and the ensemble mean exceeds 10% of the user value, the model adopts the user's values to ensure consistency.

Table 3: List of selected pedotransfer functions (PTFs) for the estimation of the Water Retention Parameters (WRPs) in ACQUAOUNT-Farm.

PTF tested	**Model type**	**Reference**
*RAW*ls et al.	Group Method Data Handling/continuous	(Rawls et al., 2003)
Zacharias & Wessolek	Regression/continuous	(Zacharias & Wessolek, 2007)
ROSETTA	Artificial neural network/continuous	(Schaap et al., 2001)
EUPTF, version 2	Machine learning/continuous	(Szabó et al., 2021)

Calibration of soil moisture for data harmonization

Divergent calibrations among *SM* sensors and retention parameter estimates can introduce bias into the water balance. To harmonize *SM* readings with the calibrated retention parameters, the model applies a linear correction:

$$SM_{calib} = m \cdot SM_{raw} + q \qquad (1)$$

where *m* and *q* are the slope and intercept of the linear calibration equation. The slope *m* is determined as the ratio between (i) the difference of the estimated field-capacity and wilting-point thresholds derived from PTFs and (ii) the difference between the corresponding values estimated from the sensor SM pattern.

$$m = \frac{\theta_{fc} - \theta_{wp}}{\theta_{fc,sensor} - \theta_{wp,sensor}} \qquad (2)$$

This transformation aligns the dynamic sensor range with the estimated thresholds, ensuring that subsequent root-zone depletion and stress calculations use a consistent moisture scale between modelled and measured values.

Reference Evapotranspiration Estimation

Hourly reference evapotranspiration (*ET0*, mm h^{-1}) is computed using the FAO Penman–Monteith equation (R. G. Allen et al., 1998b) adapted for hourly time steps:

$$ET0 = \frac{0.408\varDelta(Rn - G) + \gamma \frac{37}{T + 273} u_2 (es - ea)}{\varDelta + \gamma(1 + 0.34u_2)} \tag{3}$$

where *Rn* is the net radiation at the crop surface (MJ m^{-2} day^{-1}); *G* is the soil-heat flux density (MJ m^{-2} day^{-1}); γ is the psychrometric constant (kPa °C^{-1}); *T* is the mean hourly air temperature at 2 m (°C); u_2 is the wind speed at 2 m height (m s^{-1}); *es* and *ea* are the saturation and actual vapor pressures (kPa); and $\varDelta$ is the slope of the vapor-pressure curve (kPa °C^{-1}).

Soil Water Balance Model

The model adopts a multi-layer approach, subdividing the soil profile into layers corresponding to the depth and spacing of the *SM* probes. At each hour, the soil water balance is computed independently for each layer as a bucket, whose water content changes according to effective inputs and outputs:

$$\varDelta SM * d_i = F_{in,i} - ETa_i - F_{out,i} \tag{4}$$

where $\varDelta SM$ is the change in water content of layer *i* multiplied by its thickness *d* (mm); ET_a (mm) is the actual evapotranspiration extracted from layer *i*; $F_{in,i}$ is the water input to layer *i*, equal to the sum of effective precipitation (P_{eff}, mm) and irrigation (*Irr*, mm) for the topmost layer, and equal to the drainage flux from the overlying layer for all deeper layers, and $F_{out,i}$ is the downward drainage flux leaving layer *i*, governed by the saturated hydraulic conductivity *Ks*.

First, the irrigated area (A_{irr}), i.e., the area of the field that is wetted by the irrigation system, is computed as a fraction of the crop area (A_{crop}). For drip and subsurface systems, the model distinguishes between crop types: for tree crops, A_{irr} is assumed to be 30% of the crop area, whereas for annual crops A_{irr} corresponds to 90% of the field. For sprinkler-irrigated crops, A_{irr} is equal to A_{crop}, reflecting the uniform water distribution of sprinklers. Treating A_{irr} as equal to 90% of A_{crop} for annual crops can be an overestimation, since drip irrigation is designed to optimize water application to the root zone only. However, the model prefers to overestimate demand slightly rather than underestimate it to ensure that farmers avoid water stress.

Daily rooting depth (Z_r, m) is computed according to the FAO 56 method (R. G. Allen et al., 1998b), assuming proportional growth to the increase of the crop coefficient.

Because root density decreases with depth, water uptake is not uniform across the soil profile. A function describing root distribution must be defined to allocate *ETa* across layers. The model adopts the logistic function of Fan et al. (2016) to estimate the cumulative root density distribution:

$$Y_d = \frac{1}{1+\left(\frac{d}{0.15}\right)^{-1.117}} + \frac{\left(1+\left(\frac{Z_r}{0.15}\right)^{-1.117}\right)*d}{Z_r} \tag{5}$$

where Y_d(%) is the cumulated root density at depth d and Z_r is the daily root depth. Average coefficients (a=0.15 and b= -1.117) given in the study of Fan et al. (2016) are used for all crops, assuming a consistent root distribution pattern across species.

The model then computes the effective precipitation P_{eff} (mm), that is the amount of water that effectively infiltrates within the soil during a precipitation event. If the precipitation is very low (<20% of *ET0*), P_{eff} will be considered equal to zero, assuming that the input evaporates before entering the soil. If precipitation is very intense and infiltration exceeds saturation, the excess is treated as ponding water which remains on the surface. This ponded water is subjected to evaporation, while the remaining share infiltrates during the next step.

The model estimates the crop-specific coefficient k_c using the dual crop coefficient method of FAO 56. The crop coefficient is expressed as:

$$k_c = k_{cb} + k_e \tag{6}$$

where k_{cb} is the basal crop coefficient and k_e is the evaporation component of the shallow soil layer.

The evaporation component k_e is estimated by applying a soil water balance over the first layer of the soil profile (10–15 cm depth, depending on probe spacing) (R. G. Allen et al., 1998b).

Then, the model estimates the Total Available Water (*TAW*, mm) and the Readily Available Water (*RAW*, mm), that is the total water stored in the soil that can be extracted by the plant and the water that can be extracted before water stress develops, respectively. These variables are expressed as:

$$TAW = \left(\theta_{fc} - \theta_{wp}\right) * Z_r * 1000 \tag{7}$$

$$RAW = TAW * DF_{adj} \tag{8}$$

Where DF_{adj} is the adjusted depletion factor according to daily climate conditions. This adjustment dynamically reduces the tabulated depletion factor (from FAO) to increase irrigation frequency during particularly warm periods ($ET_0 > 4$ mm day^{-1}):

$$DF_{adj} = DF_{tab} + 0.1 * (4 - ET0) \tag{9}$$

The model estimates the root zone depletion (*Dr*, mm), that is the water deficit within the *TAW*. This parameter is used to assess the water stress coefficient k_s (-), which equals 1 when soil water content is greater than *RAW* and decreases linearly between *RAW* and *TAW*.

Using these variables, the model calculates adjusted, crop-specific evapotranspiration *ETc* and actual evapotranspiration *ETa* (mm):

$$ETc = ET0 * kc \tag{10}$$

$$ETa = ET0 * (kcb * ks + ke) \tag{11}$$

The irrigation requirements correspond to the root zone depletion (*Dr)*. *Dr* is converted into volume (V_{irr} ,m³), by multiplying it by the irrigated area (A_{irr}), and the irrigation deficit volume ($V_{irr,deficit}$,m3) is estimated using the irrigation deficit coefficient. This coefficient may vary during the growing season to modulate water stress according to phenological stages; these coefficients are provided in the crop table file.

As a final step, the model schedules irrigation dates according to the three irrigation scenarios mentioned in the introduction ("Early", "Late", "Limit"), based on root-zone depletion thresholds:

$$\begin{gathered}\text{Early: Dr} = \text{IT}_{\text{early}} * \text{RAW} \\ \text{Late: Dr} = \text{IT}_{\text{late}} * \text{RAW} \\ \text{Limit: Dr} = \text{IT}_{\text{limit}} * \text{RAW}\end{gathered} \tag{12}$$

IT coefficients are reported in the crop table file, they can vary according to the crop and its capacity to sustain water stress.

ACQUAOUNT-Farm outputs

The final output consists of three data frames:

- *Hourly_irr_final.csv*: containing hourly irrigation demand for full and deficit irrigation and soil-moisture evolution over the two-week period;
- *Daily_irr_final.csv*: with results aggregated to daily scale;
- *Irrigation_dates.csv*: a table listing the dates of Early, Late and Limit irrigation thresholds and providing irrigation recommendations for the current day (no irrigation, early, late or limit).

Validation of model performance

To validate its performance, the irrigation model has been tested in four farms located in Medenine in South of Tunisia (33°21′N 10°30′E), identified by the initials of their owners: AM, JD (citrus fields), SG, NR (potato fields) (Table 6, Supplementary material). The region is classified as an arid environment, with annual precipitation around 120 mm concentrated mainly in winter and nearly absent from June to August (Figure 6). Monthly mean temperatures range between 10-20°C in winter, and 25-35°C in summer, and temperatures exceeding 45°C are common during heat waves (Copernicus Climate Change Service, 2025).

Soil is sandy, poor in organic matter and has very low water retention (Table 6, Supplementary material). The model's performance was assessed to handle both annual (potato) and perennial (citrus) crops.

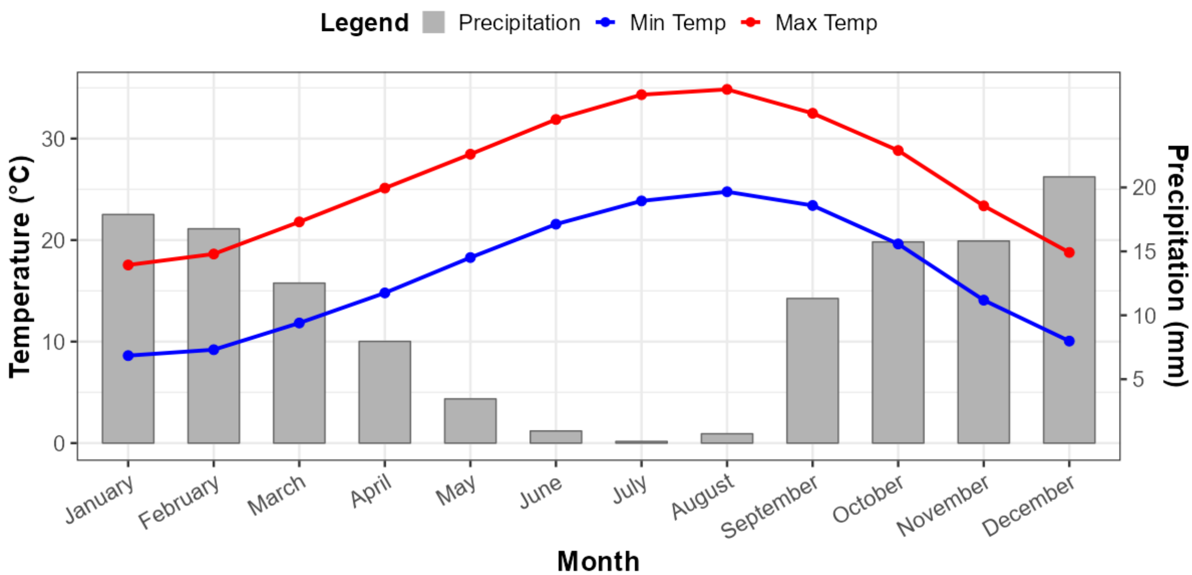

Figure 6: average monthly minimum, maximum temperature and precipitation in Medenine (South Tunisia). Data are the mean of the climatological period 1991-2020, taken from ERA5 reanalysis.

Sensors' setup

Every farm is equipped with a soil moisture sensor recording soil moisture at depths of 15, 30 and 45 cm. Irrigation water flow was measured with a water meter installed in the irrigation system. Meteorological variables, including temperature, wind speed, relative humidity, solar radiation and precipitation, were recorded at sub-hourly intervals by a single weather station installed at the NR farm. Because the farms are within 5 km of one another (Figure 12, Supplementary material), this station was considered representative for all farms. Sensors were installed in the fields and started recording from May 2024. For this reason, the simulation covered the period from May 2024 to September 2025. This period encompasses the complete growth cycles of potato (autumn 2024 and spring 2025) and most of the citrus seasons (May–December 2024 and March–September 2025).

Field data collection

Meteorological variables are used to estimate the daily reference evapotranspiration *ET0*, which is displayed in Figure 7, for the years 2024 and 2025. *ET0* ranges between 1 to 3 mm day^{-1} during the winter months, while in summer it is around 5-6 mm/day.

SM records of the four farms are reported in Figure 8 and Figure 9, for the two seasons and three depths. The plot also displays the range of *SM* available to the plant defined by the interval between field capacity and wilting point (shown in orange) and the component that translates into percolation, corresponding to the range between field capacity and saturation (shown in blue). It can be observed that the $\theta_{fc} - \theta_{wp}$ range is quite narrow for most farms, particularly for the JD and SG farms, which have sandier soils. This explains the very frequent irrigation events applied during the growing seasons, identifiable by the regular peaks in *SM*. The shallow layer (15 cm depth) shows the highest *SM* peaks, as it is the first layer to receive water during irrigation, which is then transferred to the two deeper layers. At the AM farm, *SM* frequently exceeds θ_{fc} in the deepest layer (45 cm depth), indicating that during these irrigation events part of the applied water is lost through deep percolation.

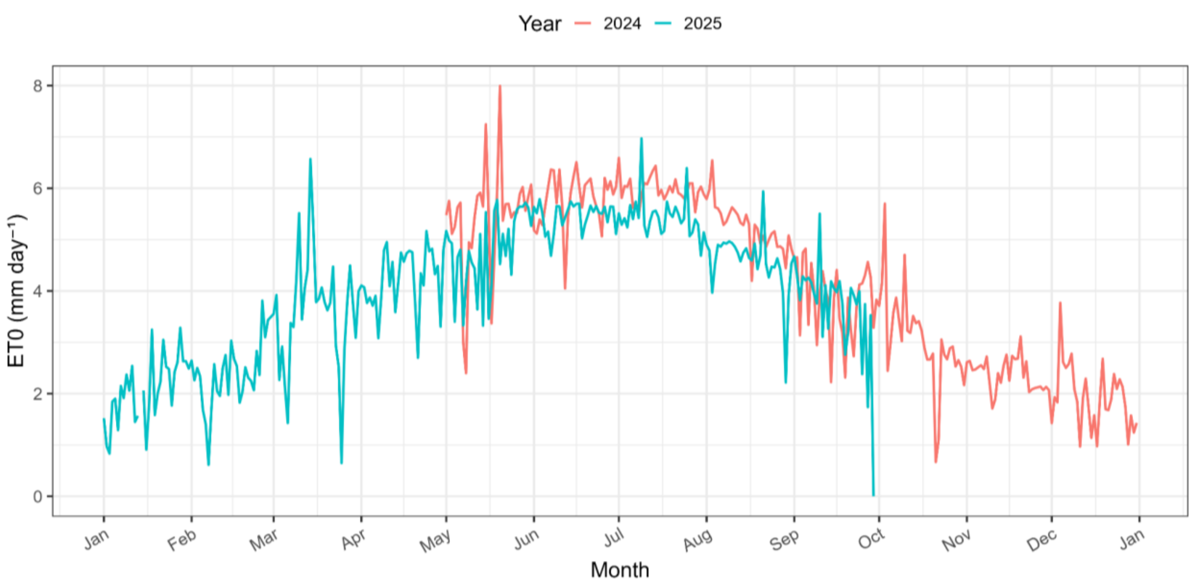

Figure 7*: Daily reference evapotranspiration (ET0) of the Tunisian pilot, calculated with the FAO Penman-Monteith equation, using the meteorological variables of the weather station installed in NR farm.*

Figure 8: Soil moisture (SM) records from sensors installed in citrus orchards (AM and JD farms) from May 2024 to September 2025, measured at depths of 15, 30, and 45 cm. The blue area represents the range between saturation and field capacity, while the orange area indicates the range from field capacity to the wilting point. Below the SM plots, the hourly precipitation recorded by the weather station at the NR farm is shown.

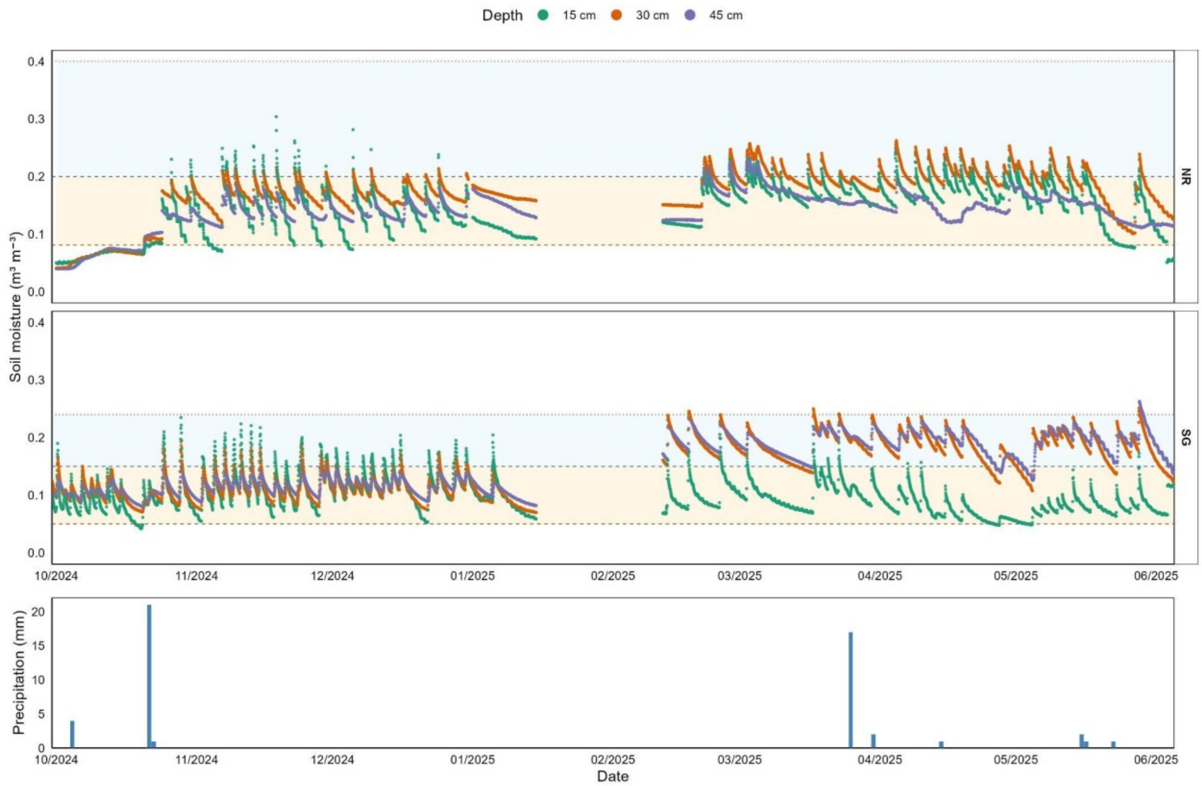

Figure 9: Soil moisture (SM) records from sensors installed in potato fields (NR and SG farms) from October 2024 to June 2025, measured at depths of 15, 30, and 45 cm. The blue area represents the range between saturation and field capacity, while the orange area indicates the range from field capacity to the wilting point. Below the SM plots, the hourly precipitation recorded by the weather station at the NR farm is shown.

Accuracy metrics

Differences between simulated soil moisture ($\hat{y}_i$) and sensor-based observations (y_i) were evaluated using a set of complementary statistical metrics, capturing both absolute and relative model performance. These include the mean bias error (*MBE*, %) the mean absolute difference (*MAD*, m^3 m^{-3}), mean absolute relative difference (*MRD*, %), root mean square error (*RMSE*, m^3 m^{-3}), and coefficient of determination (R^2):

$$MBE = \frac{1}{N}\sum_{i=1}^{N}\frac{\hat{y}_i - y_i}{y_i} \tag{13}$$

$$MAD = \frac{1}{N}\sum_{i=1}^{N}|\hat{y}_i - y_i| \tag{14}$$

$$MRD = \frac{1}{N}\sum_{i=1}^{N}\frac{|\hat{y}_i - y_i|}{y_i} \tag{15}$$

$$\text{RMSE}=\sqrt{\frac{1}{N}\sum_{i=1}^{N}(\hat{y}_i - y_i)^2} \tag{16}$$

$$R^2 = 1 - \frac{\sum_{i=1}^{N}(\hat{y}_i - y_i)^2}{\sum_{i=1}^{N}(y_i - \bar{y})^2} \tag{17}$$

where *N* is the number of paired samples and $\bar{y}$ is the mean of observations. *MAD* provides a measure of the average magnitude of difference, regardless of their direction, while *RMSE* gives greater weight to larger deviations, thus highlighting the presence of significant mismatches between simulations and observations. *MBE* indicates the tendency of the model to systematically overestimate or underestimate soil moisture. *MRD* expresses error relative to observed values, allowing comparison across different soil moisture ranges. Finally, R^2 quantifies the proportion of variance in observed soil moisture explained by the model.

Results and discussion

Model performance in reproducing soil moisture dynamics

To assess the capability of ACQUAOUNT-Farm to estimate crop irrigation demand, we evaluate its performance to reproduce *SM* dynamics. Figure 10 compares observed and simulated *SM* at the end of irrigation events across four farms during the observation period, focusing on the model's ability to capture post-irrigation *SM* decline over increasing forecast horizons. The model demonstrated good overall performance in reproducing soil moisture dynamics, with $R^2 \approx 0.65$, $RMSE \approx 0.022$ m³ m⁻³, and $MAD \approx 0.016$ m³ m⁻³. These values are consistent with those reported by comparable physically based modeling frameworks applied in soil moisture estimation. For instance, Wenzel et al. (2026) obtained $RMSE = 0.020$

$m^3\ m^{-3}$, *MAD* = 0.017 $m^3\ m^{-3}$, and $R^2 = 0.676$ using spatially distributed HYDRUS-1D simulations across a 1600 ha farm in Germany. Yu et al. (2022), reported *RMSE* values of approximately 0.054-0.066 $m^3\ m^{-3}$ across different parameterization approaches.

However, accuracy varies by site: performance is stronger in AM and NR ($R^2 > 0.7$) and weaker in JD and SG ($R^2 = 0.44$ and 0.59, respectively). Model accuracy consistently decreases with forecast length, as shown by the progressive deviation from the 1:1 line. This temporal degradation is confirmed in Table 4, which shows the model performance metrics for SM prediction after irrigation events. *MBE* values indicate that the model tends to systematically underestimate *SM* in AM, while overestimation is observed in the remaining farms. The magnitude of the deviations, quantified through *MRD* and *MAD*, reveals that JD is the farm with the largest discrepancies, with *MRD* increasing from 8% at day 1 to 52% at day 4 and *MAD* exceeding the declared sensor accuracy (±0.03 $m^3\ m^{-3}$, Delta OHM HD3910.1) from day 3 onwards. In contrast, AM, SG, and NR show *MRD* below 15% across all four prediction days, with *MAD* remaining within the sensor accuracy threshold throughout.

Considering sensor measurement's uncertainty as a threshold of acceptable *SM* prediction, model estimates can be considered reliable up to four days after irrigation in AM, SG, and NR, and up to two days in JD. It is worth noting that, from a practical perspective, reliable *SM* predictions for 2–4 days post irrigation are sufficient to capture the soil water dynamics that determine irrigation timing (R. G. Allen et al., 1998b; Pereira et al., 2020), allowing farmers to assess whether the next irrigation event is imminent or can be delayed. The difficulty in reproducing *SM* dynamics at the JD farm is also visible in Figure 8, where rapid *SM* fluctuations can drive the soil from near saturation to wilting point within just a few days. This behavior is attributable to the very sandy soil texture (Table 6, Supplementary material), which generates high drainage rates due to its poor water holding capacity (Z. Li et al., 2019; Zotarelli et al., 2010), making the estimation challenging for a soil water balance model.

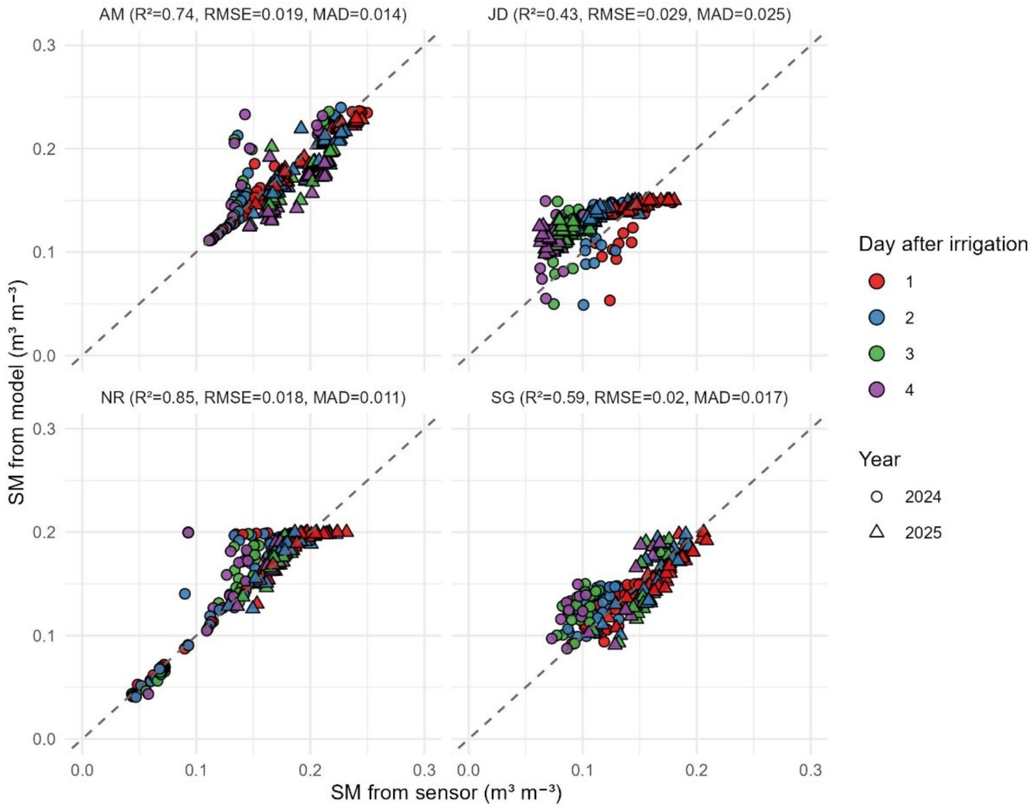

Figure 10: Comparison between predicted versus recorded soil moisture values at the end of the irrigation events applied in seasons 2024 and 2025, for the four farms under the study (AM, JD with citrus and SG and NR with potato). Values are compared from one to four days after the day of the simulations.

Table 4*: Model performance metrics for soil moisture (SM) prediction after irrigation events, for four farms (AM and JD with citrus; SG and NR with potato), seasons 2024 and 2025. Metrics are computed for each of the four days following the day after the irrigation event. Sample size reflects the number of irrigation events with a post-irrigation interval of at least the corresponding number of days. The mean bias error (MBE, %) indicates the direction of the systematic deviation between predicted and recorded SM. The mean absolute relative difference (MRD, %) and mean absolute difference (MAD, $m^3\ m^{-3}$) quantify the magnitude of the prediction error. The root mean square error (RMSE, $m^3\ m^{-3}$) penalizes larger deviations. The last column indicates whether the MAD falls within the declared measurement accuracy of the soil moisture sensors used (Delta OHM HD3910.1, ±0.03 $m^3\ m^{-3}$), which represents the minimum meaningful threshold*

for model–sensor discrepancy. Values in bold indicate days for which MAD exceeds the sensor accuracy threshold.

Farm	Day of prediction	Sample size	MBE (%)	MRD (%)	MAD (m^3 m^{-3})	RMSE (m^3 m^{-3})	Within sensor acc. (±0.03 m^3 m^{-3})
AM	1	70	-1.75	3.47	0.01	0.01	YES
AM	2	70	-0.29	5.59	0.01	0.01	YES
AM	3	69	-3.25	10.06	0.02	0.02	YES
AM	4	68	-4.81	12.81	0.02	0.03	YES
JD	1	68	-5.84	8.05	0.01	0.02	YES
JD	2	68	15.15	18.78	0.02	0.02	YES
JD	3	59	37.16	38.57	0.03	0.03	**NO**
JD	4	52	51.28	52.09	0.04	0.04	**NO**
NR	1	97	1.26	4.35	0.01	0.01	YES
NR	2	96	4.20	7.25	0.01	0.02	YES
NR	3	53	7.85	11.17	0.01	0.02	YES
NR	4	31	10.50	13.98	0.02	0.03	YES
SG	1	77	-2.92	6.87	0.01	0.01	YES
SG	2	73	5.84	13.29	0.02	0.02	YES
SG	3	47	12.79	20.94	0.02	0.03	YES
SG	4	29	14.02	22.98	0.03	0.03	YES

Compare model’s and farmer’s irrigation

In this section, the farmer's irrigation strategy is compared with the model’s recommendation for the same season. Specifically, the amount and frequency of irrigations applied by the farmer are compared with the irrigation the model would have recommended when the “Early” threshold (optimal irrigation) was reached, applying full irrigation requirements. The same comparison is considered for the “Late” threshold (mild water stress) as well, which applies deficit irrigation. This approach allows us to assess whether ACQUAOUNT-Farm enables potential water savings compared to traditional irrigation practices and to quantify these potential savings according to the followed approach.

Figure 11 and Table 5 present the comparison between the irrigation applied by farmers in the study period 2024-2025 and the irrigation recommended by the model according to crop water needs.

Potato fields

The largest potential savings are observed in the SG and NR autumn potato farms: 80–84% (“Early” threshold) and 83–88% (“Late”) in 2024 (*Table 5*). In the spring season 2025, potential savings become more moderate (SG: 17% “Early”, 32% “Late”; NR: 33% “Early”, 39% “Late”). This contrast between the autumn and spring seasons reflects the tendency to over-irrigate when actual crop water demand is low: autumn rainfall and reduced evapotranspiration rates reduce soil water extraction, yet farmers continue to irrigate at the same intensity as in the drier spring season, likely due to lack of real-time crop water information. For autumn potato in Médenine, ETc under full irrigation conditions ranges from ~2500 to 3500 m^3/ha (El Mokh et al., 2024), while for spring potato in semi-arid Mediterranean conditions, seasonal ETc is approximately ~5900–6200 m^3/ha (Karam et al., 2014). Comparing these values against the farmer irrigation volumes recorded at NR and SG (7407 and 9830 m^3 ha^{-1}, respectively), farmers over-irrigated by a factor of 2.5–3.3×, supporting the potential savings proposed by ACQUAOUNT-Farm. In the spring season, the same farms applied 7485–8310 m^3 ha^{-1} against the reference demand of 5900–6200 m^3 ha^{-1}, yielding over-irrigation ratios of 1.3–1.5×. In this case, ACQUAOUNT-Farm recommends 5580-6200 m^3 ha^{-1} under the “Early” approach, in line with the Etc reported by (Karam et al., 2014) and ~4200 m^3 ha^{-1} under “Late” approaches, considering a moderate water stress. Regarding the frequency of irrigation events during the autumn season, the model prescribes far fewer applications than farmer (<10 vs. 50–53 by the farmer), while larger per-event volumes (~179–216 vs. ~148–185 m^3 ha^{-1}). During the spring season, the model-farmer’s differences reduce (frequency: ~25-34 vs. 40-48; volume: ~180-220 vs. 170-190, model vs farmer, respectively). Comparing the “Early” and “Late” irrigations, the “Early” strategy consistently prescribes more frequent events with greater average per-event volumes.

Citrus orchards

For AM farm, consistent potential savings are observed in both seasons (~63–65% “Early” and ~68–70% “Late”). AM farm represents a case of systematic over irrigation: the farmer applied between 28000 and 31000 m^3 ha^{-1} per season, while reference *ETc* ranges between 7000 and 13000 m^3 ha^{-1} in southern Tunisia (El Mokh et al., 2021; El-Otmani et al., 2020; Nagaz et al., 2020). This means that AM is applying about 3 times the estimated crop water requirement.

In contrast, JD farm applied 7100-9000 m^3/ha, closely matching the reference *ETc* range and suggesting that the farm was already irrigating at deficit irrigation regime. In this context, any additional model-prescribed irrigation to meet the “Early” threshold constitutes a marginal top-up rather than a correction of gross over-irrigation, which explains the negative savings observed at this farm. However, under the "Late" approach, recommendations closely align with actual farmer's practices: 7120-9060 m³ ha⁻¹ (farmer) vs. 6670-7430 m³ ha⁻¹ (model). The different irrigation strategy between AM and JD comes from the size of their fields and their water availability. In Southern Tunisian farms, farmers with larger irrigated areas often face greater pressure on available water and are more likely to distribute water across plots, resulting in deficit irrigation practices (Toumi et al., 2022; Yacoubi et al., 2022).

Regarding frequency and event volumes, in AM, the model recommends fewer applications than the farmer (34–41 under "Early" vs. 55–56), with per-event volumes approximately halved (~266–303 vs. ~504–560 m³ ha⁻¹). Conversely, in JD the model recommends more applications than the farmer in 2024 (57 "Early" vs. 48), with per-event volumes also larger (206–236 vs. 148–162 m³ ha⁻¹), consistent with the higher total volumes prescribed. In 2025, JD application frequency is similar between model and farmer (45 vs. 56). The difference between "Early" and "Late" approaches is the same as for the potato crops.

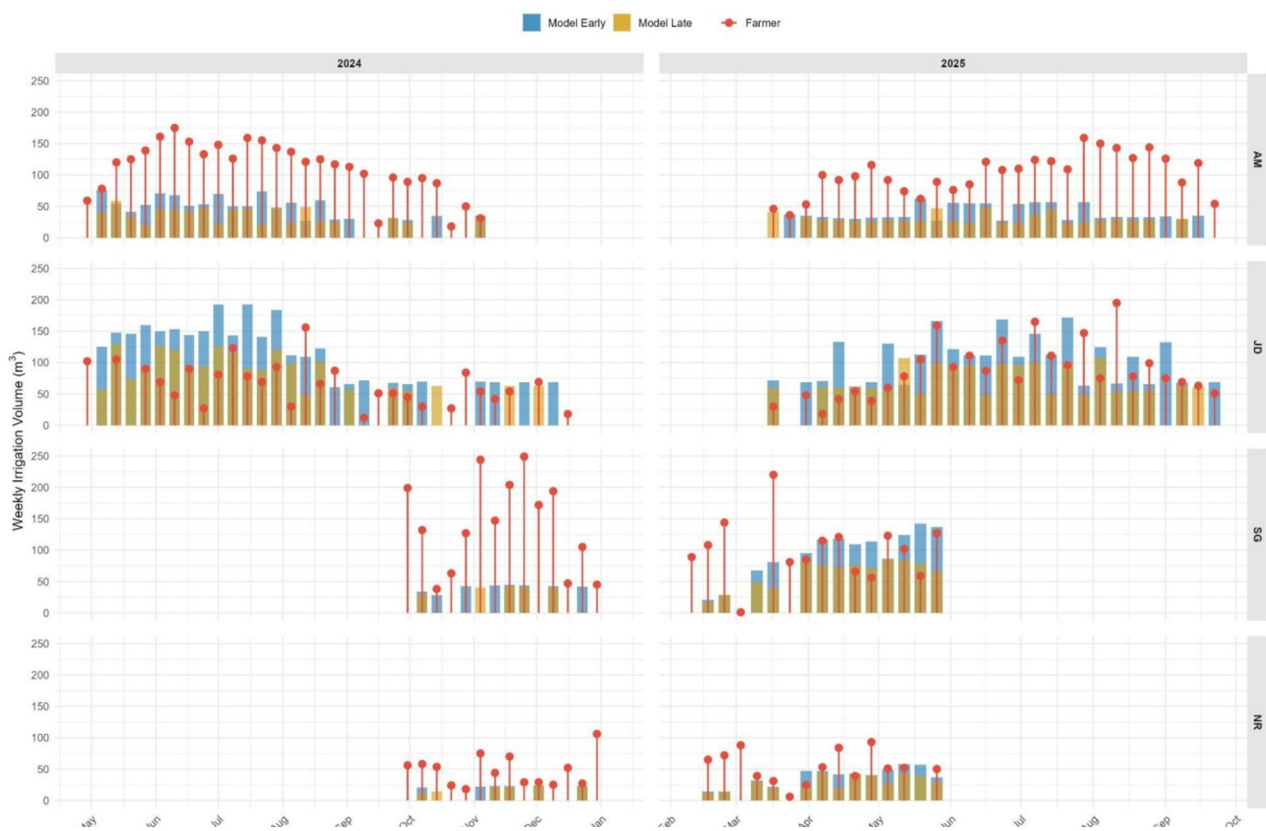

Figure 11: Comparison between the irrigation water (m3) applied by the farmer and the one suggested by the ACQUAOUNT-Farm model following the "Early" (optimal irrigation) and "Late" (mild water stress) thresholds for the four farms, seasons 2024 and 2025.

Table 5: Comparison of the aggregated irrigation water applied by the farmer versus what recommended by the ACQUAOUNT-Farm model following the "Early" (optimal irrigation) and "Late" (mild water stress) thresholds for the four farms, seasons 2024 and 2025.

Farm	**AM**		**JD**		**NR**		**SG**	
	2024	**2025**	**2024**	**2025**	**2024**	**2025**	**2024**	**2025**
Irrigated area (ha)	0.1	0.1	0.26	0.26	0.09	0.09	0.2	0.2
Total irrigation Farmer (m^3 ha^{-1})	30780	28230	7119	9058	7407	8310	9830	7485
Total irrigation Model Early vs. (Late) (m^3 ha^{-1})	10913 (7224)	10306 (7280)	11720 (7433)	10380 (6669)	1510 (1254)	5584 (4226)	1614 (967)	6201 (4114)
Water savings Early vs. (Late) (%)	65% (77%)	63% (74%)	-65% (-4%)	-15% (26%)	80% (83%)	33% (49%)	84% (90%)	17% (45%)
Frequency of applications Farmer (days)	55	56	48	56	50	48	53	40
Frequency of applications Model vs. Early (Late) (days)	41 (31)	34 (28)	57 (42)	45 (33)	7 (6)	25 (20)	9 (6)	34 (23)
Average irrigation event Farmer (m^3 ha^{-1})	560	504	148	162	148	173	185	187
Average irrigation event Model vs. Early (Late) (m^3 ha^{-1})	266 (233)	303 (260)	206 (177)	231 (202)	216 (209)	223 (211)	179 (161)	182 (179)

Limitations and future perspectives

Because this study was conducted under uncontrolled, real-world farm conditions, it was not possible to implement a simultaneous comparison between the farmer's and the model's approaches; consequently, the estimated water savings remain potential rather than empirically realized. A critical next step will involve testing ACQUAOUNT-Farm in plots where irrigation is fully based on model recommendations. Results would be compared with plots managed according to farmer practices, to better compare results in terms of yield and water productivity. This prospective design would also allow a dynamic k_c correction to be formally assessed. This would maintain the mechanistic interpretability of the physically based framework while allowing IoT observations to dynamically correct model parameters, connecting theoretical estimates with observed field behavior.

Additionally, the quality of *SM* monitoring is a critical factor: in the context of small holder farms operating with limited budgets, access to high-accuracy sensor equipment may be restricted, while low-cost alternatives may affect the precision of soil water content measurements (Sharma et al., 2025). These constraints are recognized and have informed the design of ACQUAOUNT-Farm. This constitutes a deliberate trade-off between scientific rigor and operational simplicity, in line with similar decision-support tools developed for smallholder irrigation management (Nigussie et al., 2020; Saputri et al., 2025; Todorovic et al., 2016). Providing farmers in water-scarce regions with a user-friendly, real-time estimate of crop water demand, grounded in the FAO-56 soil water balance framework (R. G. Allen et al., 1998b), can meaningfully improve their irrigation decisions, reduce unnecessary groundwater depletion, and build awareness of the actual water needs of their crops without requiring advanced agronomic expertise.

Conclusion

This study presented ACQUAOUNT-Farm, a platform integrating IoT with a physical based model, providing real-time irrigation scheduling for multiple crops under water-scarce conditions, built around farmer-accessible inputs and a user-friendly interface. ACQUAOUNT-Farm performance was evaluated across four farms in southern Tunisia over two consecutive growing seasons (2024–2025), analyzing two full potato cycles and two active periods for citrus.

The model reliably reproduced short-term post-irrigation *SM* dynamics in three of the four farms ($R^2 \approx 0.65$, RMSE ≈ 0.022 m³ m⁻³, and MAD ≈ 0.016 m³ m⁻³), with prediction errors within sensor accuracy (0.03 m^3 m^{-3}) for up to four days in AM, NR and SG farms, and up to two days in the JD farm. Comparison of observed and model-recommended irrigation volumes highlighted substantial water-saving potential: approximately 63–65% for the over-irrigated AM citrus farm, and 80–84% for autumn potato (SG and NR farms), where farmers consistently applied water in excess of seasonal crop demand. For spring potato, potential savings ranged from 17 to 33%. In JD citrus farm, where the farmer already practices deficit irrigation, model-recommended volumes exceeded observed applications, reinforcing the suitability of the "Late" threshold for this specific management context.

Data availability statement

The ACQUAOUNT-Farm platform is publicly accessible at https://farm.acquaount.development.abidevops.website/login upon free registration and creation of a personal profile. A trial version of the irrigation model script is available on GitHub at https://github.com/andrea261097/ACQUAOUNT-Farm/tree/main.

CRediT authorship contribution statement

Andrea Borgo: Conceptualization, Methodology, Software, Validation, Formal analysis, Investigation, Writing-Original Draft, Visualization. **Fathia Elmokh**: Validation, Data Curation, Writing – Review & Editing. **Kameleddine Nagaz**: Validation, Resources, Writing – Review & Editing, Project administration. **Simone Mereu**: Conceptualization, Writing - Review & Editing, Project administration, Funding acquisition. **Guido Rianna**: Conceptualization, Project administration. **Gennaro Sequino**: Data Curation, Writing - Review & Editing. **Francesco Martini**: Software, Validation, Data Curation. **Josep Pijuan Parra**: Software, Validation, Data Curation. **Mauro Lo Cascio**: Resources, Writing - Review & Editing. **Serena Marras**: Project administration, Funding acquisition. **Antonio Trabucco**: Writing - Review & Editing, Supervision. **Marta Debolini**: Methodology, Writing - Review & Editing, Supervision, Project administration, Funding acquisition.

Acknowledgments

This work was supported by the ACQUAOUNT project funded under the Grant Agreement number: [2021] [ACQUAOUNT] [Call 2020 Section Water IA**]** of the PRIMA program. The work was developed within the Ph.D program in Agrometeorology and Ecophysiology of Agricultural and Forestry Ecosystems at the University of Sassari in collaboration with the CMCC Foundation and the Institut des Régions Arides (IRA).

Declaration of competing interests

The authors declare that they have no known competing financial interests or personal relationships that could have appeared to influence the work reported in this paper.

References

Ali, A., Hussain, T., & Zahid, A. (2025). Smart Irrigation Technologies and Prospects for Enhancing Water Use Efficiency for Sustainable Agriculture. AgriEngineering, 7(4), 106. https://doi.org/10.3390/agriengineering7040106

Allen, R. G., Pereira, L. S., Raes, D., & Smith, M. (1998). FAO Irrigation and Drainage Paper No. 56—Crop Evapotranspiration (Fascicolo 56). FAO - Food and Agriculture Organization of the United Nations.

Bellvert, J., Pelechá, A., Pamies-Sans, M., Virgili, J., Torres, M., & Casadesús, J. (2023). Assimilation of Sentinel-2 Biophysical Variables into a Digital Twin for the Automated Irrigation Scheduling of a Vineyard. Water, 15(14), 2506. https://doi.org/10.3390/w15142506

Copernicus Climate Change Service (C3S). (2025). Interactive Climate Atlas (Versione 2.0) [Dataset]. https://climate-atlas.copernicus.eu/

Cramer, W., Guiot, J., Fader, M., Garrabou, J., Gattuso, J. P., Iglesias, A., Lange, M. A., Lionello, P., Llasat, M. C., Paz, S., Peñuelas, J., Snoussi, M., Toreti, A., Tsimplis, M. N., & Xoplaki, E. (2018). Climate change and interconnected risks to sustainable development in the Mediterranean. Nature Climate Change, 8(11), 972–980. https://doi.org/10.1038/s41558-018-0299-2

Delta OHM. (2021). HD3910.1 – HD3910.2 Probes for soil volumetric water content measurement. https://environmental.senseca.com/wp-content/uploads/document/DeltaOHM_HD3910_datasheet_ENG.pdf

El Mokh, F., Nagaz, K., & Masmoudi, M. M. (2024). Long-term potato response to different irrigation scheduling methods using saline water in an arid environment. Frontiers in Agronomy, 6, 1426034. https://doi.org/10.3389/fagro.2024.1426034

El Mokh, F., Nagaz, K., Masmoudi, M. M., Ben Mechlia, N., & Ghiglieri, G. (2021). Deficit Irrigation Using Saline Water of Fruit Trees under Water Scarcity Conditions of Southern Tunisia. Atmosphere, 12(7), 864. https://doi.org/10.3390/atmos12070864

El-Otmani, M., Chouaibi, A., Azrof, C., Bouchaou, L., & Choukr-Allah, R. (2020). Response of Clementine Mandarin to Water-Saving Strategies under Water Scarcity Conditions. Water, 12(9), 2439. https://doi.org/10.3390/w12092439

Fan, J., McConkey, B., Wang, H., & Janzen, H. (2016). Root distribution by depth for temperate agricultural crops. Field Crops Research, 189, 68–74. https://doi.org/10.1016/j.fcr.2016.02.013

FAO. (2017). Water for Sustainable Food and Agriculture. www.fao.org/publications

Fernandes De Oliveira, A., Mameli, M. G., Lo Cascio, M., Sirca, C., & Satta, D. (2021). An Index for User-Friendly Proximal Detection of Water Requirements to Optimized Irrigation Management in Vineyards. Agronomy, 11(2), 323. https://doi.org/10.3390/agronomy11020323

Ferragina, E., & Canitano, G. (2014). Water and Food Security in the Arab Countries: National and Regional Implications. Global Environment, 7(2), 326–351. https://doi.org/10.3197/ge.2014.070204

Granados-Olivas, A., Bravo-Peña, L. C., Salas-Aguilar, V. M., Brown, C., Gandara-Ruiz, A., Esquivel-Ceballos, V. H., Vázquez-Gálvez, F. A., Heerema, R., Heyman, J. M., Aguilar-Benitez, I., Fernald, A., Rincón-Zuloaga, J. M., Hargrove, W. L., & Alatorre-Cejudo, L. C. (2026). Smart Farming Technologies for Groundwater Conservation in Transboundary Aquifers of Northwestern México. Water, 18(6), 755. https://doi.org/10.3390/w18060755

Hendrickx, M. G. A., Vanderborght, J., Janssens, P., Laloy, E., Bombeke, S., Matthyssen, E., Waverijn, A., & Diels, J. (2026). Field-Scale Soil Moisture Predictions in Real Time Using In Situ Sensor Measurements in an Inverse Modeling Framework: SWIM2. Water Resources Research, 62(2), e2025WR041324. https://doi.org/10.1029/2025WR041324

IPCC. (2023). IPCC, 2023: Summary for Policymakers. In: Climate Change 2023: Synthesis Report. Contribution of Working Groups I, II and III to the Sixth Assessment Report of the Intergovernmental Panel on Climate Change. https://www.unep.org/resources/report/climate-change-2023-synthesis-report

Karam, F., Amacha, N., Fahed, S., El Asmar, T., & Domínguez, A. (2014). Response of potato to full and deficit irrigation under semiarid climate: Agronomic and economic implications. Agricultural Water Management, 142, 144–151. https://doi.org/10.1016/j.agwat.2014.05.007

Li, Z., Liu, H., Zhao, W., Yang, Q., Yang, R., & Liu, J. (2019). Quantification of soil water balance components based on continuous soil moisture measurement and the Richards equation in an irrigated agricultural field of a desert oasis. Hydrology and Earth System Sciences, 23(11), 4685–4706. https://doi.org/10.5194/hess-23-4685-2019

Lionello, P., Abrantes, F., Gacic, M., Planton, S., Trigo, R., & Ulbrich, U. (2014). The climate of the Mediterranean region: Research progress and climate change impacts. Regional Environmental Change, 14(5), 1679–1684. https://doi.org/10.1007/s10113-014-0666-0

Malek, Ž., & Verburg, P. H. (2018). Adaptation of land management in the Mediterranean under scenarios of irrigation water use and availability. Mitigation and Adaptation Strategies for Global Change, 23(6), 821–837. https://doi.org/10.1007/s11027-017-9761-0

MedECC. (2020). Current situation and risks for the future First Mediterranean Assessment Report (p. 632). https://zenodo.org/record/4768833

Morchid, A., Et-taibi, B., Oughannou, Z., Alami, R. E., Qjidaa, H., Jamil, M. O., Boufounas, E.-M., & Abid, M. R. (2025). IoT-enabled smart agriculture for improving water management: A smart irrigation control using embedded systems and Server-Sent Events. Scientific African, 27, e02527. https://doi.org/10.1016/j.sciaf.2024.e02527

Nagaz, K., El Mokh, F., Ben Hassen, N., Masmoudi, M. M., Ben Mechlia, N., Baba Sy, M. O., Belkheiri, O., & Ghiglieri, G. (2020). Impact of Deficit Irrigation on Yield and Fruit Quality of Orange Trees (CITRUS SINENSIS , L. Osbeck, CV. Meski Maltaise) in Southern Tunisia. Irrigation and Drainage, 69(S1), 186–193. https://doi.org/10.1002/ird.2201

Nasim, S. F., & Khurram, M. (2025). Integrated Satellite Driven Machine Learning Framework for Precision Irrigation and Sustainable Cotton Production. Algorithms, 18(12), 740. https://doi.org/10.3390/a18120740

Nigussie, E., Olwal, T., Musumba, G., Tegegne, T., Lemma, A., & Mekuria, F. (2020). IoT-based Irrigation Management for Smallholder Farmers in Rural Sub-Saharan Africa. Procedia Computer Science, 177, 86–93. https://doi.org/10.1016/j.procs.2020.10.015

Noun, G., Lo Cascio, M., Spano, D., Marras, S., & Sirca, C. (2022). Plant-Based Methodologies and Approaches for Estimating Plant Water Status of Mediterranean Tree Species: A Semi-Systematic Review. Agronomy, 12(9), 2127. https://doi.org/10.3390/agronomy12092127

Nsoh, B., Katimbo, A., DeJonge, K. C., Liang, W., Guo, H., Ge, Y., Heeren, D. M., Shi, Y., Qiao, X., Rudnick, D. R., Nakabuye, H. N., Birru, G., Kabenge, I., & Wanyama, J. (2025). Crop2Cloud platform: Real-time data integration for agricultural water monitoring. Smart Agricultural Technology, 12, 101166. https://doi.org/10.1016/j.atech.2025.101166

Open-Meteo. (2025). Open-Meteo: Free Weather API. https://open-meteo.com/

Pereira, L. S., Paredes, P., & Jovanovic, N. (2020). Soil water balance models for determining crop water and irrigation requirements and irrigation scheduling focusing on the FAO56 method and the dual Kc approach. Agricultural Water Management, 241, 106357. https://doi.org/10.1016/j.agwat.2020.106357

Rawls, W. J., Pachepsky, Y. A., Ritchie, J. C., Sobecki, T. M., & Bloodworth, H. (2003). Effect of soil organic carbon on soil water retention. Geoderma, 116(1–2), 61–76. https://doi.org/10.1016/S0016-7061(03)00094-6

Saadi, S., Todorovic, M., Tanasijevic, L., Pereira, L. S., Pizzigalli, C., & Lionello, P. (2015). Climate change and Mediterranean agriculture: Impacts on winter wheat and tomato crop evapotranspiration, irrigation requirements and yield. Agricultural Water Management, 147, 103–115. https://doi.org/10.1016/j.agwat.2014.05.008

Santos Pereira, L., Cordery, I., & Iacovides, I. (2009). Coping with Water Scarcity. Addressing the Challenges. In L. Santos Pereira, I. Cordery, & I. Iacovides, Coping with Water Scarcity (pp. 1–6). Springer Netherlands. https://doi.org/10.1007/978-1-4020-9579-5_1

Saputri, F. R., Linelson, R., Salehuddin, M., Nor, D. M., & Ahmad, M. I. (2025). Design and development of an irrigation monitoring and control system based on blynk internet of things and thingspeak. PLOS ONE, 20(4), e0321250. https://doi.org/10.1371/journal.pone.0321250

Schaap, M. G., Leij, F. J., & Van Genuchten, M. Th. (2001). rosetta: A computer program for estimating soil hydraulic parameters with hierarchical pedotransfer functions. Journal of Hydrology, 251(3–4), 163–176. https://doi.org/10.1016/S0022-1694(01)00466-8

Sharma, V., Kaur, G., S., S., Chhabra, V., & Kashyap, R. (2025). Smart irrigation systems in agriculture: An overview. Computers and Electronics in Agriculture, 239, 111008. https://doi.org/10.1016/j.compag.2025.111008

Szabó, B., Weynants, M., & Weber, T. K. D. (2021). Updated European hydraulic pedotransfer functions with communicated uncertainties in the predicted variables (euptfv2). Geoscientific Model Development, 14(1), 151–175. https://doi.org/10.5194/gmd-14-151-2021

Todorovic, M., Riezzo, E. E., Buono, V., Zippitelli, M., Galiano, A., & Cantore, V. (2016). Hydro-Tech: An automated smart-tech decision support tool for eco-efficient irrigation management. 25(2), 44–56.

Toumi, I., Zarrouk, O., Ghrab, M., & Nagaz, K. (2022). Improving Peach Fruit Quality Traits Using Deficit Irrigation Strategies in Southern Tunisia Arid Area. Plants, 11(13), 1656. https://doi.org/10.3390/plants11131656

Wenzel, J. L., Conrad, C., Mahmood, T., Kunz, M., Volk, M., & Pöhlitz, J. (2026). Spatio-temporal HYDRUS-1D soil water balance simulations as support for precision irrigation in North-Eastern Germany. Agricultural Water Management, 325, 110157. https://doi.org/10.1016/j.agwat.2026.110157

Yacoubi, S., Slatni, A., Azzi, R., & Oueslati, T. (2022). Impact of deficit irrigation strategies on water use and productivity of vegetable crops in a semi-arid context of Tunisia. Desalination and Water Treatment, 263, 109–115. https://doi.org/10.5004/dwt.2022.28212

Yu, J., Wu, Y., Xu, L., Peng, J., Chen, G., Shen, X., Lan, R., Zhao, C., & Zhangzhong, L. (2022). Evaluating the Hydrus-1D Model Optimized by Remote Sensing Data for Soil Moisture Simulations in the Maize Root Zone. Remote Sensing, 14(23), 6079. https://doi.org/10.3390/rs14236079

Zacharias, S., & Wessolek, G. (2007). Excluding Organic Matter Content from Pedotransfer Predictors of Soil Water Retention. Soil Science Society of America Journal, 71(1), 43–50. https://doi.org/10.2136/sssaj2006.0098

Zia, H., Rehman, A., Harris, N. R., Fatima, S., & Khurram, M. (2021). An Experimental Comparison of IoT-Based and Traditional Irrigation Scheduling on a Flood-Irrigated Subtropical Lemon Farm. Sensors, 21(12), 4175. https://doi.org/10.3390/s21124175

Zotarelli, L., Dukes, M. D., & Morgan, K. T. (2010). Interpretation of Soil Moisture Content to Determine Soil Field Capacity and Avoid Over-Irrigating Sandy Soils Using Soil Moisture Sensors: AE460/AE460, 2/2010. EDIS, 2010(2). https://doi.org/10.32473/edis-ae460-2010

Supplementary material

Table 6*: Soil, crop and irrigation system's features of the four farms (AM, JD, SG, NR) in the Tunisian pilot. Farms are called with the initial letters of the farm's owner.*

Variable	**AM**	**JD**	**SG**	**NR**
Crop	Citrus	Citrus	Potato	Potato
Crop Area (ha)				
2024	0.44	0.90	0.25	0.1
2025	0.44	0.90	0.25	0.1
Planting/Activation* date (2024)	10/03/2024	10/03/2024	30/09/2024	01/10/2024
Harvesting date (2024)	15/11/2024	15/12/2024	15/01/2025	15/01/2025
Planting/Activation* date (2025)	10/03/2025	10/03/2025	12/02/2025	12/02/2025
Harvesting date (2025)	15/11/2025	31/12/2025	05/06/2025	05/06/2025
Sand (%)	63.8	85	90.8	75.5
Silt (%)	20.9	6.1	1.6	13.3
Clay (%)	15.3	8.9	7.6	11.2
Organic matter content (%)	0.7	0.7	0.7	0.7
Saturated hydraulic conductivity	2.78	2.78	2.78	2.78

(cm/h)				
Bulk density (g cm^{-3})	1.40	1.40	1.40	1.40
Irrigation method	Drip	Drip	Drip	Drip
Dripper spacing (m)	1	2	0.4	0.4
Dripper rate (L h^{-1})	4	8	4	4
Total length of drip lines (m)	800	1560	1120	1260

*Activation refers to the date at which the irrigation period for orange trees usually starts

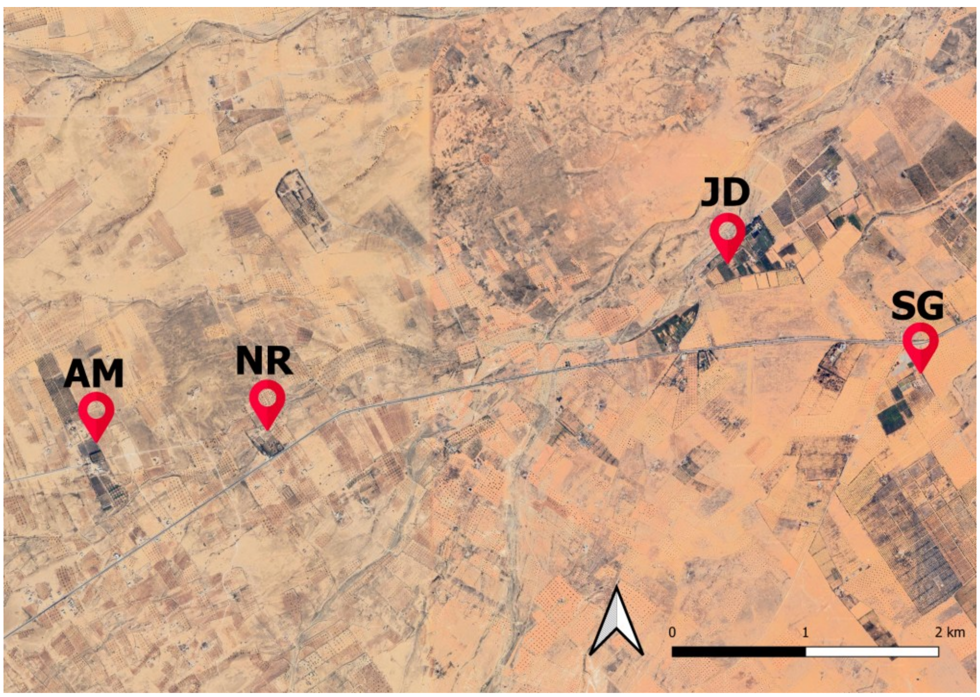

Figure 12: displacement of the four Tunisian farms AM, JD (citrus) and NR, SG (potato)

Abbreviation	**Description**
ACQUAOUNT	Adapting to Climate Change by QUantifying Optimal Allocation of Water Resources and Socio-Economic Interlinkages

API	Application Programming Interface
CMCC	Euro-Mediterranean Center on Climate Change
DF	Depletion Factor
DP	Deep percolation
Dr	Root-zone depletion
DSS	Decision Support System
e_a	Actual vapor pressure
e_s	Saturation vapor pressure
ET_0	Reference evapotranspiration
ETa	Actual evapotranspiration
ETc	Crop evapotranspiration
FAO	Food and Agriculture Organization of the United Nations
G	Soil heat flux density
h	Crop height
IoT	Internet of Things
Irr	Irrigation
IT	Irrigation threshold coefficients
IWRM	Integrated Water Resources Management
k_c	Crop coefficient
k_{cb}	Basal crop coefficient

k_e	Soil evaporation coefficient
k_s	Water stress coefficient
Ks	Saturated hydraulic conductivity
MAD	Mean Absolute Difference
MRD	Mean Relative Difference
P	Precipitation
Pb	Bulk density
PRIMA	Partnership for Research and Innovation in the Mediterranean Area
PTFs	Pedotransfer Functions
R^2	Coefficient of determination
RAW	Readily Available Water
RH	Relative humidity
RMSE	Root Mean Square Error
Rn	Net radiation at the crop surface
SM	Soil Moisture (volumetric soil water content)
SWrad	Solar radiation
T	Air temperature
TAW	Total Available Water in the root zone
u_2	Wind speed at 2 m height

WEFE	Water–Energy–Food–Ecosystems Nexus
WFD	Water Framework Directive
WoT	Web of Things
WRPs	Water Retention Parameters
γ	Psychrometric constant
Δ	Slope of the vapor-pressure curve
ΔSM	Change in volumetric soil moisture

Chapter 4. Automatic and high-resolution crop map production in Mediterranean environments applying IOTA^2 chain

Andrea Borgo[1,2], Vincent Thierion[3], Gabriele Giuseppe Antonio Satta[2], Antonio Trabucco[1], Marta Debolini[1]

1. CMCC Foundation – Euro-Mediterranean Centre on Climate Change, Italy
2. Department of Agriculture, University of Sassari, Viale Italia 39A, Sassari, 07100, Italy
3. Centre d'Etudes Spatiales de la Biosphère (CESBIO), Université de Toulouse, CNES/CNRS/INRAE/IRD/UT3-Paul Sabatier, 31401, Toulouse, France

Abstract

Reliable crop mapping is essential to understand agricultural practices, resource use, and rural dynamics, as well as to support modelling and planning for sustainable crop distribution. However, obtaining high-resolution crop distribution maps remains challenging in Mediterranean regions, where data availability is often limited and landscapes fragmented. The main European land use dataset, Corine Land Cover (CLC), lacks both the crop specificity required for accurate crop differentiation and the temporal frequency needed for timely monitoring. This study addresses these limitations by implementing the IOTA^2 automatic chain in Sardinia (Italy), for the creation of a first crop map specifically targeting Mediterranean crops. The methodology leverages open-source satellite imagery and supervised machine learning, using the 2018 Land Parcel Identification System (LPIS), CLC and Urban Atlas dataset for training. We compared two nomenclatures, a detailed (32 classes) versus a simplified (26 classes) one, across three sampling rates of the training pixels (10%, 50%, and 100%). Results indicate that the simplified nomenclature (N26) provides a more robust trade-off, achieving an Overall Accuracy (OA) of 0.66 (up to 0.77 with full sampling), compared to 0.60 for the detailed version. While high performance was achieved for specific crops like rice, citrus, and vineyards, classes such as cereals and fruit trees exhibited spectral confusion due to landscape fragmentation and uneven crop patterns. Despite these challenges, this work delivers a high-resolution (10 m) reproducible framework that improves current European datasets in thematic detail. It offers a scalable solution for rapid, annual crop monitoring in complex, data-scarce Mediterranean environments.

Introduction

Large-scale crop mapping is essential to understand the agricultural land cover of a region (Zhang et al., 2025), providing detailed spatial information to analyze the distribution of crop systems, assess agro-ecological indicators and support water management (Reumaux et al., 2023). Moreover, parcel-level crop monitoring is necessary to evaluate agricultural policies. For instance, in the framework of irrigation demand assessment, the estimation of realistic irrigation volumes requires both the individual crop irrigation demand, that can be obtained from crop models, and on a detailed crop distribution map, to understand the real surface of each crop. In addition, producing crop maps with high timeliness allows to assess the patterns, trends, as well as the crop rotations of crop systems.

The Common Agricultural Policy (CAP), which mainly regulates agricultural production, subsidies, and rural development across the European Union (EU) Member States (European Commission, 2022), also collects individual agricultural parcels within the Land Parcel Identification System (LPIS; European Court of Auditors, 2016) (Leonhardt et al., 2024; Sitokonstantinou et al., 2018). Although LPIS represents one of the most comprehensive spatial datasets on agricultural land use within the EU, data accessibility, harmonization, and completeness vary significantly across countries, as data collection is managed at the national or regional levels (Fendrich et al., 2023; Jänicke et al., 2025). Initiatives like EuroCrops, tried to address the problem of data fragmentation by merging the individual national datasets, however this procedure was possible for only 16 countries (Schneider et al., 2023). In other countries, like Italy, detailed and up-to-date crop mapping products remain scarce and highly localized. This is particularly true for Mediterranean insular regions such as Sardinia, where the combination of diverse and complex cropping systems and limited data availability makes regional-scale crop mapping especially challenging.

Among the most popular land cover services in the EU, Corine Land Cover (CLC; CLMS & EEA, 2020) builds a dataset with comprehensive, harmonized and detailed land cover maps. CLC released five land cover maps depicting the land cover distribution from 1990, 2000, 2006 and 2018, with 44 thematic classes. However, the product has a Minimum Mapping Unit (MMU) of 25 ha, and the temporal sampling remains low, also considering that no other maps have been released since 2018. Given this low update frequency, monitoring the evolution of agricultural crop systems over time is not feasible. Moreover, CLC lacks specificity in relation to agricultural classes: except for a few crop-specific classes, CLC nomenclature remains general, leaving uncertainty while conducting detailed crop studies.

Nowadays, modern satellites (Sentinel-2, Landsat 8/9) offer interesting opportunities for agricultural mapping, thanks to the high resolution (10 m) and temporal revisit time (≈ 5 days), opening new possibilities for detailed land cover classification (Zhang et al., 2025). Satellite Image Time Series (SITS) with high spatial, spectral and temporal resolution allow more accurate crop mapping, considering the possibility of distinguishing between the spectral signature of different crops and that multiple images can be collected within the crop growing season (Yi et al., 2020). In this regard, several Machine Learning (ML) algorithms can support automatic classification. Random Forest (RF) is one of the most widely used algorithms for supervised classification, thanks to its robustness towards outliers, high level of accuracy and low overfitting (Tan et al., 2024; Zhang et al., 2025). Moreover, it is particularly suitable for large-scale mapping applications (d'Andrimont et al., 2021; Pelletier et al., 2016).

By combining the observations of Sentinel-1 imagery and LUCAS in-situ observations, in 2018 the European Commission released EUCROPMAP, the first continental scale crop map, adopting RF classifier to detect 19 different crop types (d'Andrimont et al., 2021). This map has the advantage of providing a uniform mapping across the entire continent; however, it does not suit the specific conditions of individual regions, given the heterogeneity of the European landscape and its diversity in terms of crop systems. EUCROPMAP mainly focuses on annual crops (cereals, fodder, maize, root crops), but it overlooks other crop species which are particularly relevant in Mediterranean environments, such as olive groves, vineyards, vegetables, fruit trees. A crop-specific map tailored to Mediterranean agriculture is needed to gain a more precise understanding of local crop dynamics.

Moreover, timeliness is a crucial factor for many crop map applications; therefore, automated processes for repeated crop map production are needed (Inglada et al., 2017). For this reason, the Theia Land Cover SEC (Scientific Expertise Centre) deployed the IOTA^2 algorithm (Inglada et al., 2017; Theia, 2018a), a fully automatic chain of processes based on supervised RF classification, able to create land cover products from open-source SITS, given a specific nomenclature and adequate learning sample polygons. IOTA^2 is specifically designed for large-scale classification. For this reason, Theia maps cover all the French territory; they are updated once a year and contain 24 thematic classes with a 10 m resolution. Moreover, IOTA^2 offers the adoption of a climatic stratification, that is a division of the study region into different ecoclimatic regions. This ensures that pixels within the same region share similar spectral and phenological behavior, thereby improving classification accuracy (Inglada et al., 2017).

Considering that several Mediterranean countries typically lack sufficient open-source and high-quality data for spatial applications, the IOTA^2 chain can reveal a promising tool, as it mainly requires data accessible from open-source EU databases. For this reason, the main aims of this study were (i) the generation of a land cover crop-oriented map within the Sardinia region (Italy), identifying the most suitable nomenclature for the regional cropping systems, (ii) the evaluation of IOTA^2 performance in a Mediterranean context and

(iii) whether increasing the training sample size improves classification accuracy. A more detailed versus a shorter nomenclatures were compared, both tested under different sampling rates of the training pixels. This approach enables the assessment of whether a more extensive nomenclature allows satisfactory accuracy levels, and whether increasing the number of training pixels reduces or exacerbates class confusion within the classifier, given the available reference data. In doing so, this study offers a replicable approach to crop mapping in Mediterranean environments, contributing to the broader goal of timely and spatially detailed agricultural monitoring in currently data-scarce regions.

Material and Methods

Study site

The study was conducted in Sardinia, Italy, the second largest island of the Mediterranean basin (Figure 13), located in its central part and covering 24 100 km^2. Despite its extension, Sardinia has a relatively low population, with approximately 1.5 million inhabitants (ISTAT, 2025a), mainly concentrated in Cagliari and in few other towns. For this reason, the landscape is mainly dominated by natural areas, that are forests and Mediterranean shrubland. Agriculture covers 48% of the Sardinian surface, with pastures being the main agricultural activity per extension, about 67% of the total agricultural surface (ISTAT, 2018). A further 17% is dedicated to forage crops, 7% to other annual crops and the remaining 7% to woody crops, mainly olives, grapevine and citrus. Another important ecosystem is the pure cork oak forest, covering more than 4% of the total land area of the island (Mattioli et al., 2025), producing around 80% of Italian cork (MASAF, 2023). In its low-density form, it is often characterized by agroforestry practices (Paris et al., 2019; Sedda et al., 2011).

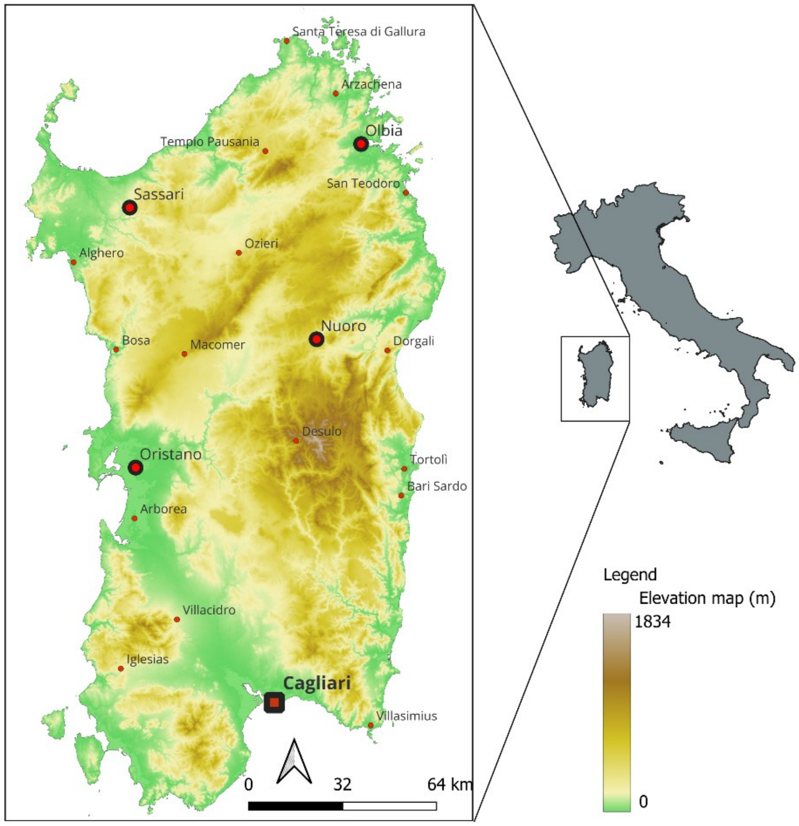

Figure 13: map of Sardinia region (Italy)

Reference data acquisition

The IOTA[2] workflow requires a set of reference data, which means training and validation samples to perform the supervised classification. This study relies on different open-source datasets provided by the European Commission, as reported in Table 1.

Table 1: Summary of the main geospatial datasets employed to collect reference data in the study area.

Dataset	Function	Source
Urban Atlas (UA)	Urban areas, roads, ports and other artificial constructions	(CLMS & EEA, 2020b)
LPIS	Agricultural areas	(AGEA, 2018)

CLCplus Backbone	Forests and shrublands	(CLMS & EEA, 2023)
Corine Land Cover (CLC)	Beaches, water bodies, non-vegetated land	(CLMS & EEA, 2020a)

Nomenclatures

The IOTA^2 algorithm has been applied to two semantic nomenclatures schemes: an extended nomenclature with 32 land cover classes (N32) and a shorter version with 26 classes (N26). This comparison aims to assess the algorithm's capacity to handle a higher level of thematic detail and to determine whether comparable classification accuracy can be maintained when the number of classes increases, given the available training samples. Although the focus is given to crop mapping, the resulting product adopts the Theia Land Cover SEC framework (Theia, 2018a), to provide a comprehensive description of artificial, agricultural, and natural areas within the region. The full list of N26 and N32 classes and their description is shown in Table 7, together with the code associated to each class.

The nomenclatures follow the approach of the land cover (Occupation des Sols, OSO) nomenclature of Theia maps, which consider these broader categories:

- Artificial areas (urban, industrial, roads and communication areas)
- Crop lands (annual and perennial crop areas)
- Natural vegetated areas (forests and shrublands)
- Other non-vegetated lands
- Water bodies

Reference data for artificial areas were collected from the 2018 Urban Atlas (UA) dataset (CLMS & EEA, 2020b), which provides high resolution land use classification (17 urban classes) of Functional Urban Areas (FUAs) with more than 50 000 inhabitants across all the European Union countries. For the Sardinia region, two cities (Cagliari and Sassari) were available for data acquisition. Natural vegetation areas were derived from the 2018 CLCplus Backbone (CLMS & EEA, 2023), a baseline land cover product with 11 classes that provides comprehensive and accurate land cover information to complement the CLC dataset. CLCplus Backbone offers a finer spatial resolution than CLC (MMU of 0.5 ha) and it explicitly accounts for overlapping land-cover characteristics. In such cases, pixels are assigned to a single land-cover class according to a majority rule. These features make the dataset particularly suitable for sampling natural vegetation areas, as they allow the selection of training samples with reduced class ambiguity. Regarding agricultural classes, reference data were collected from the 2018 LPIS database (AGEA, 2018; European Court of Auditors, 2016), which contains the georeferenced information of the crops cultivated in the region, distinguishing more than 160 crop classes. Given the high specificity of the classes involved, LPIS crop classes are aggregated in broader categories, which vary according to the N26 and N32 nomenclatures. Table 11 in the Supplementary material contains the full list of the crops cultivated in Sardinia within the LPIS dataset and their assignment to the aggregated classes of N32 and N26 nomenclatures. Finally, non-vegetated areas were taken from the 2018 CLC dataset (CLMS & EEA, 2020a) and they are common between the N26 and N32 nomenclatures.

Table 7: List of the class names and codes of N26 and N32 nomenclatures

N26 nomenclature		N32 nomenclature		Description	Original Dataset and reference class name
Class name	Code	Class name	Code	-	-
Urban dense	UDN	Urban dense	UDN	Continuous urban fabric with artificial surfaces exceeding 80%	UA 11100
Urban discontinuous	UDC	Urban discontinuous	UDC	Discontinuous urban fabric with artificial surfaces interspersed with vegetation and bare soil	UA 11210
Roads	RDS	Roads	RDS	Continuous artificial surfaces for roads, motorways, and railways, enabling motorized and rail connectivity across urban areas	UA 12210-12230
Industrial and commercial	IND	Industrial and commercial	IND	Large artificial surfaces for industrial, commercial, port, and airport activities	UA 12100, 12300, 12400
-		Isolated buildings	ISB	Single, spatially detached built-up structures surrounded by non-artificial surfaces	UA 11300

-		Mineral surfaces	MIN	Mineral extraction and dump sites	UA 13100
Cereals	CER	Cereals	CER	Annual agricultural areas with cereal crops, mainly wheat, oat, barley, mainly	LPIS
Maize	MAI	Maize	MAI	Annual agricultural areas dedicated to silage or grain maize production	LPIS
Rice	RIC	Rice	RIC	Annual agricultural areas cultivated with rice, typically cultivated in managed paddy fields with seasonal flooding	LPIS
Forage crops	FOR	Forage crops	FOR	Intensively managed fodder crops mainly irrigated and occasionally in rotation with other crops. For instance, ryegrass, clover, alfalfa, etc.	LPIS
Pastures	PAS	-		Permanent grassland, with occasional mowing or under grazing	LPIS
		Improved pasture	IMP	Actively managed pastures, usually mowed for forage harvest	LPIS
-		Permanent pasture	PAP	Pastures left to animal grazing	LPIS
-		Arboreal pasture	ARP	Permanent grasslands characterized by the presence of scattered or regularly distributed trees, forming silvo-pastoral systems	LPIS
Vegetables	VEG	Vegetables	VEG	Open-field annual or perennial herbaceous crops, like fruiting vegetables, ground-grown fruit crops, and tubers. In Sardinia, mainly tomato, potato and artichoke	LPIS
Legumes	LEG	Legumes	LEG	Mainly fava bean and pea	LPIS
Grapevine	GRA	Grapevine	GRA	Vineyards for wine or table grape production	LPIS
Olives	OLI	Olives	OLI	Olive groves for oil or table olives, organized in regular plantations or dispersed traditional systems	LPIS

Citrus	CIT	Citrus	CIT	Orange, clementine and lemon trees	LPIS
Nuts	NUT	Nuts	NUT	Nut-producing tree species, mainly almond and hazelnut	LPIS
Fruit trees	FRT	Fruit trees	FRT	Managed orchards systems with perennial fruit tree crops, mainly peach and pome fruits	LPIS
-		Tree crops	TRC	Actively managed woody perennial systems, cultivated for specific arboricultural products, including cork oaks, and other specialized trees	LPIS
Greenhouses	GRH	Greenhouses	GRH	All protected cultivation systems	LPIS
-		Ornamental and aromatics	ORA	Crops cultivated for ornamental, aromatic, medicinal, or spice uses, e.g., saffron, lavender, etc.	LPIS
Shrubland	SHR	Shrubland	SHR	Dominated by woody shrubs and bushes (woody plants < ~5 m, >50% cover); intermediate between herbaceous and forest	CLCplus 40
Broad leaved forest	BLF	Broad leaved forest	BLF	Areas dominated by deciduous or evergreen broad-leaved tree species	CLCplus 31-33
Forest coniferous	CNF	Forest coniferous	CNF	Areas predominantly covered by coniferous tree species, characterized by needle-leaved evergreen canopy	CLCplus 21 and 22
-		Shrubland and forest mix	TMM	Transitional or heterogeneous areas composed of mixed tree and shrub vegetation, where neither forest nor shrubland clearly dominates	CLCplus 51-53
Low vegetation cover	LVC	Low vegetation cover	LVC	Areas characterized by sparse or low-height vegetation, including grasslands or herbaceous cover, with limited or no tree canopy development	CLCplus 81
Non vegetated areas	NVA	Non vegetated areas	NVA	Surfaces lacking significant vegetation cover, including bare soil, exposed rock, and	CLC plus 90

				other mineral substrates where vegetation is absent or negligible	
Beaches	BCH	Beaches	BCH	Coastal depositional areas composed predominantly of sand or gravel	CLC 331
Salines	SAL	Salines	SAL	Salt extraction areas and salt-affected surfaces characterized by high salinity, including evaporation ponds and adjacent mineral crusts	CLC 422
Water	WAT	Water	WAT	Inland or coastal water bodies permanently or seasonally covered by open water, including rivers, lakes, reservoirs, lagoons, and coastal waters	CLC 511-523

Regarding the additional classes to be tested in N32, Isolated buildings class was considered to evaluate if the 10 m pixel resolution of Sentinel-2 allows the identification of buildings outside of urban perimeters. The class mineral surfaces attempted a distinction between the artificial (quarries, mines, etc.) versus the natural non-vegetated areas. Shrubland and forest mix was tested to evaluate whether IOTA^2 can identify those natural areas where shrubland and forest coexist, given their frequency in the Sardinian landscape. Regarding agricultural classes, Arboreal pasture and Tree crops classes were considered to evaluate model's performance in the attempt to distinguish agro-forestry areas and managed forests (mainly cork oak) from natural forest. Although representing a minor share of the Sardinian agricultural area (~15 ha in the LPIS samples), the Ornamental and Aromatics class was retained to evaluate performance of the classifier under conditions of extreme class imbalance and limited training availability.

Classification framework

Reference data pre-processing

Before entering the IOTA^2 chain, reference data underwent a data cleansing process to harmonize samples originating from four different datasets (Inglada et al., 2017). In the first stage, all invalid geometries and empty entities were removed and the entities larger than 100 ha were fragmented, a threshold chosen to avoid the overrepresentation of extensive land units (e.g. large pasture blocks) in the training set (C. Li et al., 2021). In a second step, features of the original datasets were merged into broader classes, according to the desired nomenclatures and the overlapping areas among samples were removed. In a further step, a negative buffering of 10 m was applied to remove boundaries of the polygons, potentially affected by mixed pixels. Then, very small geometries (smaller than 200 m^2) were eliminated. Finally, reference data were merged into single datasets (one per nomenclature), and the total per-class number of features was compared among classes. At the end of this process, a vectorized dataset containing the selected reference data was obtained, to be used in the modelling framework.

IOTA^2 workflow

IOTA^2 operates as an automated processing chain that produces a land-cover classification map and associated accuracy assessment metrics from SITS and reference data, given a predefined nomenclature. The workflow is continuously under update and it includes various stages; for a more detailed description, refer to Inglada et al. (2017) and to the IOTA^2 repository (iota2-project, 2019).

The workflow starts with folders initialization and integrity checks (step 1), where IOTA^2 verifies the consistency of the ground truth database and its spatial intersection with the SITS, preventing unnecessary processing of invalid inputs. During preprocessing (step 2), a common mask is generated for each tile across the time series to ensure geometric consistency, and pixels affected by clouds, saturation and lack of data are filtered to retain only reliable temporal observations for training and classification steps. In large-scale applications, overlapping tiles are harmonized using predefined spatial rules (step 3). Samples are then split into training and validation sets (step 4). The defined sampling rate is applied exclusively to the training polygons, selecting a percentage of pixels from each polygon to produce pixel-level training samples. For each iteration (seed), a RF model is independently calibrated on these samples and a classification map is produced; repeating this process across multiple seeds allows confidence intervals to be estimated for the validation metrics. Spectro-temporal features are extracted from the SITS (step 5) and used to train a RF classifier at the regional level. The trained model is applied to each tile, and the resulting maps are mosaicked into a single classification map covering the entire study area (step 6). Finally, accuracy assessment is performed (step 7) by computing tile-level confusion matrices aggregated into a global matrix. From this matrix, per-class (precision, recall, F-score) and global metrics (Overall Accuracy and Kappa coefficient) are derived to evaluate classification performance.

Recall (producer's accuracy) is the ratio between the correctly classified pixels to the total validation pixels of that class. It is expressed as

$$recall_i = \sum_{j=1}^{r} \frac{n_{ii}}{n_{ij}} \tag{4}$$

Where n_{ij} is the count of elements of class j classified as class i, r is the number of classes. The average recall is expressed as the mean of the recalls of each class

$$recall = \frac{1}{r} \sum_{i=1}^{r} recall_i \tag{5}$$

Precision (user's accuracy) is the ratio between the correctly classified pixels to the total pixels of that class in the final classification map. The average precision is the mean of the precisions of the classes in the test:

$$precision_i = \sum_{j=1}^{r} \frac{n_{ii}}{n_{ji}} \tag{6}$$

$$precision = \frac{1}{r} \sum_{i=1}^{r} precision_i \tag{7}$$

The F-score is the harmonic mean between recall and precision, ranging from 0 (lowest score) and 1 (highest score).

$$Fscore = \frac{2 \cdot recall \cdot precision}{recall + precision} \tag{8}$$

OA represents the ratio between the correctly classified pixels over the total pixels of the confusion matrix.

$$OA = \frac{\sum_{i=1}^{r} n_{ii}}{\sum_{i=1}^{r}\sum_{j=1}^{r} n_{ij}} \quad (9)$$

Finally, the Kappa coefficient quantifies the agreement between the classification and the reference data, accounting for the probability of chance agreement. It ranges from -1 to 1, where values lower than 0 suggest agreement is no better than random, and 1 perfect classification. It is defined as:

$$k = \frac{P_0 - P_e}{1 - P_e} \quad (10)$$

Where P_0 is the observed agreement and P_e is the agreement by chance.

Common interpretations of the Kappa coefficient consider the scale of Landis & Koch (1977): <0 (very bad), 0.1-0.20 (bad), 0.21-0.4 (weak), 0.41-0.6 (moderate), 0.61-0.8 (good), >0.81 (perfect). Although widely adopted in remote sensing applications, such thresholds should be considered indicative rather than absolute (Foody, 2020).

Simulation setup

The workflow is structured as a sequence of IOTA^2 runs based on the N26 and N32 nomenclatures and three sampling rates of training pixels (10%, 50%, and 100%), as illustrated in **Error! Reference source not found.**. Following the initial pre-processing and harmonization (section Reference data pre-processing) of the reference datasets, the IOTA^2 experiments are organized into three successive versions (V1, V2, and V3). In V1, IOTA^2 is executed using both nomenclatures and all three sampling rates. In V2, the analysis is restricted to the nomenclature obtaining the best scores, after refining the training dataset to improve classification performance. In this phase, the refinement consists in the removal of samples with mixed features (especially urban and industrial areas with large portions of vegetation) and the manual addition of samples for classes requiring more representativeness (e.g., citrus and olive groves, greenhouses and areas with low vegetation cover). Moreover, classes with higher amount of training polygons ($>10^4$) are reduced to ensure balance with classes with fewer polygons ($\approx 10^3$), following the recommendations of Belgiu & Drăguţ (2016). Overall, the total number of training polygons reduced from ≈69000 in V1 to ≈63000 in V2. Finally, V3 applies IOTA^2 using the combined training and validation datasets for model training. Given the large number of maps produced within this workflow, Table 8 summarizes the naming conventions adopted for each map, where the name indicates the corresponding version, nomenclature and sampling rate.

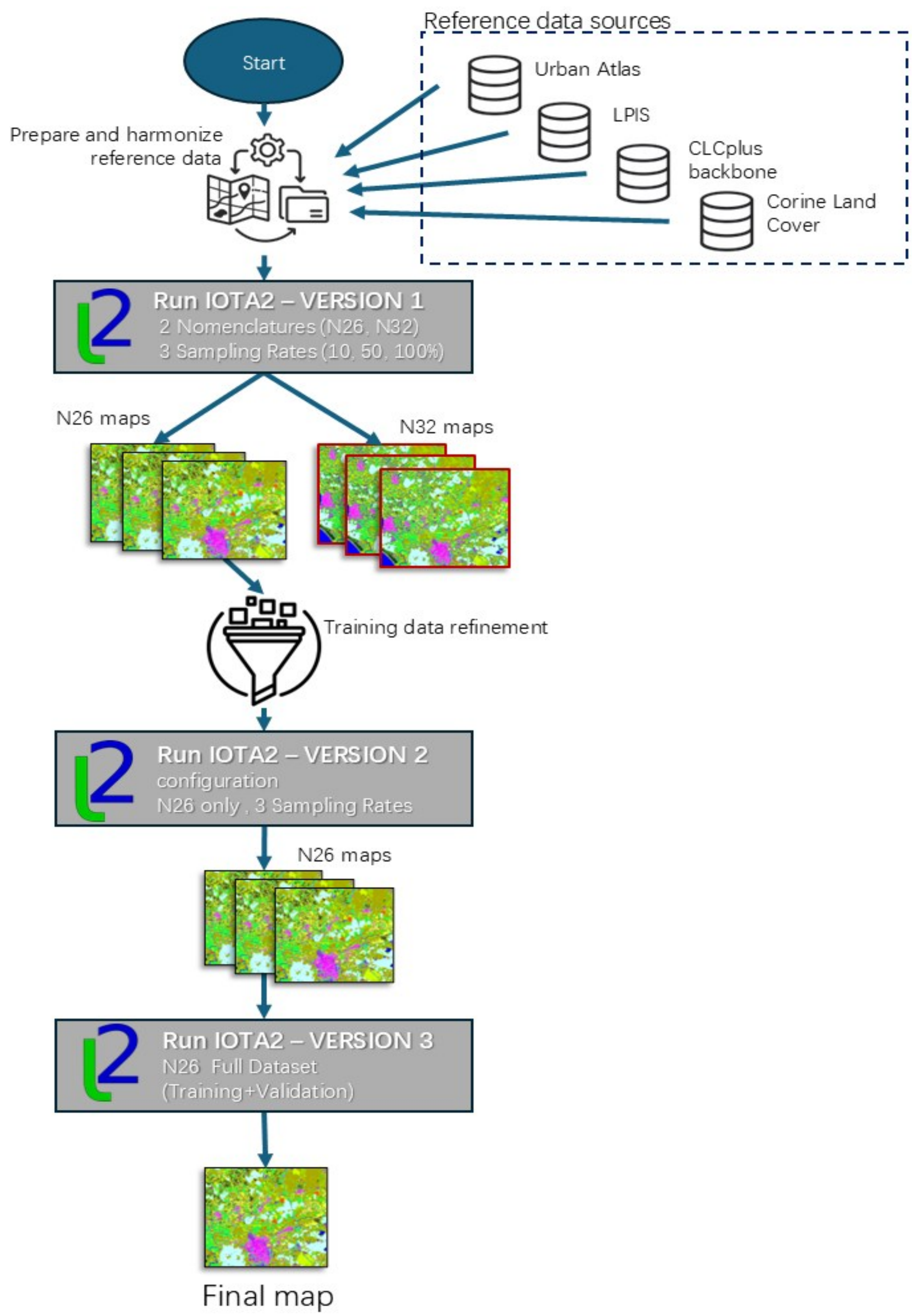

Figure 14: workflow of IOTA^2 runs, given the nomenclatures N26 (26 classes) and N32 (32 classes) and three sampling rates (10, 50, 100%). IOTA^2 runs have been divided into three versions, namely V1, V2 and V3.

Table 8: summary of the IOTA² simulations and corresponding acronyms. The maps are organized according to the two nomenclatures (N26 and N32) and three pixel-level sampling rates at the training polygon level (10, 50, 100%). Simulations are grouped in three versions: V1 includes all combinations of the two nomenclatures and the three sampling rates; V2 focuses on the samples-refined N26 nomenclature using the same three sampling rates; V3 consists of a single simulation using N26 with 100% of the reference data available (training + validation).

			Sampling rate (training)		
			10% of pixels	50% of pixels	100% of pixels
V1	Nomenclatures	N26	V1-N26-SR10	V1-N26-SR50	V1-N26-SR100
		N32	V1-N32-SR10	V1-N32-SR50	V1-N32-SR100
V 2	Nomenclature	N26	V2-N26-SR10	V2-N26-SR50	V2-N26-SR100
			Totality of reference data (training + validation)		
V 3	Nomenclature	N26	V3-TOT		

Results

The performance of the IOTA² chain across the different classification combinations, beginning with the V1 results and subsequently examining the V2 configuration, have been assessed, compared and the corresponding maps to support a qualitative interpretation of the outputs have been provided. For the V3 configuration, we present only the final map, as the accuracy metrics could not be computed. Nevertheless, we discuss the V3 results by comparing the mapped outputs with external reference datasets.

Version 1, accuracy metrics

The accuracy assessment derived from the confusion matrices for the two nomenclatures and the three sampling rates (Figure 15) reveals a clear divergence in classifier performance between the two nomenclatures. For N32, both Kappa and OA remain nearly constant across all sampling rates (Kappa: 0.53, 0.54, and 0.55; OA: 0.60, 0.60, and 0.61 at SR10, SR50, and SR100, respectively), indicating that enlarging the training set does not improve classification when class boundaries are intrinsically ambiguous. By contrast, N26 exhibits a moderate gain at intermediate sampling (Kappa: 0.54 at SR10, 0.56 at SR50; OA: 0.60, 0.61), followed by a substantial increase at full sampling (Kappa = 0.74; OA = 0.77 at SR100), an OA gain of +0.16 over SR50.

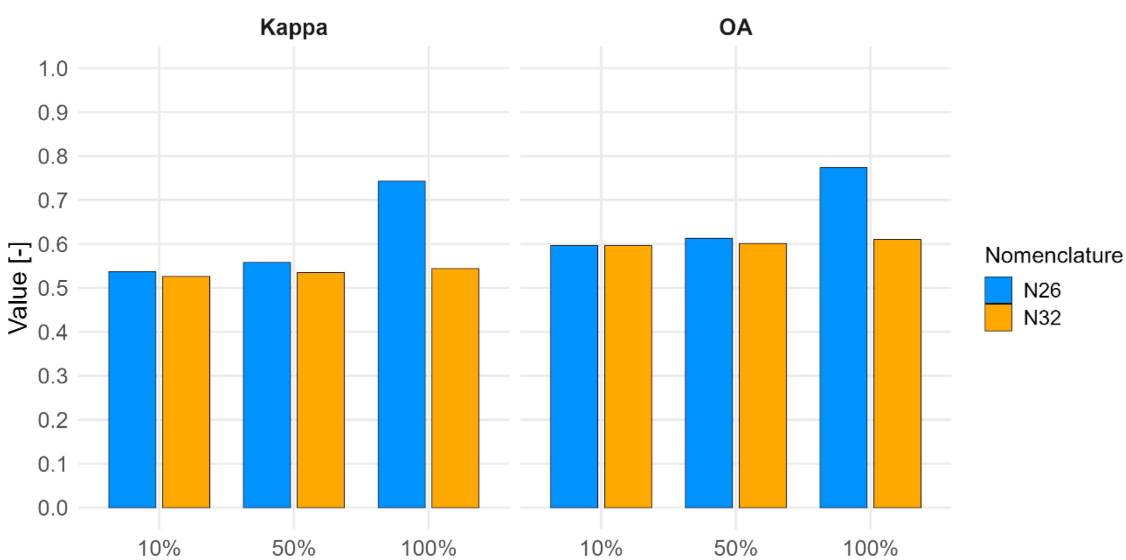

Figure 15: comparison of the Kappa score and Overall Accuracy (OA) metrics between the N26 and N32 nomenclatures and sampling rates (10, 50 100%), under version 1 (V1) of IOTA² simulations.

Regarding the per-class metrics, the F-scores comparison across the three sampling rates for each nomenclature (Figure 16), reveals a marked contrast in class-level performance between the two nomenclatures. Within N32, performance is highly heterogeneous and largely unresponsive to increasing sample size: some classes achieve high F-scores consistently above 0.90 (*Rice*, *Water*) or around 0.75 (*Arboreal Pasture*, *Vegetables*, *Citrus*), while a large group of N32-specific classes (*Mineral Surfaces*, *Tree crops*, *Ornamental and Aromatics*, *Shrubland–forest mix, Improved Pastures*, and *Broad-leaved forest*) exhibit F-scores below 0.05 at SR10 and remain below 0.20 even at SR100. Only few classes (e.g. *Mineral Surfaces, Permanent Pasture, Beaches*) show gains above 0.15, although their final F-scores at 100% sampling remain low (0.2-0.5). Conversely, the N26 nomenclature exhibits more uniform class performance, with 13 classes with F-scores above 0.5 at SR10 and only two classes with F-score ≈0.3 (*Cereals* and *Olives*) and other two with F-score <0.1 (*Nuts* and *Greenhouses*). At SR100, F-scores increase sharply in all classes, exceeding mostly 0.5 (except *Nuts*, which achieves 0.48).

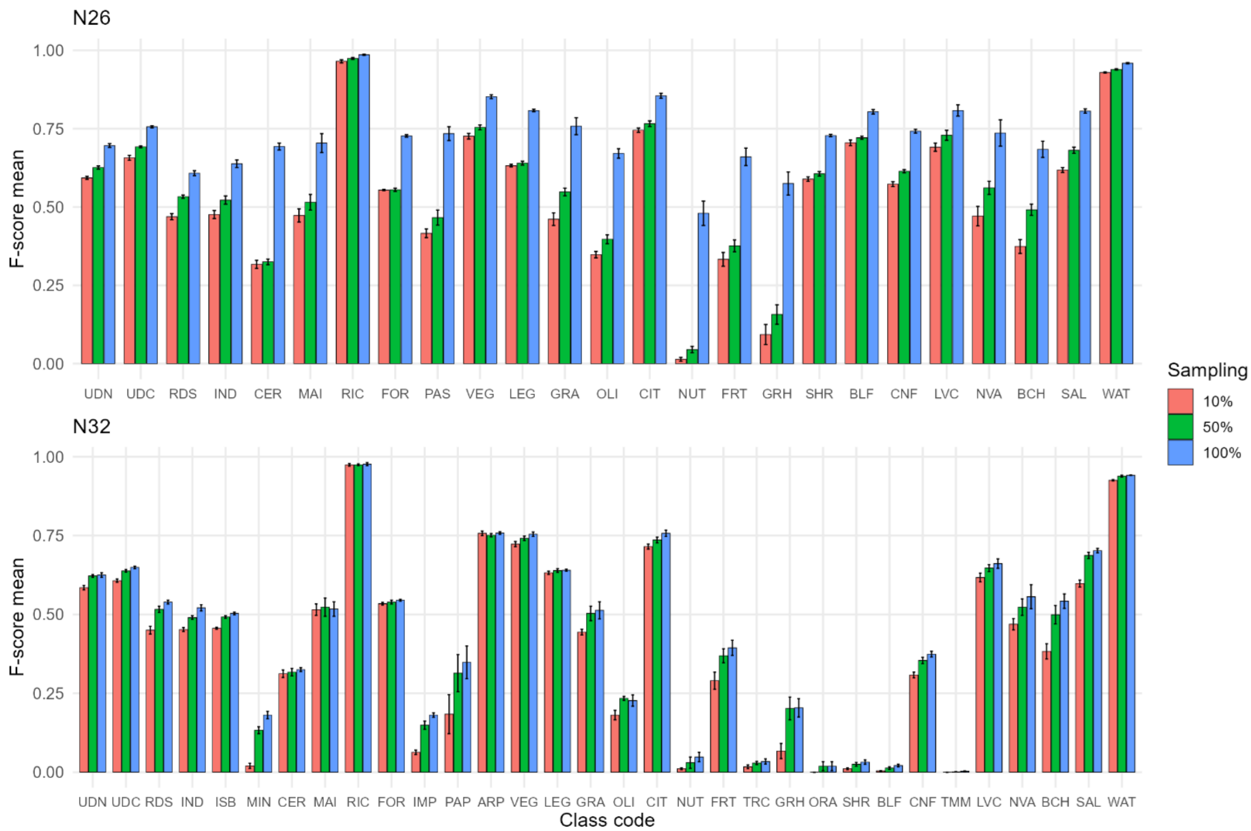

*Figure 16**:** F-score mean of the classes of N26 and N32 nomenclatures, for the three sampling rates (10, 50, 100%), under version 1 (V1) of IOTA^2 simulations.*

A visual interpretation of the V1 maps is provided in Figure 17, which compares the satellite view over a vineyard region in center Sardinia with the classification outputs V1-N32-SR100 and V1-N26-SR100 (i.e., the N32 and N26 nomenclatures at 100% sampling). In the N32 map, the class *Arboreal pasture* clearly dominates, reducing the apparent heterogeneity of land-use patterns. In contrast, the N26 map reveals a more diverse landscape, allowing the distinction among forage crops, pastures, shrublands, and forested areas (both broad-leaved and coniferous).

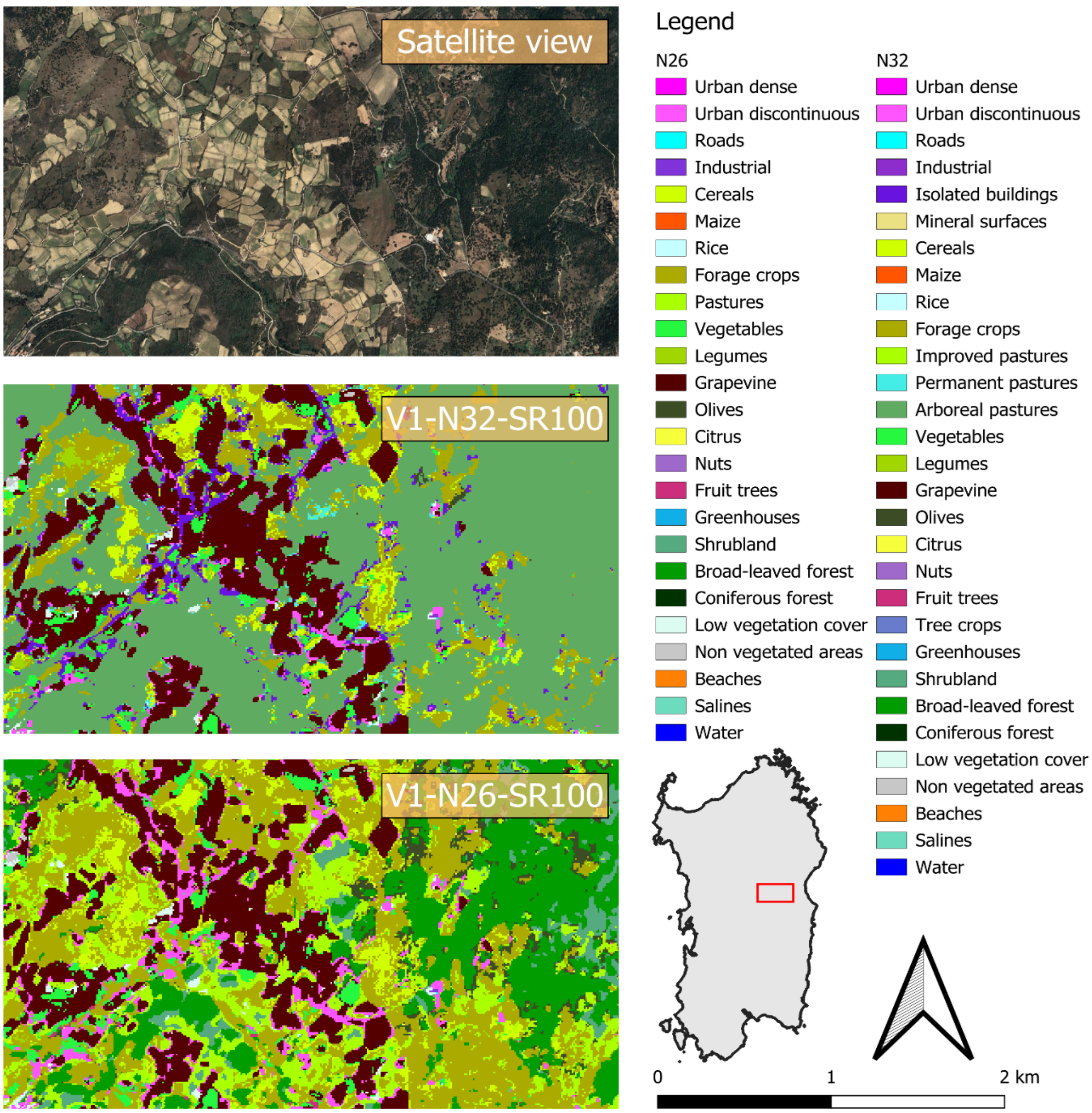

*Figure 17**:** visual interpretation of the version1 (V1) classification maps, under 100% sampling rate, for N26 (V1-N26-SR100) and N32 (V1-N32-SR100)*

Version 2, accuracy metrics

Given the lower performance of the N32 nomenclature, only N26 is retained for the V2 round of simulations. In V2, IOTA^2 is re-run for the three sampling rates after a refinement of the training samples (described in section 0) based on the evaluation of the V1 maps. The Kappa score and OA derived from the confusion matrices for the three sampling rates of this version (Figure 18) reveals flatter accuracy response to increasing training sample size compared to V1. Kappa improves by only 0.022 percentage points (from 0.544 at SR10 to 0.566 at SR100) and OA by 0.018 percentage points (from 0.601 to 0.619), compared to gains of +0.18 and +0.16 respectively observed in V1-N26 between SR10 and SR100. Moreover, V2 accuracy is consistently lower than that of V1 across all sampling rates (V1 Kappa range: 0.54–0.74; OA: 0.60–0.77; V2 Kappa range: 0.54–0.57; OA: 0.60–0.62).

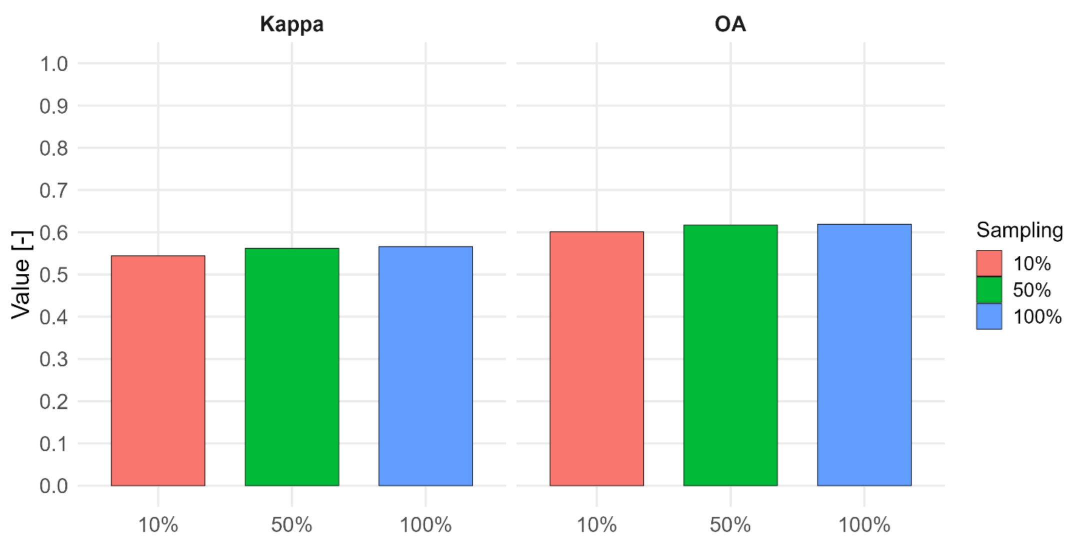

Figure 18: comparison of the Kappa score and Overall Accuracy (OA) metrics of N26 nomenclature and three sampling rates (10, 50 100%), under the version 2 (V2) of IOTA^2 simulations.

Regarding per-class performance analysis, Figure 19 reports the mean F-score per class for the three V2 sampling rates. The class ranking is consistent with V1: *Rice* and *Water* maintain the highest F-scores (above 0.97 and 0.92, respectively), followed by *Citrus* (F ≈ 0.80), *Vegetables* (F ≈ 0.77), *Broad-leaved forest* (F ≈ 0.70), and *Low vegetation cover* (F ≈ 0.75) at SR100. In contrast, *Cereals* (F ≈ 0.33), *Pastures* (F ≈ 0.45), *Olives* (F ≈ 0.40), *Fruit trees* (F ≈ 0.43), and *Nuts* (F < 0.08 at SR10 and SR50) remain poorly classified. Notably, *Grapevine* does not exceed 0.70 even at SR100 in V2, a slight regression from V1. Overall, F-scores are consistently lower in V2 than in V1 across all classes (Figure 20). The decline is driven primarily by a reduction in recall, while precision remains largely comparable between the two versions, staying above 0.50 for most classes in both. Recall drops substantially for several agricultural classes:

Cereals (V1: 0.57, V2: 0.25), *Maize* (V1: 0.60, V2: 0.40), *Pastures* (V1: 0.70, V2: 0.41), *Olives* (V1: 0.64, V2: 0.34).

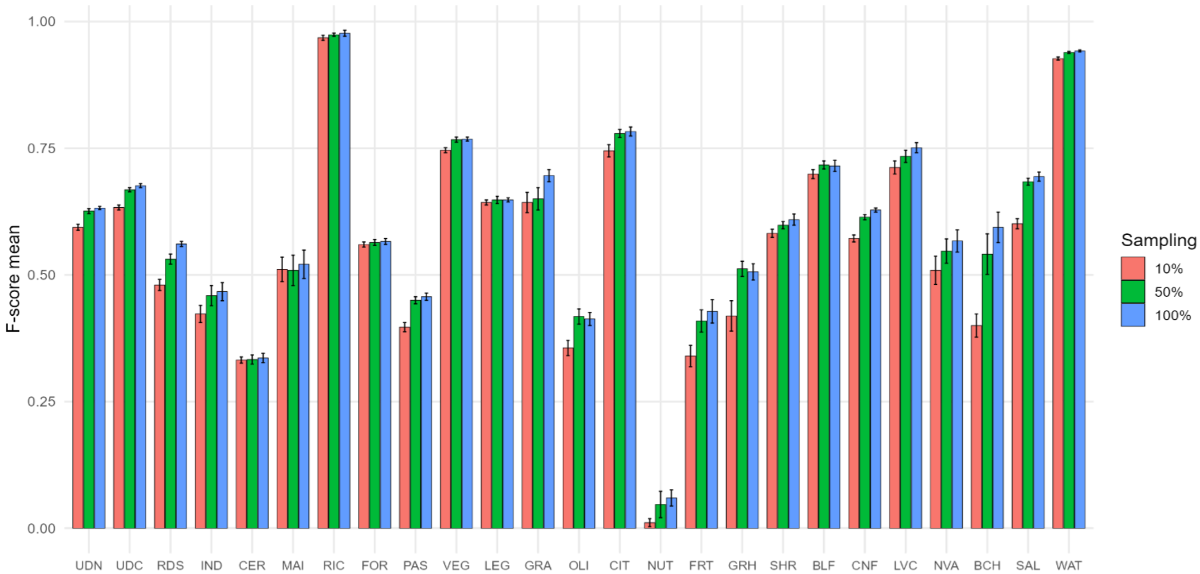

Figure 19: F-score mean of each class (indicated by its class code) of the N26 nomenclature, for the three sampling rates (10, 50, 100%), under the second round of IOTA² simulations (V2).

Figure 20: comparison of precision, recall and F-score between V1-N26-SR100 and V2-N26-SR100 (version 1 and version 2 of N26 nomenclature, under 100% sampling, respectively) maps.

Confusion matrix of the best model

The confusion matrix of V2-N26-SR100 (Table 9) reports row-normalized proportions, where diagonal values correspond to the recall and off-diagonal values quantify misclassification rates. Among agricultural classes, Rice achieves the highest recall (97%), followed by *Vegetables* (77%), *Citrus* (77%), and *Forage crops* (74%), all exhibiting limited off-diagonal spread. In contrast, *Cereals* (24%), *Olives* (32%), and *Nuts* present the lowest recall values, indicating severe omission errors for these classes. A dominant misclassification pattern is observed toward the *Forage crops* class, which accumulates a substantial proportion of pixels from *Cereals* (47%), *Pastures* (50%), *Maize* (30%), *Legumes* (27%), *Olives* (34%), *Nuts* (62%), and *Fruit Trees* (24%).

*Table 9**:** Confusion matrix of the classes of V2-N26-SR100 map, with rows representing the classes of the validation samples and columns the predicted classes. Values are normalized and according to the validation samples (rows), that is, the proportion of pixels belonging to a given class that were assigned to each predicted class. Diagonal values indicate correctly classified pixels, whereas off-diagonal values represent misclassifications, showing how pixels of one ground-truth class were attributed to other classes. Colors are assigned to indicate the percentage of correspondence between validation and predicted pixels: the higher the percentage, the greater the number of predicted pixels associated to that validation sample.*

Code N26	UD N	UD C	RD S	IN D	CE R	MA I	RI C	FO R	PA S	VE G	LE G	GR A	OL I	CI T	NU T	FR T	GR H	SH R	BL F	CN F	LV C	NV A	BC H	SA L	WA T	Code N26
UDN	62	28	0	6	0	0	0	1	0	1	0	0	0	0	0	0	0	0	0	0	0	0	0	0	0	UDN
UDC	15	75	0	3	0	0	0	2	0	2	0	0	1	1	0	0	0	0	0	0	0	0	0	0	0	UDC
RDS	5	10	50	17	0	0	0	5	0	3	1	0	2	0	0	0	0	2	1	1	1	0	0	0	1	RDS
IND	8	13	1	42	0	0	0	15	1	4	7	0	2	1	0	0	1	1	0	0	1	1	0	0	1	IND
CER	0	0	0	0	24	0	0	47	3	3	22	0	0	0	0	0	0	0	0	0	0	0	0	0	0	CER
MAI	0	0	0	0	1	43	2	30	0	9	14	0	0	0	0	0	0	0	0	0	0	0	0	0	0	MAI
RIC	0	0	0	0	0	0	97	1	0	1	1	0	0	0	0	0	0	0	0	0	0	0	0	0	0	RIC
FOR	0	0	0	0	3	1	0	74	6	3	11	0	0	0	0	0	0	0	0	0	0	0	0	0	0	FOR
PAS	0	0	0	0	1	0	0	50	41	1	2	0	1	0	0	0	0	2	1	0	1	0	0	0	0	PAS
VEG	0	0	0	0	3	0	0	12	0	77	5	0	0	0	0	0	1	0	0	0	0	0	0	0	0	VEG
LEG	0	0	0	0	4	1	0	27	1	3	63	0	0	0	0	0	0	0	0	0	0	0	0	0	0	LEG
GRA	0	4	0	0	0	0	0	16	3	14	1	58	1	1	0	1	0	1	1	0	0	0	0	0	0	GRA
OLI	0	2	0	0	0	0	0	34	7	4	1	0	32	4	0	0	0	7	8	1	0	0	0	0	0	OLI
CIT	0	1	0	0	0	0	0	7	1	6	1	1	3	77	0	2	0	1	1	0	0	0	0	0	0	CIT
NUT	0	2	0	0	1	0	0	62	5	6	6	0	5	2	3	0	0	4	2	0	0	0	0	0	0	NUT
FRT	0	2	0	0	1	0	0	24	4	10	1	2	4	14	0	30	0	4	4	0	0	0	0	0	0	FRT
GRH	2	3	3	17	0	0	0	6	1	17	1	0	2	1	0	0	43	1	1	0	0	0	0	0	1	GRH

SHR	0	0	0	0	0	0	0	3	3	0	0	0	3	0	0	0	0	64	19	3	4	0	0	0	0	SHR
BLF	0	0	0	0	0	0	0	2	4	0	0	0	2	0	0	0	0	11	78	3	1	0	0	0	0	BLF
CNF	0	0	0	0	0	0	0	2	1	0	0	0	1	0	0	0	0	20	21	52	1	0	0	1	0	CNF
LVC	0	2	0	1	0	0	0	1	3	0	0	0	0	0	0	0	0	6	1	0	83	3	0	0	0	LVC
NVA	3	2	1	20	0	0	0	3	0	0	0	0	0	0	0	0	0	1	0	0	23	44	1	0	1	NVA
BCH	2	8	2	26	0	0	0	1	0	1	0	0	0	0	0	0	0	1	0	0	2	3	48	3	2	BCH
SAL	0	1	0	3	0	0	0	7	0	1	2	0	1	1	0	0	0	2	1	2	0	0	1	61	16	SAL
WAT	0	0	0	0	0	0	0	1	0	0	0	0	0	0	0	0	0	0	0	0	0	0	0	2	94	WAT

Final map

Although in V2 each incremental increase in training samples yielded only modest improvements in OA, still the cumulative effect of using the full reference dataset for training is expected to produce a more accurate final product. For this reason, a final classification map, referred to as V3_TOT (Figure 21), was generated by training IOTA^2 on the complete set of available reference data, without retaining any samples for independent validation. This map represents the definitive output of the IOTA^2 workflow for the entire

Sardinia region. Since all reference data were used exclusively for training, no independent samples remain for quantitative accuracy assessment, and formal metrics cannot be reported.

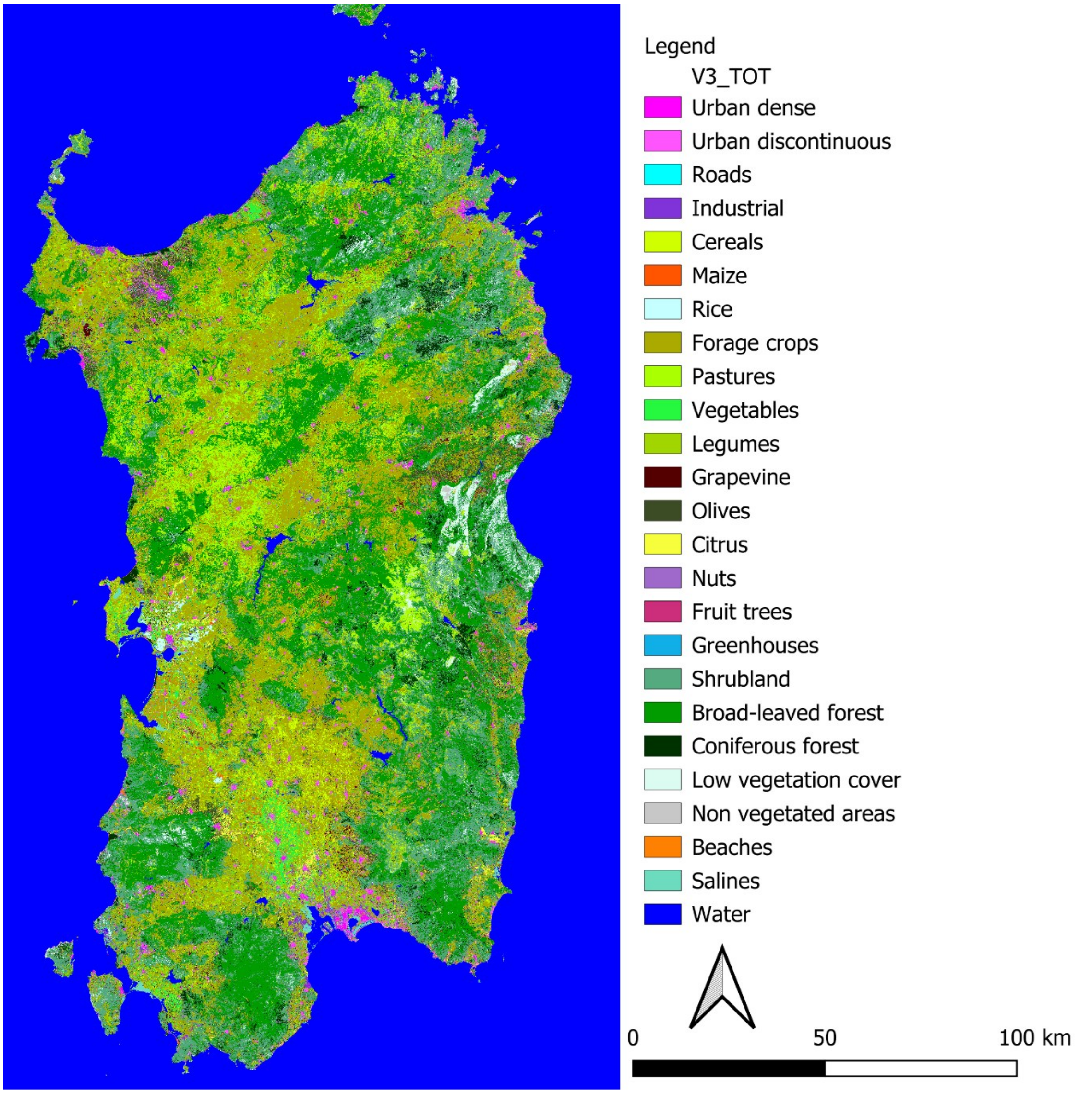

*Figure 21**:** classification map of version 3 (V3_TOT), adopting the N26 nomenclature and the full set of reference data as training.*

Considering that the calculation of the accuracy metrics for V3_TOT map was not possible, the aggregated areas of the original reference data were compared with the areas of the V3_TOT map beneath the reference data polygons (Table 10). Unlike pixel-based accuracy metrics, this aggregated approach only checks whether class areas match in order of magnitude, not their spatial distribution.

Overall, the differences between the aggregated reference data and V3_TOT datasets are smaller than those observed in the pixel-level accuracy assessment. *Rice*, *Forage crops*, and *Water* show the smallest discrepancies (≤3%), followed by *Legumes*, *Vegetables*, *Broad-leaved forest*, *Low vegetation cover*, *Maize*, *Cereals*, and *Citrus*, all with relative differences below 10%. The largest discrepancies (above 30%) are concentrated in few classes: *Nuts* (48%), *Roads* (41%), *Industrial and commercial* (32%), *Fruit trees* (29%), and *Greenhouses* (26%).

Coherently with what emerged in Table 9, *Forage crops* class emerges as the dominant confusion target across nearly all agricultural classes. Among natural vegetation classes, *Shrubland* is the most frequent misclassification destination, while urban classes tend to be confused with one another, particularly towards *Urban discontinuous*.

*Table 10**:** Comparison between the total area of the reference data dataset and the area classified by V3_TOT within those same polygons, aggregated by class across the entire Sardinia region. The table reports the absolute and relative difference between the two area estimates, as well as the most frequent misclassification target (i.e., the class that received the largest share of misassigned pixels).*

N26 nomenclature	Code	LPIS area (ha)	V3_TOT map area (ha)	Difference (ha)	Difference (%)	Major misclassified class name	Major misclassified class (ha)
Urban dense	UDN	830	621	208	25	UDC	154
Urban discontinuous	UDC	1199	1014	185	15	UDN	109
Roads	RDS	154	91	62	41	IND	21
Industrial and commercial	IND	759	519	240	32	UDC	86
Cereals	CER	6103	5537	566	9	FOR	343
Maize	MAI	1035	944	91	9	FOR	45
Rice	RIC	2484	2420	64	3	FOR	14
Forage crops	FOR	11187	10903	284	3	LEG	54
Pastures	PAS	3383	2980	403	12	FOR	288
Vegetables	VEG	5654	5310	344	6	FOR	161
Legumes	LEG	10268	9791	477	5	FOR	266

Grapevine	GRA	725	652	73	10	FOR	36
Olives	OLI	1236	1007	229	19	FOR	101
Citrus	CIT	1022	932	91	9	FOR	26
Nuts	NUT	414	217	197	48	FOR	119
Fruit trees	FRT	467	334	133	29	FOR	52
Greenhouses	GRH	169	125	44	26	VEG	11
Shrubland	SHR	1644	1433	211	13	BLF	122
Broad leaved forest	BLF	2058	1909	148	7	SHR	77
Forest coniferous	CNF	1040	776	264	25	SHR	111
Low vegetation cover	LVC	755	699	56	7	SHR	27
Non vegetated areas	NVA	515	420	95	18	LVC	61
Beaches	BCH	134	104	29	22	IND	11
Salines	SAL	437	370	67	15	FOR	17
Water	WAT	1534	1485	49	3	SAL	8

Discussion

This study had the objective of creating a first high-resolution (10 m) crop map specifically designed for Mediterranean crops. IOTA² was used for this purpose, as it contains a fully automatic workflow for map generation from satellite time series: in this way, it is possible to create updated crop maps every year, overcoming the timeliness limitation of most of existing land cover products (CLMS & EEA, 2020a; d'Andrimont et al., 2021) and the national agricultural census (ISTAT, 2020). EUCROPMAP (d'Andrimont et al., 2021) represents the most comprehensive crop map at European scale, but its focus on annual crops leaves Mediterranean perennial crops (olive groves, vineyards, citrus) uncharted, a gap that this study directly addresses. Unlike the original IOTA² application (Inglada et al., 2017), which considered a balanced land cover nomenclature across France, this study deliberately extended the agricultural component of the nomenclature to capture the diversity of Mediterranean cropping systems, while maintaining non-agricultural classes as contextual background following the Theia framework. As IOTA² was not initially developed for a highly fragmented and heterogeneous Mediterranean landscape (De Montis et al., 2017; Pelletier et al., 2016), the study also assessed how nomenclature complexity (26 vs. 32 classes) and training-sample size (10%, 50%, 100%) affect classification performance.

The comparison between N26 and N32 nomenclatures under different sampling rates (V1 experiments) highlighted that increasing the number of training samples can improve accuracy only if the nomenclature contains clear and spectrally distinguishable classes. This suggests that intrinsic class ambiguity, rather than insufficient training data, limits model performance (D'Amico et al., 2024; Fu et al., 2023). N32's low accuracy mainly derives from classes with overlapping ecological and spectral characteristics (e.g., *Arboreal pasture* confused with *Broad-leaved Forest*, *Shrubland*, and *Improved pastures*).

The V2 experiment highlighted the effects of a reduced (from 69000 to 63000 polygons), but more balanced training dataset on classification accuracy: OA decreased from 0.77 (V1) to 0.61 (V2), driven primarily by a reduction in recall while precision remained high. This pattern is consistent with a classifier trained on a narrower spectral representation of each class. With fewer training polygons, the RF learns from a more restricted portion of each class's spectral variability. The classifier maintains the ability to correctly identify the most common spectral signatures, but it misses the less frequent variants (for instance, crops with different cultivation patterns, phenology, or irrigation regimes) (Belgiu & Drăguţ, 2016). This happens even if sample size is more balanced among classes, in line with the findings of Ghassemi et al. (2022). On the other hand, a visual analysis on the maps highlights that the differences between the V1 and V2 maps are less substantial than what metrics might suggest: disagreements are concentrated mainly at field margins rather than constituting the misclassifications of entire parcels. Considering that the field margins are many (due to small and fragmented crop parcels), this leads to a high number of mixed pixels, reducing classification power, as also reported by Orynbaikyzy et al. (2020). Notably, land parcels of grapevine, olives (both relevant for Sardinian agriculture), and greenhouses are more accurately represented in V2, due to the more careful selection of their training polygons. Indeed, accuracy metrics are computed at the pixel-level, while visual analysis allows the observation of landscape patterns and their match with the satellite view.

Regarding the final V3_TOT map, this shows much better agreement with reference data on the regional scale (Table 10), with average differences across agricultural classes below 15%, substantially better than what reported by the pixel-level accuracy metric. This parcel-level validation approach is appropriate for the large-scale mapping initiative, which prioritizes regional accuracy over individual-pixel precision. Indeed, the V3_TOT map's agricultural class predictions align closely with the LPIS dataset (AGEA, 2018; Reumaux et al., 2023), which represents the most accurate and authoritative reference data available for the Sardinia region, validating the map's utility for policy and land-management applications.

Visual inspection

The V3_TOT's crop patterns can be better visualized in Figure 22, which shows a zoom across the agricultural districts of Alghero (Figure 22a, grapevine), Arborea (Figure 22b, maize-forage rotation), and Villacidro (Figure 22c, tree orchards) (ISTAT, 2020). In Alghero, large vineyards can be identified, but smaller fields are more frequently confused with spectrally similar crops such as vegetables and forage systems. The Arborea case illustrates a critical limitation of pixel-based classification: despite being dominated by maize-forage rotations, the map shows mostly forage crops. This occurs because training samples are heavily imbalanced (11000 ha of *Forage crops* vs. 1000 ha of *Maize*), causing the classifier to assign pixels to the dominant class (Belgiu & Drăguţ, 2016; Inglada et al., 2017). In Villacidro, characterized by a mosaic of tree orchards, V3_TOT map shows systematic differences with the official statistics of the agricultural census (ISTAT, 2020). Specifically, V3_TOT map identified around 1500 ha of *Olives*, 1700 ha of *Citrus*, and 200 ha of *Fruit trees*, versus 1066, 500 and 341 ha declared by ISTAT (2020), respectively. This comparison shows the difficulty of the classifier to distinguish citrus and fruit trees due to structural and phenological similarity, as documented by Campos-Taberner et al. (2020).

Inter-class confusion (Table 9 and Table 10) is dominated by *Forage crops*, which absorb validation pixels from multiple annual crops (cereals, maize, legumes, pastures) and tree crops (olives, nuts, fruit trees). This pattern reflects the wide within-class spectral and phenological variability of *Forage crops* (driven by different crop rotations, perennial mowed systems, and agroforestry contexts), as illustrated by the contrasting parcel types shown in Figure 23 (Supplementary material). Such structural and phenological variability, combined with frequent crop coexistence within fields increases the difficulty for the classifier to generate a clear and consistent map (Crespin-Boucaud et al., 2020).

Overall, this visual inspection confirms that the fragmented landscape structure of Sardinian agriculture, characterized by small parcel sizes (0.96 ha average) and high crop diversity, poses inherent challenges for achieving high classification accuracy at the regional scale (Crespin-Boucaud et al., 2020; De Montis et al., 2017; Siachalou et al., 2015).

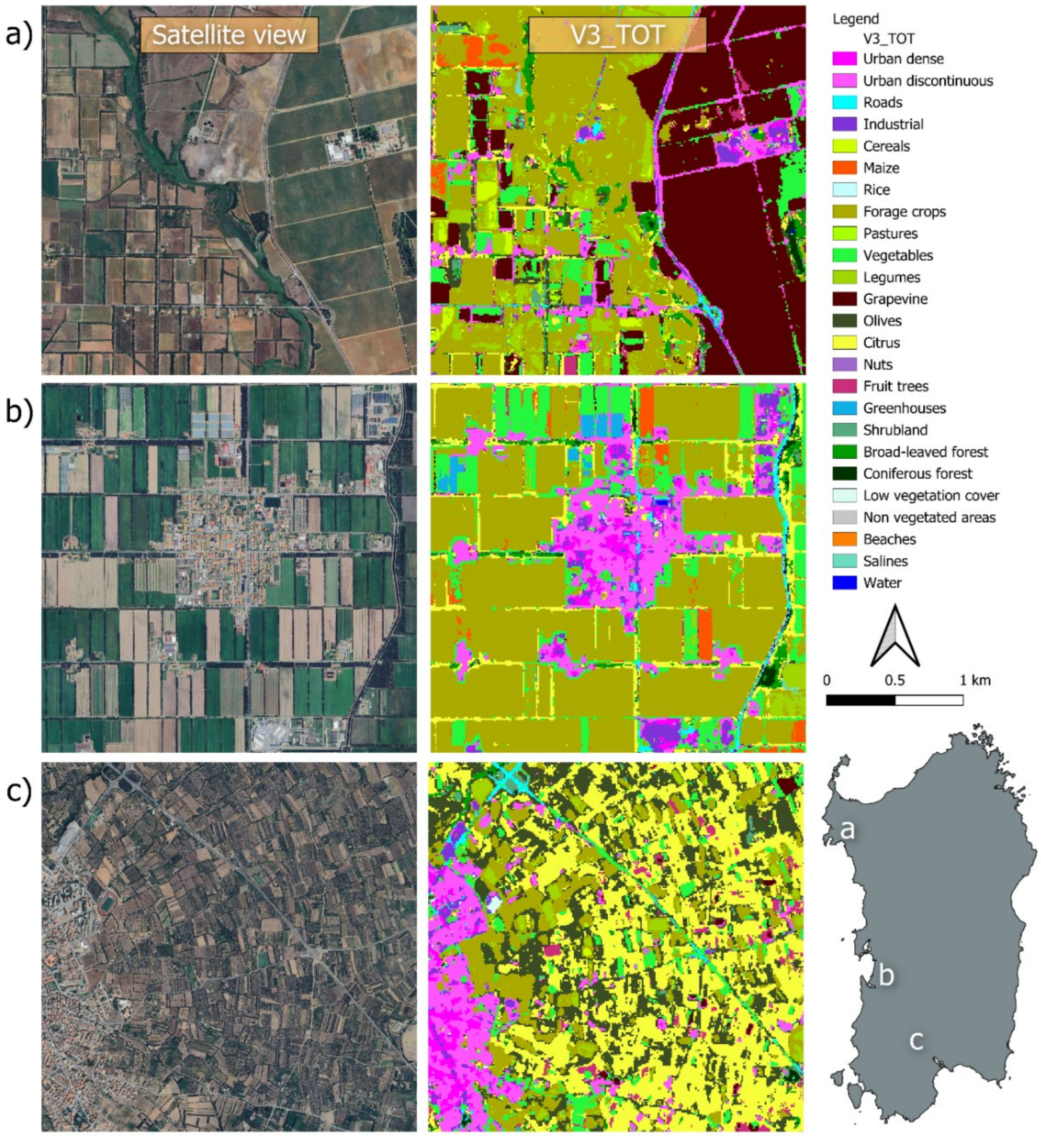

Figure 22: visual inspection of the V3_TOT map, with a zoom in three different areas of Sardinia (a. Alghero, b. Arborea, c. Villacidro) and comparison with the Satellite view.

Limitations and future perspectives

The classification performance observed in this study is fundamentally constrained by the trade-off between thematic detail and quality of the reference data. While Inglada et al. (2017) achieved an OA > 0.85 using the French RPG (Registre Parcellaire Graphique), the Italian LPIS may suffer from spatial imprecision, given the complex cultivation patterns in Sardinia (European Court of Auditors, 2016). LPIS polygons, by design, typically assign a single class to an entire field (Leonhardt et al., 2024; Reumaux et al., 2023; Schneider et al., 2023), while IOTA^2 conducts a pixel-based classification. If parcels are internally heterogeneous this leads to lower accuracy. For a Mediterranean landscape, pixel-based approaches may produce less spatially consistent maps compared to object-based methods (Belgiu & Csillik, 2018; Immitzer et al., 2016).

To address the observed confusion in complex classes like *Forage crops*, future developments will implement a multitemporal splitting strategy, creating two maps separating winter and summer vegetative cycles. In this way, it would be possible to distinguish perennial forages from the annual forages in rotation with other crops. Beyond class refinement, the crop mapping initiative can be extended to multiple years, to have a multi-year analysis of the dynamics of Sardinian crop systems. Thanks to the automatic feature of IOTA², this process can be conducted in a short time, with a significantly low computational cost compared to other methods.

Conclusion

This study generated the first high-resolution (10m) crop-specific land cover map for Mediterranean agriculture using the fully automated IOTA² processing chain applied to Sentinel-2 time series. A key contribution is the systematic evaluation of the trade-offs between thematic detail and classification performance, which is critical for crop monitoring in Mediterranean environments characterized by small, fragmented farms. The comparison between two nomenclatures with different specificity levels (N26 with 26 classes and N32 with 32 classes) demonstrated that the shorter nomenclature consistently outperforms the more detailed one across all sampling rates, achieving an OA of 0.75 at 100% sampling of training pixels, compared to 0.60 of N32. Per-class analysis reveals that crops with evident spectral signatures (e.g., *Rice*, *Vegetables*, *Grapevine*, *Citrus*) achieve higher accuracy (F-score > 0.7), while heterogenous classes (e.g., *Cereals*, *Pastures*, *Fruit trees*) show weaker performance (F-score < 0.5). The *Forage crops* class, due to its structural heterogeneity and high representativeness among reference data, tends to be over-classified and generate confusion with most of other crop classes. The automated and scalable nature of IOTA² classification enables annual updates, addressing the temporal gaps currently presents in the existing dataset (LPIS, ISTAT). This capability is essential for monitoring crop rotations and management shifts over time.

References

AGEA. (2018). OPENIACS Project—Land Parcel Identification System (LPIS) (EU Open Data Portal) [Dataset]. https://data.europa.eu/data/datasets/agea-openiacs-lpis-m002?locale=en

Belgiu, M., & Csillik, O. (2018). Sentinel-2 cropland mapping using pixel-based and object-based time-weighted dynamic time warping analysis. Remote Sensing of Environment, 204, 509–523. https://doi.org/10.1016/j.rse.2017.10.005

Belgiu, M., & Drăguţ, L. (2016). Random forest in remote sensing: A review of applications and future directions. ISPRS Journal of Photogrammetry and Remote Sensing, 114, 24–31. https://doi.org/10.1016/j.isprsjprs.2016.01.011

Campos-Taberner, M., García-Haro, F. J., Martínez, B., Izquierdo-Verdiguier, E., Atzberger, C., Camps-Valls, G., & Gilabert, M. A. (2020). Understanding deep learning in land use classification based on Sentinel-2 time series. Scientific Reports, 10(1), 17188. https://doi.org/10.1038/s41598-020-74215-5

CLMS & EEA. (2020a). CORINE Land Cover 2018 (CLC2018) (Copernicus Land Monitoring Service, European Environment Agency) [Dataset]. https://doi.org/https://doi.org/10.2909/71c95a07-e296-44fc-b22b-415f42acfdf0

CLMS & EEA. (2020b). Urban Atlas Land Cover/Land Use 2018 (vector), Europe, 6-yearly (Copernicus Land Monitoring Service, European Environment Agency) [Dataset]. https://doi.org/https://doi.org/10.2909/fb4dffa1-6ceb-4cc0-8372-1ed354c285e6

CLMS & EEA. (2023). CLCplus Backbone 2018 (vector), Europe (Copernicus Land Monitoring Service, European Environment Agency) [Dataset]. https://doi.org/https://doi.org/10.2909/d45d5114-fb86-4265-9c5a-a7225a511f7c

Crespin-Boucaud, A., Lebourgeois, V., Lo Seen, D., Castets, M., & Bégué, A. (2020). AGRICULTURALLY CONSISTENT MAPPING OF SMALLHOLDER FARMING SYSTEMS USING REMOTE SENSING AND SPATIAL MODELLING. The International Archives of the Photogrammetry, Remote Sensing and Spatial Information Sciences, XLII-3/W11, 35–42. https://doi.org/10.5194/isprs-archives-XLII-3-W11-35-2020

d'Andrimont, R., Verhegghen, A., Lemoine, G., Kempeneers, P., Meroni, M., & Van Der Velde, M. (2021). From parcel to continental scale – A first European crop type map based on Sentinel-1 and LUCAS Copernicus in-situ observations. Remote Sensing of Environment, 266, 112708. https://doi.org/10.1016/j.rse.2021.112708

D'Amico, G., Nilsson, M., Axelsson, A., & Chirici, G. (2024). Data homogeneity impact in tree species classification based on Sentinel-2 multitemporal data case study in central Sweden. International Journal of Remote Sensing, 45(15), 5050–5075. https://doi.org/10.1080/01431161.2024.2371082

De Montis, A., Martín, B., Ortega, E., Ledda, A., & Serra, V. (2017). Landscape fragmentation in Mediterranean Europe: A comparative approach. Land Use Policy, 64, 83–94. https://doi.org/10.1016/j.landusepol.2017.02.028

European Commission. (2022). Common agricultural policy. https://agriculture.ec.europa.eu/common-agricultural-policy_en

European Court of Auditors (A c. Di). (2016). The Land Parcel Identification System: A useful tool to determine the eligibility of agricultural land - but its management could be further improved; Special report No 25, 2016. Publications Office. https://doi.org/10.2865/19472

Fendrich, A. N., Matthews, F., Van Eynde, E., Carozzi, M., Li, Z., d'Andrimont, R., Lugato, E., Martin, P., Ciais, P., & Panagos, P. (2023). From regional to parcel scale: A high-resolution map of cover crops across Europe combining satellite data with statistical surveys. Science of The Total Environment, 873, 162300. https://doi.org/10.1016/j.scitotenv.2023.162300

Foody, G. M. (2020). Explaining the unsuitability of the kappa coefficient in the assessment and comparison of the accuracy of thematic maps obtained by image classification. Remote Sensing of Environment, 239, 111630. https://doi.org/10.1016/j.rse.2019.111630

Fu, Y., Shen, R., Song, C., Dong, J., Han, W., Ye, T., & Yuan, W. (2023). Exploring the effects of training samples on the accuracy of crop mapping with machine learning algorithm. Science of Remote Sensing, 7, 100081. https://doi.org/10.1016/j.srs.2023.100081

Ghassemi, B., Dujakovic, A., Żółtak, M., Immitzer, M., Atzberger, C., & Vuolo, F. (2022). Designing a European-Wide Crop Type Mapping Approach Based on Machine Learning Algorithms Using LUCAS Field Survey and Sentinel-2 Data. Remote Sensing, 14(3), 541. https://doi.org/10.3390/rs14030541

Immitzer, M., Vuolo, F., & Atzberger, C. (2016). First Experience with Sentinel-2 Data for Crop and Tree Species Classifications in Central Europe. Remote Sensing, 8(3), 166. https://doi.org/10.3390/rs8030166

Inglada, J., Vincent, A., Arias, M., Tardy, B., Morin, D., & Rodes, I. (2017). Operational High Resolution Land Cover Map Production at the Country Scale Using Satellite Image Time Series. Remote Sensing, 9(1), 95. https://doi.org/10.3390/rs9010095

iota2-project. (2019). Iota2 [Source code] [Framagit]. https://framagit.org/iota2-project/iota2/

ISTAT. (2018). IstatData—Superfici agricole in Sardegna [Dataset]. https://esploradati.istat.it/databrowser/#/it/dw/categories/IT1,Z1000AGR,1.0/AGR_CRP/DCSP_COLTIVAZIONI

ISTAT. (2020). Censimento dell'Agricoltura 2020—Unità agricole con superficie agricola utilizzata per tipo di coltivazione e zona altimetrica [Dataset]. https://esploradati.istat.it/databrowser/#/it/censimentoagricoltura/categories/IT1,Z1100AGR,1.0/AU/IT1,DF_DCAT_CENSAGRIC2020_UA_CROPS_2,1.0

ISTAT. (2025). Bilancio demografico mensile anno 2025 (dati provvisori) [Dataset]. https://doi.org/https://demo.istat.it/app/?i=D7B

Jänicke, C., Petersen, K. A., Schmidts, P., Müller, D., & Jepsen, M. R. (2025). Field and farm-level data on agricultural land use for the European Union. Scientific Data, 12(1), 1050. https://doi.org/10.1038/s41597-025-05210-6

Landis, J. R., & Koch, G. G. (1977). The Measurement of Observer Agreement for Categorical Data. Biometrics, 33(1), 159. https://doi.org/10.2307/2529310

Leonhardt, H., Wesemeyer, M., Eder, A., Hüttel, S., Lakes, T., Schaak, H., Seifert, S., & Wolff, S. (2024). Use cases and scientific potential of land use data from the EU's Integrated Administration and Control System: A systematic mapping review. Ecological Indicators, 167, 112709. https://doi.org/10.1016/j.ecolind.2024.112709

Li, C., Ma, Z., Wang, L., Yu, W., Tan, D., Gao, B., Feng, Q., Guo, H., & Zhao, Y. (2021). Improving the Accuracy of Land Cover Mapping by Distributing Training Samples. Remote Sensing, 13(22), 4594. https://doi.org/10.3390/rs13224594

MASAF. (2023). Piano del settore sughericolo 2022-2026. Ministero dell'agricoltura, della sovranità alimentare e delle foreste. https://www.masaf.gov.it/flex/cm/pages/ServeBLOB.php/L/IT/IDPagina/19802

Mattioli, W., Romano, R., Botticelli, D., Chirici, G., D'Amico, G., Giuliarelli, D., Pecchi, M., & Corona, P. (2025). The Forest Map of Italy (CFI2020): An updated portrait of Italian forests. Forest@ - Rivista di Selvicoltura ed Ecologia Forestale, 22(3), 39–44. https://doi.org/10.3832/efor4836-022

Orynbaikyzy, A., Gessner, U., Mack, B., & Conrad, C. (2020). Crop Type Classification Using Fusion of Sentinel-1 and Sentinel-2 Data: Assessing the Impact of Feature Selection, Optical Data Availability, and Parcel Sizes on the Accuracies. Remote Sensing, 12(17), 2779. https://doi.org/10.3390/rs12172779

Paris, P., Camilli, F., Rosati, A., Mantino, A., Mezzalira, G., Dalla Valle, C., Franca, A., Seddaiu, G., Pisanelli, A., Lauteri, M., Brunori, A., Re, G. A., Sanna, F., Ragaglini, G., Mele, M., Ferrario, V., & Burgess, P. J. (2019). What is the future for agroforestry in Italy? Agroforestry Systems, 93(6), 2243–2256. https://doi.org/10.1007/s10457-019-00346-y

Pelletier, C., Valero, S., Inglada, J., Champion, N., & Dedieu, G. (2016). Assessing the robustness of Random Forests to map land cover with high resolution satellite image time series over large areas. Remote Sensing of Environment, 187, 156–168. https://doi.org/10.1016/j.rse.2016.10.010

Reumaux, R., Chopin, P., Bergkvist, G., Watson, C. A., & Öborn, I. (2023). Land Parcel Identification System (LPIS) data allows identification of crop sequence patterns and diversity in organic and conventional farming systems. European Journal of Agronomy, 149, 126916. https://doi.org/10.1016/j.eja.2023.126916

Schneider, M., Schelte, T., Schmitz, F., & Körner, M. (2023). EuroCrops: The Largest Harmonized Open Crop Dataset Across the European Union. Scientific Data, 10(1), 612. https://doi.org/10.1038/s41597-023-02517-0

Sedda, L., Delogu, G., & Dettori, S. (2011). Forty-Four Years of Land Use Changes in a Sardinian Cork Oak Agro- Silvopastoral System: A Qualitative Analysis. The Open Forest Science Journal, 4(1), 57–66. https://doi.org/10.2174/1874398601104010057

Siachalou, S., Mallinis, G., & Tsakiri-Strati, M. (2015). A Hidden Markov Models Approach for Crop Classification: Linking Crop Phenology to Time Series of Multi-Sensor Remote Sensing Data. Remote Sensing, 7(4), 3633–3650. https://doi.org/10.3390/rs70403633

Sitokonstantinou, V., Papoutsis, I., Kontoes, C., Lafarga Arnal, A., Armesto Andrés, A. P., & Garraza Zurbano, J. A. (2018). Scalable Parcel-Based Crop Identification Scheme Using Sentinel-2 Data Time-Series for the Monitoring of the Common Agricultural Policy. Remote Sensing, 10(6), 911. https://doi.org/10.3390/rs10060911

Tan, Y.-C., Duarte, L., & Teodoro, A. C. (2024). Comparative Study of Random Forest and Support Vector Machine for Land Cover Classification and Post-Wildfire Change Detection. Land, 13(11), 1878. https://doi.org/10.3390/land13111878

Theia. (2018). Land Cover Map. https://www.theia-land.fr/en/blog/product/land-cover-map/

Yi, Z., Jia, L., & Chen, Q. (2020). Crop Classification Using Multi-Temporal Sentinel-2 Data in the Shiyang River Basin of China. Remote Sensing, 12(24), 4052. https://doi.org/10.3390/rs12244052

Zhang, C., Kerner, H., Wang, S., Hao, P., Li, Z., Hunt, K. A., Abernethy, J., Zhao, H., Gao, F., Di, L., Guo, C., Liu, Z., Yang, Z., Mueller, R., Boryan, C., Chen, Q., Beeson, P. C., Zhang, H. K., & Shen, Y. (2025). Remote sensing for crop mapping: A perspective on current and future crop-specific land cover data products. Remote Sensing of Environment, 330, 114995. https://doi.org/10.1016/j.rse.2025.114995

Supplementary material

Table 11: Crop classes of the LPIS database in Sardinia, selecting the classes with at least 0.1 ha and aggregated in the extended (N32) versus simplified (N26) nomenclature.

Crop name	Area (ha)	N32 name	N26 name
WHEAT (DURUM WHEAT)	2541.6	Cereals	Cereals
SPELLED (EINKORN / FARRO)	14.3	Cereals	Cereals
TRITICALE	280.8	Cereals	Cereals
TURANICUM WHEAT OR ORIENTAL WHEAT OR KHORASAN WHEAT	5.1	Cereals	Cereals
OAT	4058.6	Cereals	Cereals
WHEAT (BREAD WHEAT / COMMON WHEAT)	0.6	Cereals	Cereals
MILLET	2.7	Cereals	Cereals
RYE	0.9	Cereals	Cereals
SORGHUM	29.3	Cereals	Cereals
BARLEY	2486.4	Cereals	Cereals
MAIZE (CORN)	140.4	Maize	Maize
PADDY RICE	376.2	Rice	Rice
RYEGRASS (LOLLIUM)	516.3	Forage crops	Forage crops

RYEGRASS	2.1	Forage crops	Forage crops
VETCHES	404.4	Forage crops	Forage crops
CLOVER	4258.0	Forage crops	Forage crops
TURF (SOD)	7.3	Forage crops	Forage crops
ALFALFA (MEDICAGO SATIVA L. VARIETIES)	5.6	Forage crops	Forage crops
RYEGRASS (LOLIUM × BOUCHEANUM KUNT.)	1.3	Forage crops	Forage crops
CLOVER (TRIFOLIUM ALEXANDRINUM L.)	98.9	Forage crops	Forage crops
CLOVER (TRIFOLIUM HYBRIDUM L.)	10.5	Forage crops	Forage crops
CLOVER (TRIFOLIUM PRATENSE L.)	1.0	Forage crops	Forage crops
COMMON VETCH	57.2	Forage crops	Forage crops
HAIRY VETCH	15.9	Forage crops	Forage crops
ALFALFA	595.9	Forage crops	Forage crops
ARABLE LAND	411.7	Forage crops	Forage crops
CLOVER (TRIFOLIUM SQUARROSUM L.)	23.3	Forage crops	Forage crops
FORAGE CROP	9941.9	Forage crops	Forage crops
SULLA (HEDYSARUM CORONARIUM)	327.7	Forage crops	Forage crops
MEADOW-PASTURE	12456.3	Improved pasture	Pastures
POLYPHYTIC PASTURE WITH OUTCROPPING ROCK TARE 20%	13906.3	Pastures	Pastures
POLYPHYTIC PASTURE WITH OUTCROPPING ROCK TARE 50%	251.7	Pastures	Pastures
POLYPHYTIC PASTURE	10202.9	Pastures	Pastures
POLYPHYTIC MEADOW	4030.0	Pastures	Pastures
NATURAL PERMANENT GRASSLAND WITH ENVIRONMENTAL CONSTRAINTS - TARE 50%	1.9	Pastures	Pastures
PASTURE WITH TRADITIONAL PRACTICES	14586.1	Arboreal pasture	-
WOOD PASTURE - TARE 50%	17909.1	Arboreal pasture	-
WOOD PASTURE WITH SHRUBS TARE 20%	6155.5	Arboreal pasture	-
CARROT	6.2	Vegetables	Vegetables
SWEET POTATO	0.7	Vegetables	Vegetables
CAULIFLOWER	5.5	Vegetables	Vegetables
LETTUCE (BABY LETTUCE / CUT LETTUCE)	11.1	Vegetables	Vegetables
MELON	17.3	Vegetables	Vegetables
OPEN-FIELD VEGETABLES	267.0	Vegetables	Vegetables
TOMATO	26.2	Vegetables	Vegetables
HOUSEHOLD VEGETABLE GARDENS	22.4	Vegetables	Vegetables
POTATO	68.3	Vegetables	Vegetables
ASPARAGUS	20.5	Vegetables	Vegetables
ARTICHOKE	652.9	Vegetables	Vegetables
CHICORY	3.0	Vegetables	Vegetables
ONION (INCLUDING LONG TYPE / ECHALION)	5.9	Vegetables	Vegetables
WATERMELON	9.7	Vegetables	Vegetables
FENNEL	21.0	Vegetables	Vegetables
STRAWBERRY	1.7	Vegetables	Vegetables
PEPPER	1.1	Vegetables	Vegetables

COURGETTE (ZUCCHINI)	1.7	Vegetables	Vegetables
EGGPLANT (AUBERGINE)	1.4	Vegetables	Vegetables
LENTILS	12.5	Legumes	Legumes
PEA	294.5	Legumes	Legumes
GRASS PEA	1.9	Legumes	Legumes
CHICKPEA	44.8	Legumes	Legumes
FAVA BEAN (BROAD BEAN)	1249.1	Legumes	Legumes
GRAIN LEGUMES	34.0	Legumes	Legumes
LUPIN	44.4	Legumes	Legumes
VINEYARD	1300.5	Grapevine	Grapevine
OLIVE GROVE	2310.3	Olives	Olives
ORANGE	78.4	Citrus	Citrus
MANDARIN	3.2	Citrus	Citrus
TANGERINE (CLEMENTINE)	13.2	Citrus	Citrus
LEMON	5.4	Citrus	Citrus
CITRUS FRUITS	89.8	Citrus	Citrus
NUT TREE CROPS	1.3	Nuts	Nuts
ALMOND TREE	84.8	Nuts	Nuts
HAZELNUT TREE	3.1	Nuts	Nuts
APPLE TREE	7.6	Fruit trees	Fruit trees
PEAR TREE	13.1	Fruit trees	Fruit trees
MYRTLE	18.4	Fruit trees	Fruit trees
PRICKLY PEAR	1.9	Fruit trees	Fruit trees
PERSIMMON (KAKI, INCLUDING FUYU-TYPE)	2.9	Fruit trees	Fruit trees
APRICOT TREE	3.0	Fruit trees	Fruit trees
CHERRY TREE	2.4	Fruit trees	Fruit trees
PLUM TREE	2.3	Fruit trees	Fruit trees
FAMILY ORCHARDS	0.6	Fruit trees	Fruit trees
PEACH TREE	33.6	Fruit trees	Fruit trees
NECTARINE PEACH TREE	1.1	Fruit trees	Fruit trees
CHESTNUT TREE	40.4	Tree crops	-
CITRON TREE	0.8	Tree crops	-
POPPLAR	15.0	Tree crops	-
PAULOWNIA TOMENTOSA	3.5	Tree crops	-
MARITIME PINE	0.5	Tree crops	-
CYPRESS	0.8	Tree crops	-
PINE	3.2	Tree crops	-
HOLM OAK	3.2	Tree crops	-
CORK OAK	1.5	Tree crops	-
TREE CROPS (ARBORICULTURE)	741.7	Tree crops	-
FOREST	3447.1	Tree crops	-
SPECIALIZED TREE CROPS	600.4	Tree crops	-
AGROFORESTRY SYSTEM (WITH HERBACEOUS CROPS)	49.8	Tree crops	-

EUCALYPTUS	239.8	Tree crops	-
MIXED TREE CROPS (SEVERAL TREE SPECIES)	33.2	Tree crops	-
TREES IN ROWS	8.8	Tree crops	-
GROUPS OF TREES AND GROVES	34.5	Tree crops	-
ISOLATED TREES	1.6	Tree crops	-
DOWNY OAK	50.2	Tree crops	-
MILK THISTLE	5.6	Ornamental and Aromatics	-
HELICHRYSUM	1.3	Ornamental and Aromatics	-
LAVENDER	1.1	Ornamental and Aromatics	-
AROMATIC, MEDICINAL AND SPICE PLANTS	1.6	Ornamental and Aromatics	-
ORNAMENTAL PLANTS	3.4	Ornamental and Aromatics	-
SAFFRON	2.6	Ornamental and Aromatics	-
GREENHOUSES	22.2	Greenhouses	Greenhouses

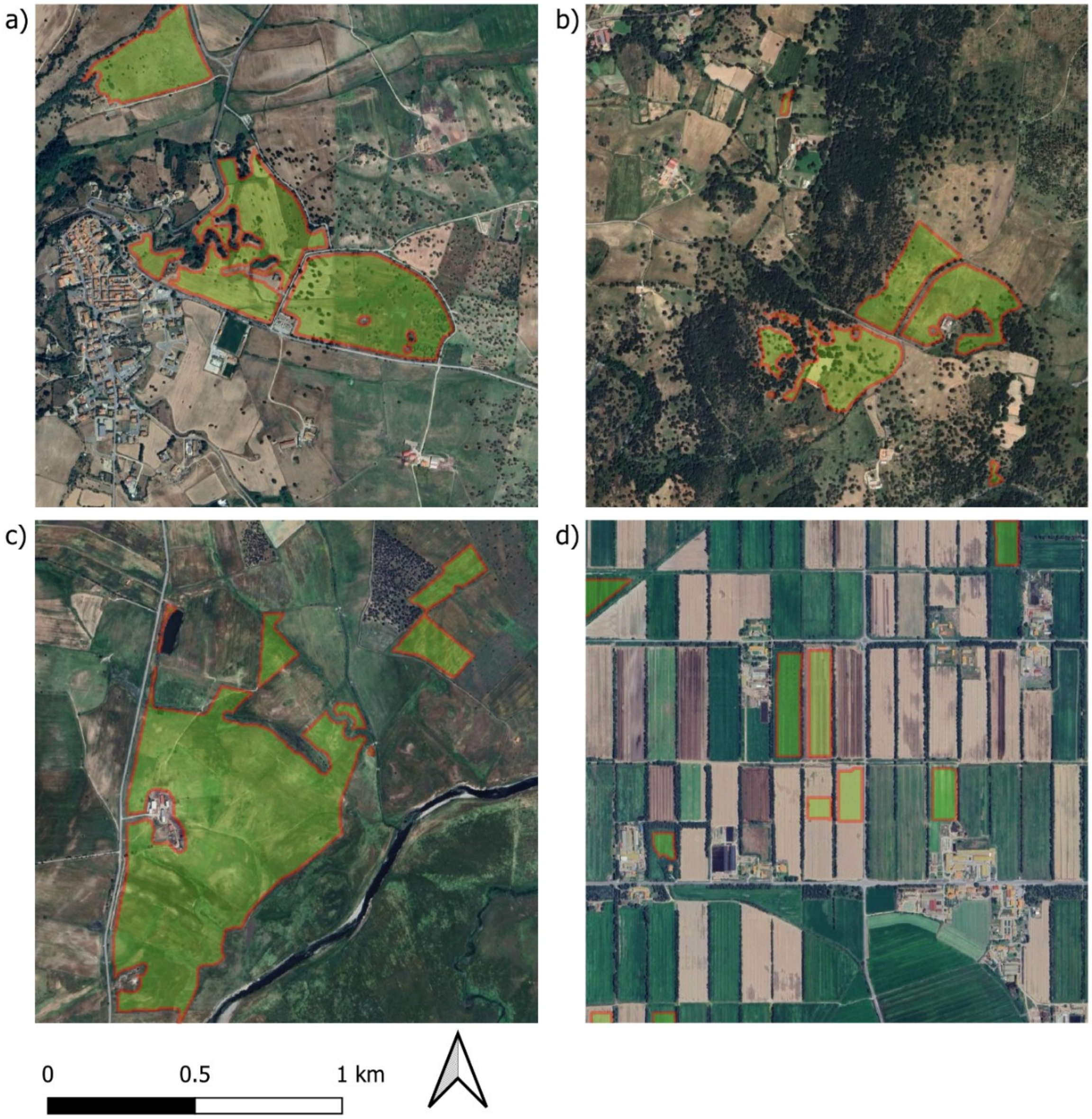

Figure 23: visual inspection of the LPIS class Forage crop across Sardinian landscape

Chapter 5. Exploring basin-level water management strategies under climate change: a narrative-based decision support tool applied to Sardinia

Andrea Borgo[a,b], Annamaria Mazzoni[b], Elisa Delpiazzo[b], Lisa Napolitano[b], Guido Rianna[b], Simone Mereu[b,c], Serena Marras[a,b], Antonio Trabucco[b], Muhammad Faizan Aslam[b], Marta Debolini[b]

(a) Department of Agriculture, University of Sassari, Viale Italia, 39a, 07100 Sassari, Italy

(b) CMCC Foundation – Euro-Mediterranean Centre on Climate Change, Italy

(c) Institute of BioEconomy, Italian National Research Council, Italy

Abstract

Agriculture is the largest water-consuming sector in the Mediterranean, where climate change and socio-economic pressures intensify hydro-climatic stress and competition among sectors, especially during peak demand. Evidence shows that farm-level irrigation efficiency does not automatically lead to basin-wide water savings. The ACQUAOUNT project addresses this challenge by testing digital tools for sustainable irrigation and Integrated Water Resources Management (IWRM) in Sardinia, Tunisia, Lebanon, and Jordan. One of the core innovations is ACQUAOUNT-DST, a narrative-based Decision Support Tool (DST), which integrates climate projections, hydrological modeling, agricultural water demand, and socio-economic evaluation. This study addresses the application of ACQUAOUNT-DST in Sardinia region, specifically in the Tirso district, characterized by an intense exploitation of water for agricultural purposes. ACQUAOUNT-DST is built on a modular framework: a climate module that estimates hydrological inflows combining observational data with bias-corrected CMIP6 ensemble and ERA5-Land reanalysis, a sectoral demand module that estimates water demand for the different sectors, a water budget model that combines inflows and outflows and evaluates reservoir's storage changes and an avoided losses module which estimates the avoided losses of each narrative based on a set of co-designed socio-economic indicators. The DST investigates a set of narratives which span from business-as-usual to the application of farm and basin level management strategies, under current (1991-2020) and future (2021-2070) climate conditions, under the shared socio-economic pathways SSP1-2.6 and SSP3-7.0. Results tested in Sardinia reveal a persistent

paradox: while optimized irrigation reduces water shortages and enhances crop yields and farmer income, especially under SSP1-2.6 and partly under SSP3-7.0 scenarios to 2070, these gains do not automatically translate into basin-level water conservation. Economic accessibility and reinvestment of efficiency gains often drive expanded water use, exacerbating competition among agriculture, urban, and ecosystem needs. Complementary measures, such as reducing distribution losses, show limited direct impact when combined with measures that intensify productivity and water use exploitation.

These findings highlight that technical efficiency alone is insufficient for climate-resilient water management. Instead, basin-level sustainability requires aligning farmers' incentives with collective governance goals. ACQUAOUNT-DST proves valuable not only as a modeling platform but also as a strategic dialogue tool: through co-designed narratives, it enables stakeholders to test "what-if" scenarios, negotiate trade-offs, and propose equitable water allocation strategies.

Introduction

Mediterranean regions are widely recognized as climate change hotspots, where rising temperatures, declining precipitation and increasing climate variability are expected to intensify water scarcity and hydrological extremes (Lionello et al., 2014). Recent assessments highlight that the Mediterranean basin is warming faster than the global average, with significant implications for water availability, agricultural productivity and ecosystem stability (Cramer et al., 2018b; Giorgi & Lionello, 2008). These trends are particularly critical in semi-arid island contexts such as Sardinia, where water resources are highly dependent on reservoir systems and strongly influenced by interannual climate variability. In such environments, water availability is already characterized by structural imbalances between supply and demand, and climate change is expected to exacerbate these pressures over the coming decades.

In a context of water scarcity, available water for human purposes is subjected to more intense competition among sectors (Adamovic et al., 2019a; Carmona-Moreno et al., 2021; Ferragina & Canitano, 2014a). Irrigated agriculture often represents the dominant water use among sectors and plays a key role in regional economies and food production (Rodríguez Díaz et al., 2007b). With climate change, irrigation water is expected to increase of 10% to 16% by 2050 (Crovella et al., 2022; Daccache et al., 2014; Masia et al., 2021b). At the same time, urban water demand needs to be addressed considering demographic and tourism dynamics, while environmental policies require the maintenance of ecological flows and the protection of aquatic ecosystems. In addition, reservoir systems often serve multiple purposes, including hydropower generation and flood regulation. These concurrent demands generate complex trade-offs among agricultural productivity, energy production, ecosystem protection and urban supply. Managing these competing objectives requires integrated approaches capable of capturing interactions among water, energy, food and ecosystems, as emphasized by the Water–Energy–Food–Ecosystem (WEFE) Nexus framework (Adamovic et al., 2019a; De Roo et al., 2021; European Commission, 2024; Lucca et al., 2023).

In this context, Decision Support Tools (DSTs) have emerged as a key instrument to support water management under uncertainty (Koutsoyiannis et al., 2002; Serrat-Capdevila et al., 2011). DSTs are designed to integrate data, models and stakeholder knowledge to explore alternative management strategies and support transparent decision-making processes (Serrat-Capdevila et al., 2009). Within water resources management, DSTs typically combine hydrological models with socio-economic and policy components to evaluate the consequences of different allocation rules, infrastructure operations or demand-management measures. Their relevance has increased in recent years due to the growing need to evaluate climate change impacts and identify adaptive strategies for water systems.

Several studies have developed integrated modelling frameworks to support water management decisions. Andreu et al., (1996) deployed AQUATOOL, a generalized DST for decision-making in complex basins, with multiple reservoirs, aquifers and water demands. Giupponi et al. (2004) released a DST software for the sustainable management of water resources at the catchment scale, providing quantitative indicators co-developed with the end-users. One of the most widely adopted tools is WEAP (Yates et al., 2005), a demand-driven, scenario-based decision support model for integrated water resource planning. The main feature of WEAP is its ability to link hydrology with water infrastructure and socio-economic water demands inside a single modelling framework. More recent studies have also applied nexus-oriented modelling frameworks to evaluate cross-sectoral interactions among water, energy, food and ecosystems, demonstrating the importance of integrated tools for addressing resource conflicts under climate change (Correa-Cano et al., 2022; Martinez et al., 2018; Ramirez et al., 2022; Trabucco et al., 2018).

Despite these advances, many existing tools require large datasets and complex calibration procedures, which may limit their applicability in regions where monitoring systems are incomplete or fragmented. Mediterranean basins often face such data constraints, while at the same time requiring flexible tools capable of exploring climate uncertainty and competing sectoral demands. There is therefore a need for modelling approaches that balance integration across sectors with practical usability for decision-making processes.

This study presents ACQUAOUNT-DST, a decision support tool designed to simulate water availability and allocation dynamics within the Tirso River Basin in Sardinia. The tool integrates climate projections, hydrological processes and sectoral water demands within a modelling framework that links environmental, economic and social indicators. The system allows the exploration of alternative management strategies by combining CMIP6 climate pathways (SSP1-2.6 and SSP3-7.0) with different reservoir operation and irrigation efficiency scenarios, also called as “narratives”. Through this integrated approach, the tool aims to support the evaluation of trade-offs among agricultural production, ecosystem pressures and water allocation equity, while providing stakeholders with a transparent framework to explore future water management pathways under climate uncertainty.

Materials and Methods

Study Area

The study focuses on the Tirso River basin located in central–western Sardinia (Italy), one of the main hydrological systems of the island. The Tirso River extends for approximately 152 km and drains a catchment area of about 3,377 km^2, representing nearly 14% of the regional territory.

Water regulation within the basin is primarily ensured by the Omodeo reservoir system, one of the largest artificial reservoirs in Italy. The reservoir acts as the central storage and regulation node for water supply, irrigation, and hydropower generation. The current reservoir system provides a maximum authorized storage of approximately 450 million cubic meters, making it the largest strategic water reserve on the island.

From a climatic perspective, Sardinia exhibits typical Mediterranean conditions characterized by hot and dry summers and mild, wet winters. Precipitation is strongly seasonal and highly variable between years (600 ± 400 mm/year, Trabucco et al., 2018), leading to recurrent drought episodes that significantly affect water availability. These climatic characteristics make reservoir-based regulation essential for ensuring water supply throughout the year.

Water use in Sardinia is highly sectorized. Irrigated agriculture represents the dominant water user (69.4%), followed by urban water use (25.4%), which depends on the seasonal fluctuations of tourist flows, and industrial (5.2%) (Trabucco et al., 2018).

Water governance in Sardinia is centrally coordinated at the regional level through the River Basin District Authority (ADIS), which defines planning and allocation rules under the EU Water Framework Directive (European Parliament and Council, 2000), while the regional water agency ENAS operates and manages the Regional Multisectoral Water System (SIMR, Regione Autonoma della Sardegna, 2022), including reservoirs, conveyance infrastructure, and operational water releases. To optimize water allocation, the SIMR subdivided the region into seven districts, as illustrated in *Figure 24*. Within this framework, water stored in major reservoirs such as Lake Omodeo is allocated annually among the main sectors, irrigation, urban supply, and industrial uses, through operational plans prepared by ENAS and based on requests from users such as the Oristanese Reclamation Consortium (CBO) and the public water utility. In the Tirso basin, irrigation represents the dominant use, serving approximately 18,000 ha of agricultural land, while urban and industrial demands are partly satisfied through groundwater resources. Water allocation and reservoir operations are further regulated through a regional drought management system based on a statistical indicator of water availability, which defines four states (Normal, Pre-Alert, Alert, Emergency) and triggers progressively stricter management measures prioritizing essential uses such as drinking water.

Figure 24: Framework of Hydrographic Zone No. 2 (Tirso) and delineation of the Tirso River basin

Decision Support Tool Structure

The ACQUAOUNT-DST is a modular system that integrates climatic, hydrological and socio-economic modelling components to simulate water availability and allocation dynamics within the basin. The modular framework of the DST considers different processes affecting water resources, and the interlinkages are represented through interconnected modelling components (*Figure 25*).

ACQUAOUNT-DST consists of four main modules: the Climate Module, the Water Budget Module, the Sectoral Water Demand Module (in this case, Irrigation and urban demand) and the Avoided Losses Module. These modules are connected sequentially but exchange information dynamically. Climate variables determine inflow conditions in the Water Budget Module and the sectoral water demands of the Sectoral Demand Module. Parallelly, the resulting storage levels constrain sectoral water allocations with the application of the management rules. Finally, the Avoided Losses Module evaluates the implications of these allocations in terms of socio-economic and environmental indicators.

The modular architecture allows the tool to simulate system behavior under alternative climate scenarios and water management strategies while maintaining transparency in the representation of physical and socio-economic processes.

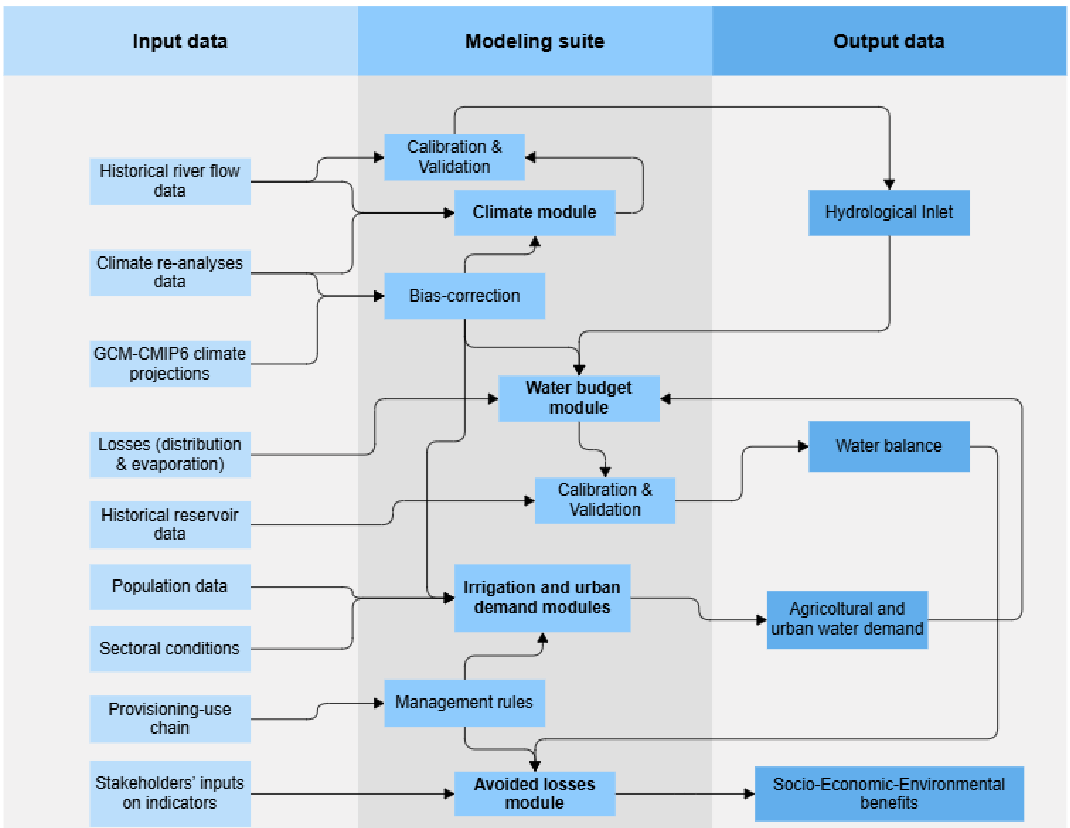

Figure 25. Workflow oft he Decision Support Tool for the Tirso water basin

Water Management Rules

As introduced in Section 2.1, the Sardinia region regulates water allocation and reservoir management by monitoring water availability in the reservoir, applying restrictions in the releases of water according to specific thresholds (Regione Autonoma della Sardegna, 2022). Operational decisions are guided by a regional drought indicator ranging from 0 to 1 that classifies water availability into four states (Normal, Pre-Alert, Alert, Emergency). The indicator is derived from long-term simulations of the regional reservoir system, where synthetic hydrological series are used to estimate the non-exceedance probability of stored water volumes for each month of the year. In this framework, lower indicator values correspond to lower storage conditions and higher drought risk. To integrate this mechanism into ACQUAOUNT-DST, the indicator was translated into operational thresholds for the Omodeo lake by associating each drought class with corresponding reservoir storage volumes. This linkage was obtained by scaling the Tirso–Flumendosa system indicator according to Omodeo lake's contribution to the total storage capacity (about 42%) and identifying storage levels that reproduce the same drought state classification. The resulting thresholds are reported in *Table 12* and ACQUAOUNT-DST to trigger management responses directly from simulated reservoir storage levels while remaining consistent with the regional drought monitoring framework.

Table 12: Correlation between drought indicator class and Omodeo Lake's storage volume

State of the World	**Drought Indicator**	**Omodeo Lake Storage Threshold**
Normal (N)	I= 1 - 0.5	250 Mm^3 and above
Pre-Alert (P-A)	I= 0.3 - 0.5	249-150 Mm^3
Alert (A)	I= 0.15 - 0.3	149-75 Mm^3
Emergency (E)	I= 0 - 0.15	74 Mm^3 and below

Climate module

The Climate Module provides the estimates of the hydrological inlet to the Omodeo Lake using a climate-responsive inflow forecasting methodology. This hydrological inlet corresponds to the flow of the Tirso River into the reservoir, which includes upstream runoff and direct precipitation. In the Sardinia application, the module uses bias-corrected CMIP6 climate projections under the socio-economic pathways SSP1-2.6 and SSP-3-7.0 (period 2021-2070), along with historical (period 1991-2020) and reanalysis climate data, to simulate both natural and treated wastewater inflows. CMIP6 data relies on seven regional climate models (*Table 16*). Bias correction adopts Empirical Quantile Mapping to remove systematic biases of climate models, by mapping the quantiles of the modeled distribution to the corresponding quantiles of the observed distribution (Gudmundsson et al., 2012; Piani et al., 2010). Input data for the Climate Module include:

- Historical river flow data (used for calibration and validation of the inflow model).
- Bias-corrected CMIP6 climate projections.
- Climate re-analysis data - ERA5-Land (1991-2020).

The hydrological inlet calculated by this module and used as a key input to the Water Budget Module represents the total inflow to Omodeo Lake. This inflow is primarily provided by the Tirso River, which constitutes the main course, and by an additional lateral contribution from the Massari River, crossing the municipality of Allai.

To simulate the natural inflow dynamics in a climate-responsive manner, a dedicated inflow forecasting methodology has been developed. The forecasting process relies on both historical and projected climate data:

- ERA5-Land Reanalysis Data (1991-2024): High-resolution gridded precipitation and temperature data are used to construct a baseline climatology and to train the forecasting model using observed inflow data, inclusive of wastewater contributions.

- Bias-Corrected CMIP6 Climate Projections: Future inflow conditions are assessed under two Shared Socioeconomic Pathways (SSPs), SSP1-2.6 and SSP3-7.0, both covering the period 2021-2070. Climate outputs are bias-corrected to ensure consistency with observed conditions, as described in *D5.2*. The historical reference period (1991-2020) is used for model validation and comparison.

The inflow to the reservoir is estimated through a climate-responsive modelling approach that links atmospheric variables with observed river discharge. The method combines historical inflow observations with climate data derived from reanalysis products and bias-corrected climate projections.
Hydrological predictors are derived from precipitation and temperature data. Evapotranspiration is estimated using a simplified Hargreaves formulation:

$$ET = 0.023 \cdot (T_{mean} + 17.8) \cdot \sqrt{T_{range}} \cdot Ra$$

Eq. 1

where T_{range} is fixed at 15°C and solar radiation (Ra) at 31 MJ/m²/day.

The water balance is computed as the difference between cumulative precipitation and cumulative evapotranspiration over selected antecedent periods (e.g., 2, 7, or 10 days). This metric provides a quick assessment of the net water input to the catchment and serves as an important predictor for inflow dynamics.

These metrics form the base hydrological predictors used in the inflow forecasting model. The core of the inflow forecasting approach is the application of the K-Nearest Neighbors (KNN) algorithm, a nonparametric, data-driven method commonly used for both classification and regression tasks. In this context, KNN operates as a regression model:

- Given a new observation defined by hydrological predictors (e.g., cumulative precipitation, water balance), the algorithm searches the historical dataset for the k most similar past observations (neighbors). Similarity is assessed using Euclidean distance in the multi-dimensional predictor space.
- The inflow associated with the new observation is estimated by averaging the observed inflow values of these k nearest neighbors. This approach is particularly suitable for hydrological applications because it does not assume any specific functional relationship between predictors and inflow, it can capture complex, non-linear interactions often present in hydrological processes and it is relatively simple and interpretable.

To test the sensitivity of predictions, two neighborhood sizes were evaluated, k = 5 and k = 20 neighbors. Several predictor combinations were explored to identify the best-performing model configurations:

- Cumulative precipitation.
- Water balance.
- Combined cumulative precipitation and water balance.
- Daily precipitation (with and without inclusion of balance).

Additionally, different temporal windows for cumulative metrics were tested, including 1, 2, 3, 4, 7, and 10 days. The model was trained using ERA5 data and observed inflow records for the Sardinia pilot site (2006-2023). Based on model calibration and validation against observed river discharge at the Omodeo Lake, the configurations used are: the Tirso River with k = 5 and a 7-day cumulative window and the Massari River with k = 5 and a 10-day cumulative window.

Model performance was evaluated through a validation against observed inflow data at the Omodeo Lake for the historical period. The comparison between simulated and observed inflows shows a good agreement in reproducing the main temporal dynamics and seasonal variability, indicating that the inflow elaboration methodology is able to reliably reproduce the main hydrological patterns of the basin. This validation supports the use of the simulated inflows as a robust input for subsequent water budget modeling and scenario analysis (*Figure 26*).

Following calibration, the model is applied to predictors generated from the bias-corrected CMIP6 climate projections. For each future day and each climate model ensemble member, predictors are computed and matched with historical analogs. Inflow forecasts are generated by averaging the inflows from the five most similar historical cases. The total inflow to the reservoir is obtained as the sum of the two contributions, the Tirso River and the Massari River. The results are illustrated in *Figure 27*, which shows the historical and projected hydrological inlet to the Omodeo Lake; the uncertainty range, representing the mean values and associated 5th-95th percentile under both SSP1-2.6 and SSP3-7.0 scenarios, corresponds to the spread of results from these seven climate model simulations. All subsequent results and analyses presented in the following sections are based on these same seven climate model simulations, ensuring methodological and dataset consistency throughout the assessment.

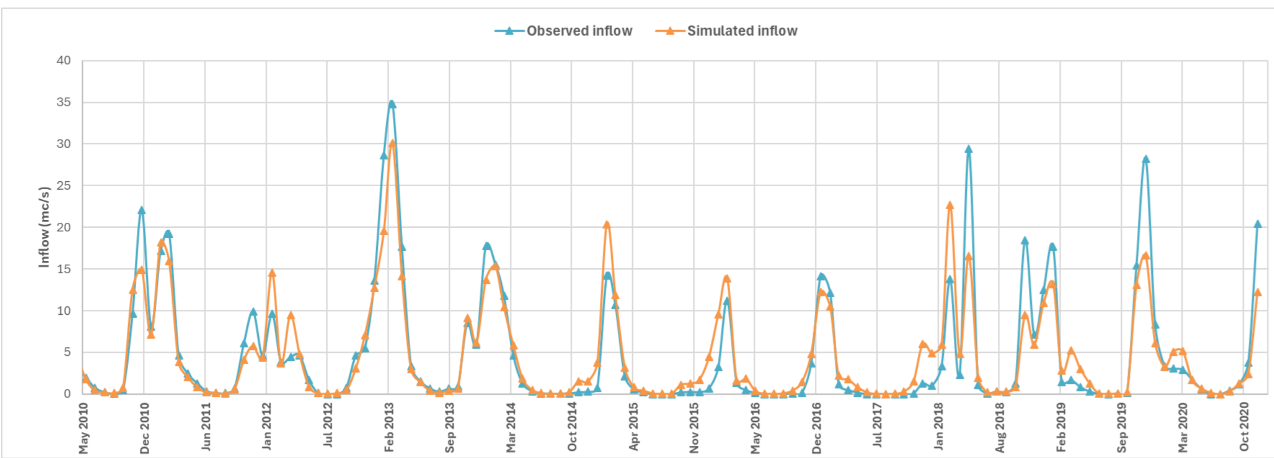

Figure 26: Hydrological Model performance: observed vs simulated inflow.

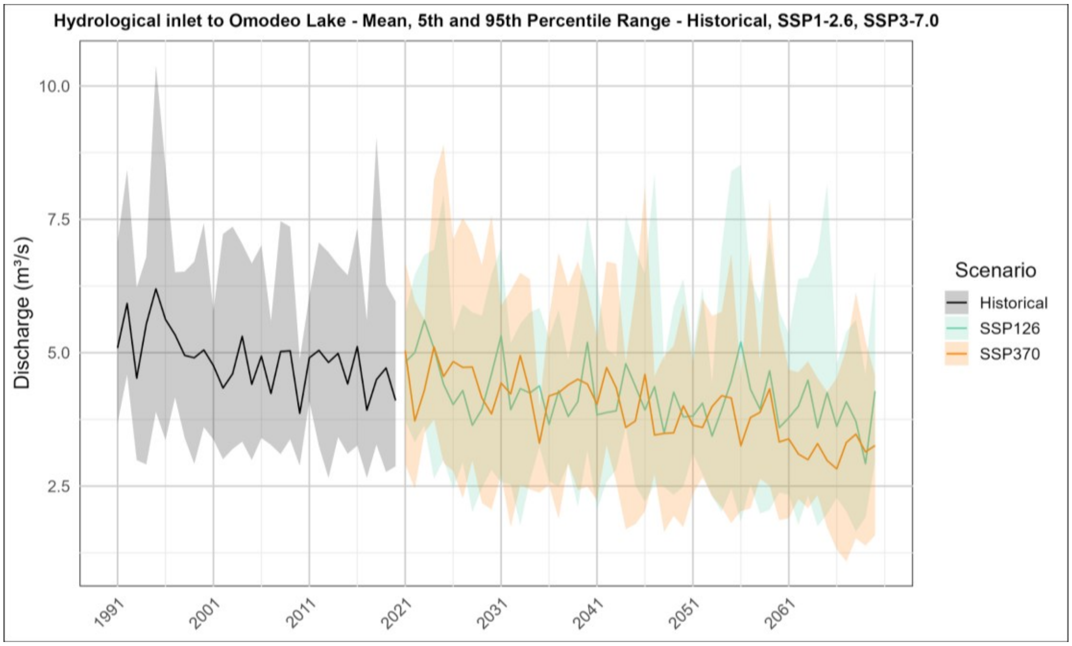

Figure 27: Historical and Projected Hydrological Inlet to Omodeo Lake.

Sectoral demand module

The Sectoral Demand Module estimates water requirements for the main water-using sectors of the Tirso basin, with a specific focus on agricultural irrigation and urban demand, including tourism flows. Industrial water demand is considered absent for the Tirso district, so it is not considered among the competing sectors.

Agricultural Water Demand Calibration

The agricultural water demand module simulates crop-specific irrigation requirements across the irrigated areas served by the Tirso basin, specifically the Irrigation Consortium of Oristano (CBO). Climate inputs are derived from bias-corrected CMIP6 projections, to compute daily reference evapotranspiration (ET_0) using the FAO Penman–Monteith equation. Crop evapotranspiration (ETc) and Actual Evapotranspiration (ETa) is then estimated through crop and water-stress coefficients (kc and ks) following FAO-56 guidelines (R. G. Allen et al., 1998a):

$$ETc = k_c \times ET_0$$

Eq. 2

$$ETa = k_s \times ET_c$$

Eq. 3

Soil moisture dynamics are simulated through a root-zone water balance integrating precipitation, evapotranspiration, infiltration and deep percolation. Irrigation requirements are computed from root-zone depletion and crop water stress conditions, and total irrigation withdrawals are obtained by multiplying the applied irrigation depth by irrigated surface and irrigation system's efficiency coefficients.

The spatial distribution of crops is derived from datasets provided by CBO and the Stati Generali dell'Agricoltura 2018 (Canu & Mameli, 2018). Historical crop distribution patterns (2004–2023) were combined in order to reconstruct irrigated surface evolution. Linear regression models were used to estimate crop-specific temporal trends:

$$Area_c(y) = m_c \cdot y + q_c$$

where $Area_c(y)$ is the irrigated area of crop c in year y, and m_c and q_c are regression coefficients derived from historical crop statistics. *Table 13* shows the main crops and their surfaces within CBO, together with the regression coefficients to reconstruct their evolution in time, created from the data in *Table 17*.

Table 13: Crop distribution across the Consorzio di Bonifica dell'Oristanese (CBO) and linear regression coefficients for time evolution. The crop distribution (Surface) is referred to the year 2023; the coefficients m and q are the linear regression coefficient.

Crop	Surface (ha)	m	q	Percentage with macro-categories (%)
Maize	6103	250	-492718	51
Rice	3473	54	-104841	100
Cereals	316	250	-492718	3
Potato	229	-39	80266	16
Vegetables	1182	-39	80266	84
Alfalfa	1596	250	-492718	13
Grapevine	129	-17	33335	100
Olives	259	-3	6812	100
Citrus	709	-5	11393	72
Fruit trees	272	-5	11393	28

Forage	3991	250	-492718	33

Urban and Tourism Water Demand Calibration

The other sectoral water use is the urban water demand, which includes the domestic and tourist sectors. Urban water demand is a dynamical value that changes according to future projections of the local population and the seasonal variations of tourism flows.

Regarding the water demand of the resident population, we consider an average daily water use per person equal to 170 l/day/person, which includes all the urban water uses (e.g. domestic use, car-washing and gardening). The future demographic trends of resident population are taken by (ISTAT, 2025b), which provides the historical pattern and the estimated trends up to 2100 at municipal level. Regarding tourist average water consumption, we split the tourist presences between hotels and other facilities (camping, B&B, agri-tourism), as the former consume approximately 40% more than the latter, 450 l/day/person and 250 l/day/person, respectively (Regione Sardegna, 2025). Tourist demand shows seasonal variations, as tourist flows fluctuate across the year, with a peak in the summer months and a minimum during winter. In this work, we adopted the approach proposed by the Joint Research Centre (JRS) of the European Commission (Matei et al., 2023), which identified a model to estimate the bed-nights as following:

$$lnBN_{itm} = \alpha_i + \beta_1 lnTCI_{itm} + \beta_2 lnGDP_{itm} + \beta_3 lnHICP_{itm} + \varepsilon_{itm}$$

where the natural logarithm (ln) of the number of bed nights (BN) from a given region i, in year t and month m is function of a regional fixed coefficient (α_i), the logarithm of a monthly climate-suitability index, that is, the Tourist Climate Index (TCI) from Mieczkowski (1985), the regional Gross Domestic Product (GDP) and the regional Harmonized Index of Consumer Prices ($HICP$), in year t and month m. This equation is applied for all Sardinia, as the predictors can be found only at regional scale.

The TCI rationale stems from the need to examine the relationship between climate and tourist flows. Studies demonstrate that the patterns of certain climate variables, that is the temperature, precipitation, wind and number of sunshine hours affect the seasonal and long-term pattern of tourist demand. For this regard, the TCI has been a common metric in research to describe the attractiveness of tourists' destinations. The TCI is expressed as:

$$TCI = 8 \cdot CID + 2 \cdot CIL + 4 \cdot PP + 4 \cdot SH + 2 \cdot W$$

where CID and CIL represent adimensional daily comfort indexes, based on the combinations of minimum, mean and maximum temperature, as well as relative humidity. PP, SH and W correspond to the partial indices of precipitation, sunshine and wind, respectively.

The GDP and $HICP$ are taken from (EUROSTAT, 2025), selecting the values for the Sardinia region of period 2016-2019. Considering the short period of available data for these variables, we approximated the values of period 1991-2015 as the values of 2016 and the future years (2019-2070) as the values of 2019.

Finally, the coefficients α_i, β_1, β_2, β_3 and ε_{itm} are calculated by training the model with the data of the period 2016-2019. Once the *BN* variable was estimated for past and future periods, the number of bed-nights for the Tirso district was calculated as 10% of Sardinia's total bed-nights, following Sardegna Turismo (Regione Sardegna, 2025). Although we acknowledge that the Tirso basin is less touristic than other coastal or insular destinations in Sardinia, this proportion is consistent with regional distribution data and provides a reasonable and conservative estimate of local tourist water demand. According to Sardegna Turismo, the proportion of tourists staying in hotels versus other facilities is approximately 60% and 40%, respectively.

Water budget model

The Water Budget Model is the core component in which the dynamic evolution of storage in the Omodeo Lake is calculated. At each daily timestep, the model updates the reservoir volume by summing all water inputs and subtracting all outputs, according to the following equation:

$$S_t = S_{t-1} + In_t + P_t - EF_t - E_t - Irr_t - DL_t - Urb_t$$

Eq. 4

Where S_t is the storage at the time step (day or month) *t*, In_t is the hydrological inflow, P_t is the precipitation occurring over the surface of the reservoir, EF_t is the natural environmental flow left to the river, E_t is the evaporation occurring over the surface of the reservoir, Irr_t is the irrigation demand, DL_t are the distribution losses over the canals and pipes, Urb_t is the urban water demand.

The Water Budget Model enables full linkage to the Climate Module (for inflows), the Sectoral Water Demand Module (for irrigation and urban demand) and empirical relationships (for distribution losses and environmental flow). The model tracks changes in reservoir storage over time, relying on observed initial conditions and updates with climate-driven hydrological and agricultural inputs.

Regarding the distribution losses, they include seepage, evaporation, and operational inefficiencies occurring along canals and distribution infrastructure. In the BAU (Business-As-Usual) configuration of the model, distribution losses are assumed to amount to 35% of the irrigation water volume.

The environmental flow corresponds to the minimum volume of water that must remain in the Tirso river downstream of the reservoir to maintain ecological functionality and meet downstream non-agricultural water demands. In our modeling framework, this outlet is set to 10% of the hydrological inlet at each time step. This value is currently in operational use in Italy, as reported in (Moccia et al., 2020).

Evaporation losses and precipitation over the Omodeo Lake represent a significant component of the water budget and are carefully accounted for in the flow management strategy. The evaporation losses are computed as the product of the Total Open Water Evaporation (OWET) and the reservoir's daily surface area. To estimate surface area, a globally validated area-volume relationship is used, derived from a regression analysis of bathymetric data from 5824 large reservoirs as part of the Global Reservoir and Dam Database (GRanDv1) (Lehner et al., 2011; Van Bemmelen et al., 2016). The empirical relationship used to approximate the reservoir's surface area $Surf_t$ (in hectares) on day t is:

$$Surf_t = \left(\frac{S_{t-1}}{30.684}\right)^{\frac{1}{0.978}} \times 100 \ \ [ha] \tag{Eq. 5}$$

Reconciling Water Allocation and Water Availability

Reconciling water allocation and availability in the Tirso Basin requires accounting for both infrastructure evolution and hydrological variability. The Omodeo Lake–Cantoniera Dam system is the main regulating structure of the basin, replacing the former Santa Chiara Dam during the transition period between 1991 and 2000. In this study, the basin is represented as a single integrated system including all upstream inflows and storage components. Model validation was performed for the period 2010–2020 by comparing simulated and observed reservoir storage (*Figure 28*). Despite gaps in observational records, particularly between 2016 and 2018, the model reproduces the main storage dynamics and interannual variability, supporting its use for basin-scale water balance simulations.

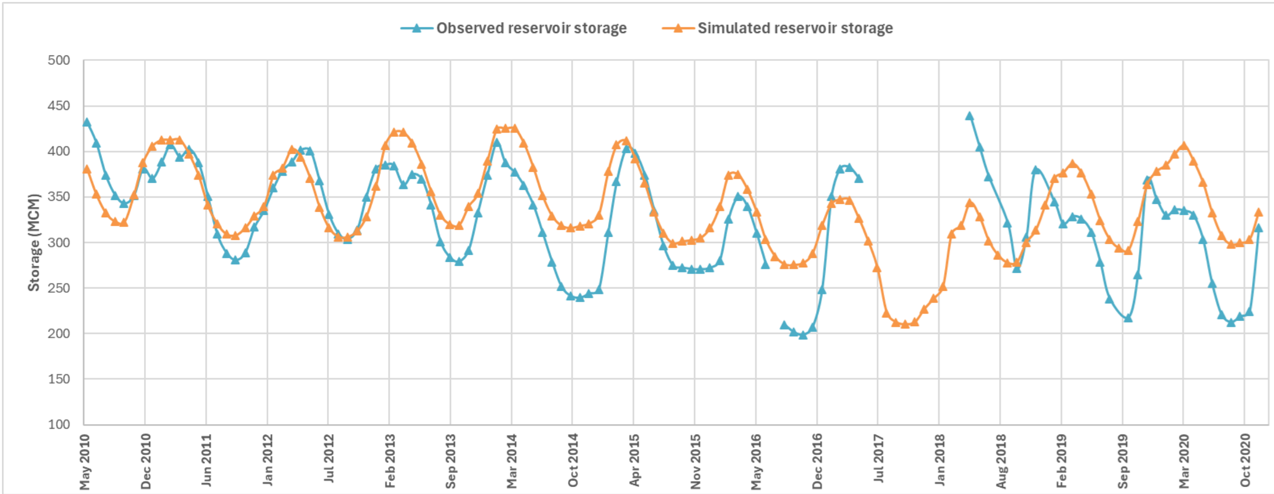

Figure 28: Observed versus simulated reservoir's storage oft he Omodeo Lake across the 2010-2020 period

Avoided Losses Module

The Avoided Loss Module assesses benefits by focusing on the timely avoidance of socio-economic and environmental damages due to changes in water availability, by means of a set of Socio-Economic and Environmental Benefits (SEEB) indicators, which have been co-developed with local stakeholders. Avoidance is operationalized through "narratives" that align with a mitigation hierarchy: sectoral prioritization, design solutions, timing strategies, and suspension of high consumption uses. The SEEB indicators help quantify changes across socio-economic and environmental conditions, allowing for the actual evaluation of the different narratives in place. By embedding this method into ACQUAOUNT-DST, the approach explicitly links States of the World (water storage changes at Omodeo Lake) to corresponding water losses/gains, enabling the benefits of adaptation strategies to be measured consistently across all pilot sites and management interventions, while maintaining comparability and scalability under climate change and alternative scenarios. The indicators selected for this pilot and their changes depending on the States of the World are outlined in *Table 14*.

Table 14: Indicators used in the Avoided Losses Module, classified by sector and associated with different States of the World (Normal, Pre-Alert, Alert, Emergency).

Indicator Class	**Name of the indicator**	**Units**	**Plant Type**	**States of the World**			
				NORMAL	*PRE-ALERT*	*ALERT*	*EMERGENCY*
Agriculture and Food Security Indicators	Crop cover	%	Forages	0	*0*	*50*	*100*
			Horticultural crops	0	0	50	100
			Trees	0	0	30	60
	Crop yield	Kg/ha	Forages	20000	20000	15000	5000
			Horticultural crops	50000	50000	30000	10000
			Trees	5000	5000	4000	3000
Water Services and Infrastructure Indicators	Irrigation costs	€/ha/year	Forages	100	100	60	10
			Horticultural crops	213	213	130	20
			Trees	20	20	10	5
	Water consumption per inhabitant (resource use)	liters/person/day		200	180	100	50
Environmental and Quality Indicators	Nitrogen leaching	kg/ha/month	Forages	10	15	30	50
			Crops	10	20	40	70
			Trees	4	5	10	20
Employment Indicators	Employment Generation	AWU/ha/year (continuous)		50	50	25	0

Narratives

The Decision Support Tool is structured around a set of narratives that combine climate projections with co-developed water management interventions at the farm and basin level. These interventions were selected based on their practical feasibility and the stakeholders' interest in implementing them in the future.

The narrative framework includes a Business-as-Usual (BAU) scenario, which serves as a benchmark and represents the continuation of current management practices without significant structural or operational changes. In comparison with BAU, more advanced management strategies are explored, targeting both water supply and water demand. These measures considers both strategies aimed at improving water-use efficiency and savings, as well as strategies with the goal of intensifying production and water exploitation. ACQUAOUNT-DST then evaluates the trade-offs between these narratives by reflecting their impacts through the indicators reported on Table 14. The list of narratives is reported in Table 15, which summarizes their names and features. In particular, the features consider the increase of storage capacity in time, the expansion of the irrigated area served by the Omodeo Lake, the application of irrigation optimization at farm scale, and finally the eventual transfer of water from the Tirso to the neighboring (Campidano) water district. Specifically, the baseline narratives (BAU and ACQUAOUNT) represent reference configurations with and without the ACQUAOUNT-Farm Tool, i.e. the water use optimization in agriculture. Then, the Soft Strategies introduce a moderate, sustainability-driven expansion strategy, reflecting adaptive but realistic improvements in infrastructure and efficiency. Finally, the Hard Strategies reflect aggressive water use expansion and infrastructural intensification. They represent a stress-test of Tirso system capacity and resilience. Each narrative is tested under the historical period and two climate projections (SSP1-2.6 and SSP3-7.0), with the Soft and Hard strategies being tested with and without the optimization in irrigation management.

Table 15: Main feautures of the narratives considered fort he Tirso water basin

Narrative	**Reservoir capacity (2020–2070)**	**Irrigated area (2020–2070)**	**Irrigation management**	**Annual water transfer to neighbouring district**
Business-as-usual	450 Mm^3 (constant)	18 258 ha (constant)	Non-optimised	–

ACQUAOUNT	450 Mm^3 (constant)	18 258 ha (constant)	Optimised	–
Soft Strategies	790 Mm^3 (target 2070); increase of 340 Mm^3	18 258 ha (target 2070); increase of 1 000 ha	Optimised (ON/OFF)	10 Mm^3 per year
Hard Strategies	450 Mm^3 (no increase)	35 338 ha (target 2070); increase of 17 080 ha	Optimised (ON/OFF)	70 Mm^3 per year

Results

State of the World Frequency

ACQUAOUNT-DST first translates the reservoir storage evolution of the different narratives into the frequency analysis of the four States of the World, as illustrated in *Figure 29*. Under current climate conditions (1991–2020), Business as Usual (BAU) maintains Normal condition in more than 90% of months, whereas Hard Strategies reduce it to 43% and increase Alert and Emergency levels (20% and 19%). The introduction of ACQUAOUNT almost fully restores Normal conditions (~100%) and offsets Soft Strategies, indicating that irrigation optimization compensates for increased irrigation demand and transfers to the neighboring district. However, ACQUAOUNT cannot fully counterbalance Hard Strategies, as expanded irrigated areas and additional transfers increase basin-scale demand and largely re-consume field-level efficiency gains. Under SSP1-2.6, system performance deteriorates markedly, with BAU Normal states dropping to 25% and Alert and Emergency conditions increasing substantially; ACQUAOUNT improves performance (≈60% Normal states) and largely offsets Soft Strategies but remains insufficient when combined with Hard Strategies. Under SSP3-7.0, conditions worsen further, particularly in the long term, when Emergency states become dominant and only limited recovery of Normal conditions occurs even with optimized irrigation, reflecting intensified rainfall variability and more frequent prolonged droughts.

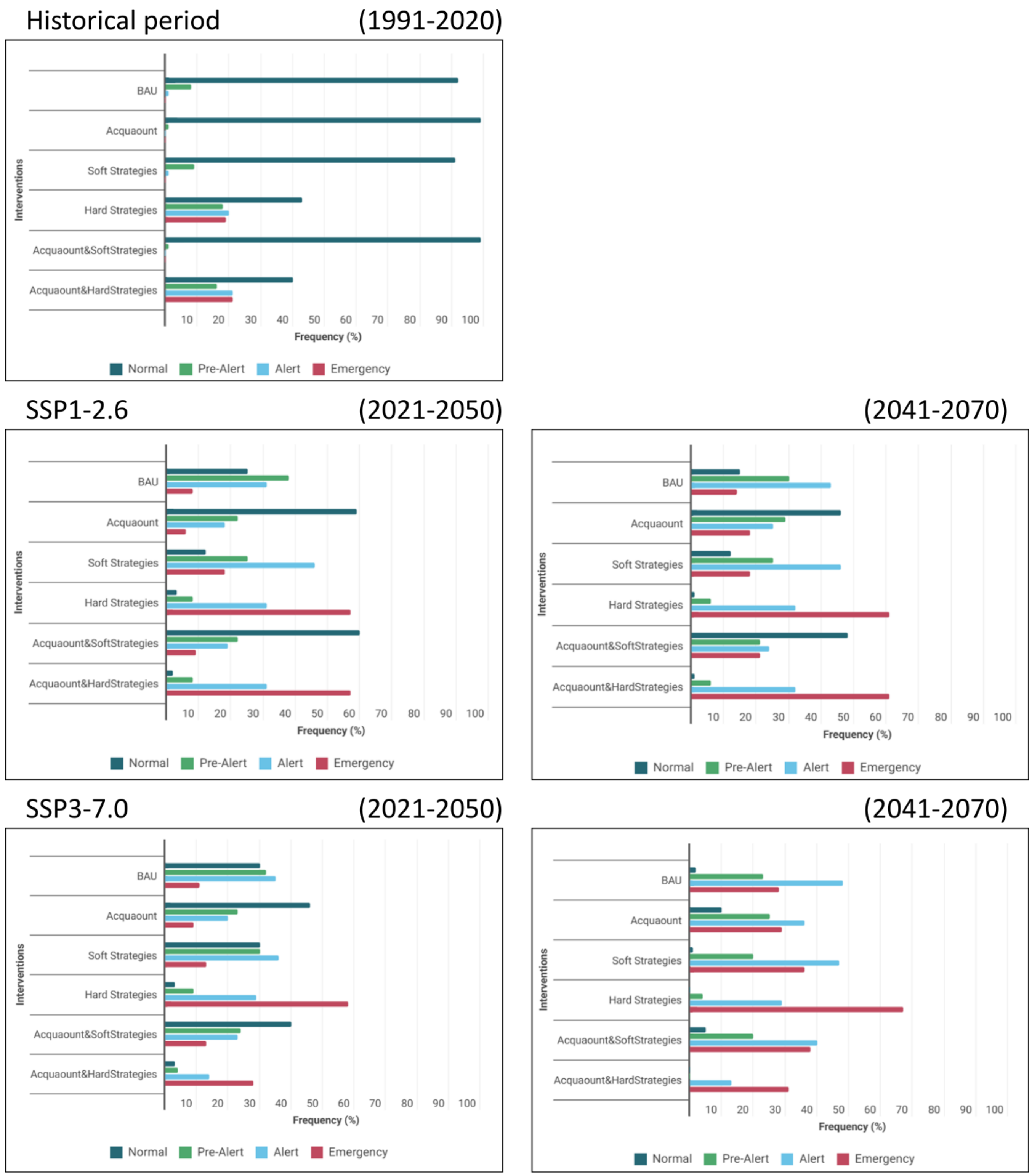

Figure 29: Slacked bars for frequencies of States of the World in the historical period (1991-2020), and future period (2021-2050 and 2041-2070) under SSP1-2.6 and SSP3-7.0 climate scenarios.

Agriculture and Food Security indicators

Indicators for agriculture production and food security include Crop yield (*Figure 30*), expressed as ton/ha, and Crop cover (*Figure 31*), as percentage losses. The linkage between these indicators and drought events is straightforward. If water availability for irrigation decreases, it compromises plant growth and development, leading to a reduction in agricultural production per unit of land area. Similarly, drought stimulates reduction in crop cover.

In the period 1991-2020, the average Crop yield does not change significantly across interventions if Hard Strategies are not applied. Indeed, when Hard Strategies are implemented and compared with BAU, the indicator falls by 19.5% and 21% when they are coupled with the introduction of ACQUAOUNT. BAU management cannot cope with changing climate conditions thus Crop yield reduces by 13.4% in SSP1-2.6 in 2021-2050 and 22.5% in 2041-2070 with respect to current climate conditions. Crop yield further reduces in SSP3-7.0 with the biggest drop in the period 2041-2070 when the indicator falls by 15.6% with respect to the same period in SSP1-2.6. Either Soft Strategies alone or ACQUAOUNT do not greatly modify the pattern of the Crop yield indicator. The indicator falls when Hard Strategies are considered. The reduction is more evident in the long term both in SSP1-2.6 and in SSP3-7.0. In these cases, indeed, Crop yield is nearly halved with respect to the same intervention in 1991-2020. Adding ACQUAOUNT on top of Hard Strategies does not affect Crop yield and the indicators are almost unchanged.

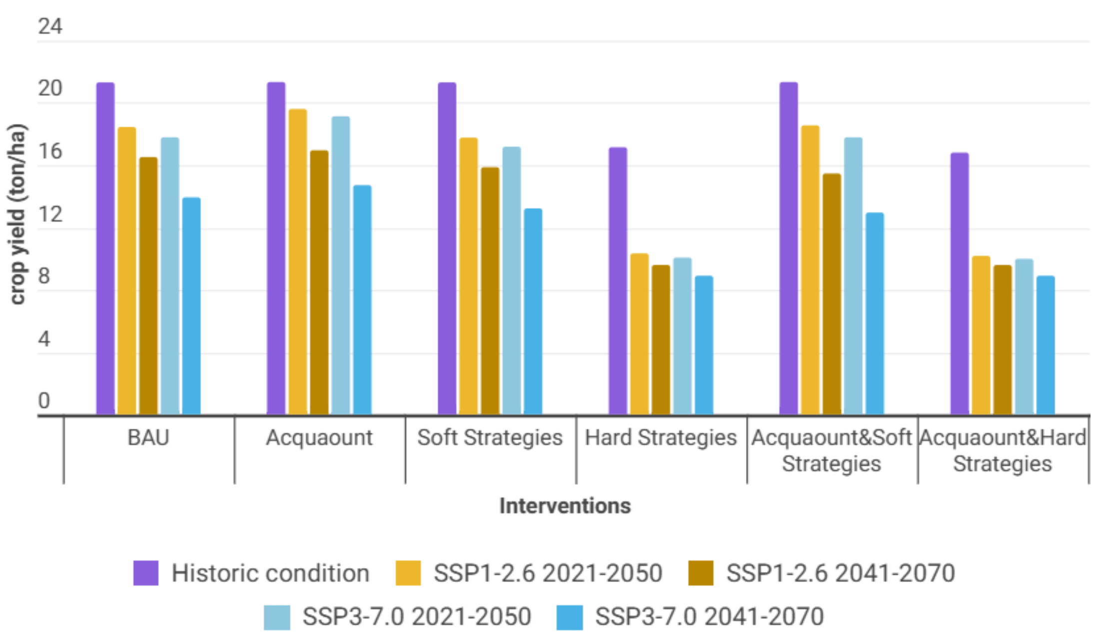

Figure 30: Stacked bars for Crop yield indicator according to climate conditions and interventions

In the period 1991-2020 under current climate conditions the indicator Crop cover is not affected by interventions in most of the cases, only the introduction of Hard Strategies shows a negative impact. Indeed, in these cases Crop cover declines by 28% when only the Strategies are implemented and 30% when they are coupled with ACQUAOUNT. ACQUAOUNT allows to reduce Crop cover losses when climate change is added both in SSP1-2.6 and SSP3-7.0. In SSP1-2.6 ACQUAOUNT reduces Crop cover mostly in the short run. In the period 2021-2050, indeed, Crop cover reduces by 8 percentage points with respect to BAU management in the same scenario (13% vs 21%) while in the long run (2041-2070) the reduction is just 2% more (31% vs 33%). Similarly, in SSP3-7.0 ACQUAOUNT adoption reduces Crop cover to 16% in the short run and to 45% in the long run showing a much more constant trend than SSP1-2.6. Soft Strategies increase Crop cover reductions both in the short and in the long run with average losses higher than using BAU management in both SSPs. Adding ACQUAOUNT on top of Soft Strategies lowers the negative effect on this indicator in the short run (-2% than in BAU in SSP1-2.6 and null with respect to BAU in SSP3-7.0) while the effect in the long run remains almost unaffected with respect to introducing Soft Strategies alone in SSP3-7.0 and slightly worse in SSP1-2.6 (+1% than with only Soft Strategies). Hard Strategies, instead, push Crop cover losses up to at least 70% both in the short and in the long run in both SSPs, demonstrating that the Strategies' effects prevail on the ACQUAOUNT benefits.

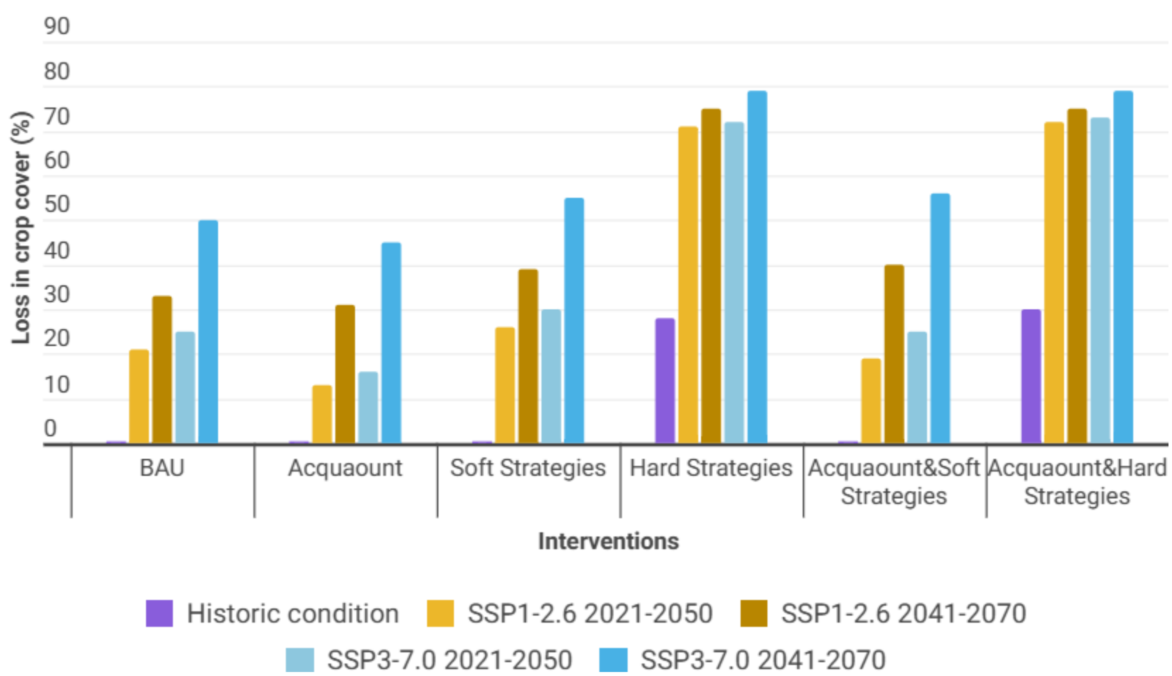

Figure 31: Stacked bars for Crop cover indicator according to climate conditions and interventions.

Water Services and Infrastructure indicators

Irrigation costs (graphically shown in *Figure 32*) under current climate conditions are almost stable across interventions. A significant change, with a 20% drop, is seen only when Hard Strategies are implemented with respect to BAU management. This is the resulting effects of both a reduction in water availability and an increase in irrigated area that is one of the assumptions of the scenario (see Sub-Section 6.1). Although Hard Strategies under current climate conditions reduce the costs with respect to BAU, the effect is much more evident for SSP1-2.6 and SSP3-7.0 where the indicator falls by 55% in 2021-2050 and 52% in 2041-2070 with respect to BAU under the same climate conditions.

In general SSP1-2.6 has higher Irrigation costs than SSP3-7.0 due to the higher water availability for the agricultural sector. Moreover, in both SSPs there are slightly higher costs in the medium run (2021-2050) than in the long run (2041-2070) independently of the intervention. On average costs in the medium run are 18% and 13% higher than in the long run in SSP1-2.6 and SSP3-7.0, respectively. The adoption of ACQUAOUNT allows it to have the highest level of water resources thus the costs are the highest in the medium run (+22% and +18% with respect to BAU management in SSP1-2.6 and SSP3-7.0, respectively).

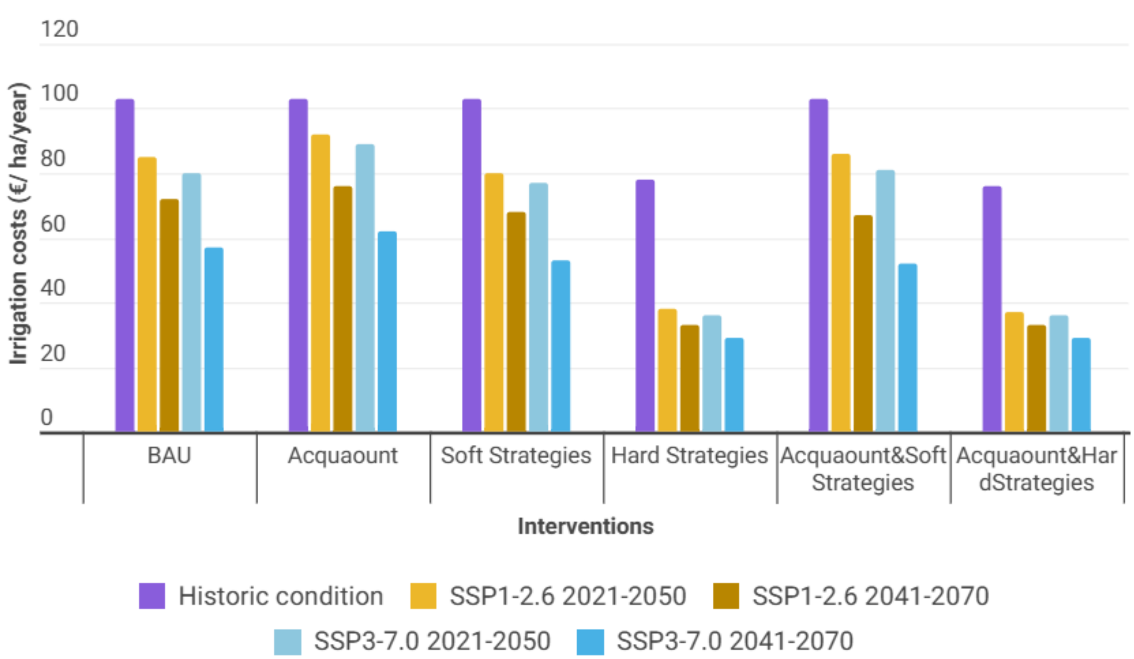

Figure 32: Stacked bars for Irrigation costs indicator according to climate conditions and interventions.

Per capita water consumption (*Figure 33*) is not sensitive to interventions supposing BAU management although Hard Strategies are implemented. In those cases the indicator declines by nearly 44%. In both SSPs Per capita water consumption is higher with ACQUAOUNT (+25% with respect to BAU management) in the medium run. However, the effectiveness reduces in the long run, when the indicator is 20% lower in SSP1-2.6 and 30% in SSP3-7.0. Coupling ACQUAOUNT with Soft Strategies improves the indicator as the optimized irrigation can partially counterbalance the negative effect of Strategies in the short run. In SSP1-2.6 the increase with respect to Soft Strategies is nearly 10% in 2021-2040 but only 2% in 2041-2070. In SSP3-7.0, instead, the positive effect of ACQUAOUNT lowers and the indicator increases with respect to Soft Strategies only by 9% in the medium run and it is almost null in the long run. Finally, Hard Strategies negative impact on the indicator is not positively affected by the introduction of ACQUAOUNT.

Figure 33: Stacked bars for Per capita water consumption indicator according to climate conditions and interventions.

Employment indicators

To consider the effects of drought on employment, Stakeholders in the Sardinian pilot case study suggested the use of the Employment generation in the agricultural sector (*Figure 34*) as the annual work units (AWU) related to crop management expressed in AWU/ha/year.

In the period 1991-2020 under current climate conditions the indicator reaches its maximum value according to each intervention. While there are no differences in terms of Employment generation in BAU and with the introduction of ACQUAOUNT and Soft Strategies, there is an evident reduction, nearly 30%, when Hard Strategies are pursued. In SSP1-2.6 and in SSP3-7.0 ACQUAOUNT adoption boosts average employment per hectare higher than the level in BAU (+9.4% in the short run and +5.9% in the long run in SSP1-2.6 and +13.3% in the short run and +12.6% in the long run in SSP3-7.0). Adopting Hard Strategies drastically reduces the indicator that respect to BAU falls between 14 AWU/ha/year and 10 AWU/ha/year in case of changing climate conditions. Coupling these Strategies with ACQUAOUNT does not affect the indicator.

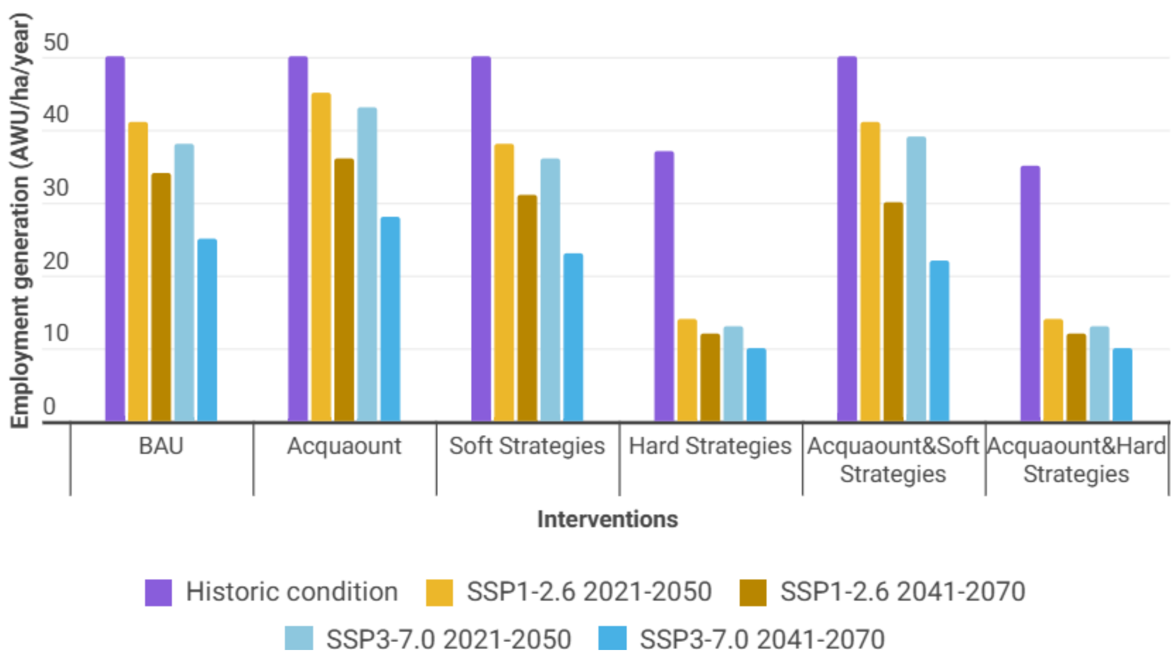

Figure 34: Stacked bars for Employment generation indicator according to climate conditions and interventions.

Environmental and Quality indicators

As visible in Figure 35, in the period 1991-2020 Nitrogen leaching indicator does not change among interventions (nearly 10 kg/ha per month) unless Hard interventions are assumed. In this case it is more than double, reaching 23 kg/ha per month. Supposing BAU management in climate change conditions the indicator increases both in the short and in the long run. Being in SSP1-2.6 or SSP3-7.0 does not affect the indicator in the short run (20 kg/ha per month vs 22 kg/ha per month), while in the longer run SSP3-7.0 shows a higher indicator (up to 32 kg/ha per month). Trends are constant across interventions, although the adoption of ACQUAOUNT can lower Nitrogen leaching due to an optimized use of water resources. The maximum average level is 29 kg/ha per month in SSP3-7.0 in the period 2041-2070. Nevertheless, when the intervention is coupled with Soft Strategies the benefits minimize and the indicator values are close to BAU management.

In case of Hard Strategies (with or without ACQUAOUNT) Nitrogen leaching indicator increases up to 42 kg/ha per month in SSP3-7.0 in the period 2041-2070. However, these interventions are characterized by a lower indicator difference in terms of short and long run within each SSP. Moreover, the indicator is very close among SSPs.

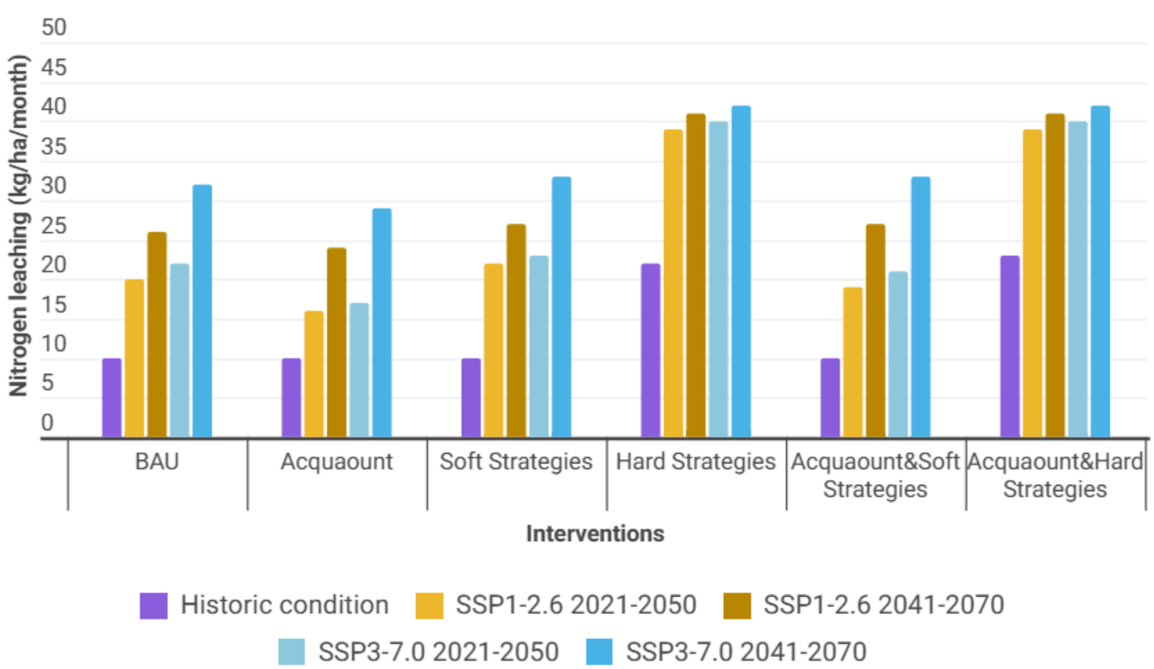

Figure 35*: Stacked bars for Nitrogen leaching indicator according to climate conditions and interventions.*

Conclusions and policies recommendations

The application of ACQUAOUNT-DST in Sardinia provided a valuable test for analyzing multi-sector water pressures in the Tirso Basin, where agricultural and urban demands interact within a highly regulated infrastructure system. In this context, ACQUAOUNT-DST proved useful for integrating hydrological, operational, and socio-economic dimensions and for supporting a shift from static allocation rules toward a more predictive and adaptive water management approach. Considering a set of 18 narratives allowed a more detailed representation of basin-specific governance questions, including farm-level water savings, system-wide implications mediated by the CBO, transfers to the Campidano area, and the possible buffering role of increased Cantoniera storage. Across the analysed indicators, the results consistently show that coordinated interventions outperform isolated actions, whereas business-as-usual trajectories tend to increase vulnerability under climate change.

The State-of-the-World analysis confirms that under historical conditions the system remains generally stable under BAU and Soft Strategies, while Hard Strategies sharply increase the frequency of Alert and Emergency states. ACQUAOUNT is the most effective stabilizing option, almost fully restoring Normal states under current climate and substantially improving performance under future scenarios, although it cannot fully offset the additional pressures generated by Hard Strategies. Under both SSP1-2.6 and SSP3-7.0, and especially in the long term, the system experiences a general deterioration, with more frequent and severe drought conditions driving downstream effects on crop productivity, crop cover, per-capita water consumption, employment, irrigation costs, and nitrogen leaching.

Across indicators, Hard Strategies consistently produce the most extreme trade-offs, reducing crop yields and crop cover, per-capita consumption, and employment, while increasing nitrogen leaching; irrigation costs decline under these strategies mainly because of reduced water availability. By contrast, ACQUAOUNT generally mitigates negative impacts, especially in the short to medium term, but its benefits become more limited when combined with Soft or Hard Strategies under persistent future stress.

Overall, to strengthen the resiliency of basin management, it is necessary to adopt basin-wide operational rules informed by dynamic forecasts of water availability, crop water requirements, and urban demand; strengthening coordination and information exchange between basin authorities and Land Reclamation Consortia; embedding narrative-based stress testing in annual planning cycles; promoting hybrid solutions that combine efficiency gains with moderate storage improvements; using evidence on crop cover, irrigation technology, and cost structures to guide incentives that stabilize basin-scale demand; and carefully evaluating transfers to the Campidano area against basin reliability, urban needs, and ecological thresholds.

Future developments should extend ACQUAOUNT-DST to additional ecological indicators, farmer decision-making, investment costs, urban conservation behaviour, and seasonal to sub-seasonal forecasting, in order to further strengthen its applicability for adaptive water management planning.

Acknowledgements

This work was supported by the ACQUAOUNT project funded under the Grant Agreement number: [2021] [ACQUAOUNT] [Call 2020 Section Water IA] of the PRIMA program.

References

Adamovic, M., Al-Zubari, W., Amani, A., Ameztoy Aramendi, I., Bacigalupi, C., Barchiesi, S., Bisselink, B., Bodis, K., Bouraoui, F., Caucci, S., Dalton, J., De Roo, A., Dudu, H., Dupont, C., El Kharraz, J., Embid, A., Farajalla, N., & Fernandez Blanco Carra, G. (2019). Position Paper on Water, Energy, Food and Ecosystems (WEFE) Nexus and Sustainable Development Goals (SDGS). https://doi.org/10.2760/5295

Allen, R. G., Pereira, L. S., Raes, D., & Smith, M. (1998). FAO Irrigation and Drainage Paper No. 56—Crop Evapotranspiration (Fascicolo 56). FAO - Food and Agriculture Organization of the United Nations.

Andreu, J., Capilla, J., & Sanchís, E. (1996). AQUATOOL, a generalized decision-support system for water-resources planning and operational management. Journal of Hydrology, 177(3–4), 269–291. https://doi.org/10.1016/0022-1694(95)02963-X

Canu, V., & Mameli, M. G. (2018). Stati generali dell'agricoltura 2018, Report tavolo 11, Gestione delle risorse idriche (No. 11). https://www.agenzialaore.it/documenti/14_43_20181203131540.pdf

Carmona-Moreno, C., Crestaz, E., Cimmarrusti, Y., Farinosi, F., Biedler, M., Amani, A., Mishra, A., & Carmona-Gutierrez, A. (2021). Implementing the Water–Energy–Food–Ecosystems Nexus and Achieving the Sustainable Development Goals. United Nations Educational, Scientific and Cultural Organization (UNESCO). ISBN 978-92-3100473-5

Correa-Cano, M. E., Salmoral, G., Rey, D., Knox, J. W., Graves, A., Melo, O., Foster, W., Naranjo, L., Zegarra, E., Johnson, C., Viteri-Salazar, O., & Yan, X. (2022). A novel modelling toolkit for unpacking the Water-Energy-Food-Environment (WEFE) nexus of agricultural development. Renewable and Sustainable Energy Reviews, 159, 112182. https://doi.org/10.1016/j.rser.2022.112182

Cramer, W., Guiot, J., Fader, M., Garrabou, J., Gattuso, J. P., Iglesias, A., Lange, M. A., Lionello, P., Llasat, M. C., Paz, S., Peñuelas, J., Snoussi, M., Toreti, A., Tsimplis, M. N., & Xoplaki, E. (2018). Climate change and interconnected risks to sustainable development in the Mediterranean. Nature Climate Change, 8(11), 972–980. https://doi.org/10.1038/s41558-018-0299-2

Crovella, T., Paiano, A., & Lagioia, G. (2022). A meso-level water use assessment in the Mediterranean agriculture. Multiple applications of water footprint for some traditional crops. Journal of Cleaner Production, 330, 129886. https://doi.org/10.1016/j.jclepro.2021.129886

Daccache, A., Ciurana, J. S., Rodriguez Diaz, J. A., & Knox, J. W. (2014). Water and energy footprint of irrigated agriculture in the Mediterranean region. Environmental Research Letters, 9(12), 124014. https://doi.org/10.1088/1748-9326/9/12/124014

De Roo, A., Trichakis, I., Bisselink, B., Gelati, E., Pistocchi, A., & Gawlik, B. (2021). The Water-Energy-Food-Ecosystem Nexus in the Mediterranean: Current Issues and Future Challenges. Frontiers in Climate, 3, 782553. https://doi.org/10.3389/fclim.2021.782553

European Commission. (2024). Water-Energy-Food-Ecosystem Nexus. https://international-partnerships.ec.europa.eu/policies/climate-environment-and-energy/water-energy-food-ecosystem-nexus_en

European Parliament and Council. (2000, ottobre 23). Directive 2000/60/EC of the European Parliament and of the Council of 23 October 2000 establishing a framework for Community action in the field of water policy. https://eur-lex.europa.eu/eli/dir/2000/60/oj

EUROSTAT. (2025). Gross domestic product (GDP) and main components (output, expenditure and income). https://ec.europa.eu/eurostat/databrowser/view/namq_10_gdp/default/table?lang=en

Ferragina, E., & Canitano, G. (2014). Water and Food Security in the Arab Countries: National and Regional Implications. Global Environment, 7(2), 326–351. https://doi.org/10.3197/ge.2014.070204

Giorgi, F., & Lionello, P. (2008). Climate change projections for the Mediterranean region. Global and Planetary Change, 63(2–3), 90–104. https://doi.org/10.1016/j.gloplacha.2007.09.005

Giupponi, C., Mysiak, J., Fassio, A., & Cogan, V. (2004). MULINO-DSS: A computer tool for sustainable use of water resources at the catchment scale. Mathematics and Computers in Simulation, 64(1), 13–24. https://doi.org/10.1016/j.matcom.2003.07.003

Gudmundsson, L., Bremnes, J. B., Haugen, J. E., & Engen-Skaugen, T. (2012). Technical Note: Downscaling RCM precipitation to the station scale using statistical transformations – a comparison of methods. Hydrology and Earth System Sciences, 16(9), 3383–3390. https://doi.org/10.5194/hess-16-3383-2012

ISTAT. (2025). Population and Households [Software]. https://esploradati.istat.it/databrowser/#/en/dw/categories/IT1,POP,1.0

Koutsoyiannis, D., Efstratiadis, A., & Karavokiros, G. (2002). A DECISION SUPPORT TOOL FOR THE MANAGEMENT OF MULTI-RESERVOIR SYSTEMS1. JAWRA Journal of the American Water Resources Association, 38(4), 945–958. https://doi.org/10.1111/j.1752-1688.2002.tb05536.x

Lehner, B., ReidyLiermann, C., Revenga, C., Vorosmarty, C., Fekete, B., Crouzet, P., Doll, P., Endejan, M., Frenken, K., Magome, J., Nilsson, C., Robertson, J. C., Rodel, R., & Sindorf, N. (2011). Global Reservoir and Dam Database, Version 1 (GRanDv1): Dams, Revision 01 (Versione 1.01) [Dataset]. Palisades, NY: NASA Socioeconomic Data and Applications Center (SEDAC). https://doi.org/10.7927/H4N877QK

Lionello, P., Abrantes, F., Gacic, M., Planton, S., Trigo, R., & Ulbrich, U. (2014). The climate of the Mediterranean region: Research progress and climate change impacts. Regional Environmental Change, 14(5), 1679–1684. https://doi.org/10.1007/s10113-014-0666-0

Lucca, E., El Jeitany, J., Castelli, G., Pacetti, T., Bresci, E., Nardi, F., & Caporali, E. (2023). A review of water-energy-food-ecosystems Nexus research in the Mediterranean: Evolution, gaps and applications. Environmental Research Letters, 18(8), 083001. https://doi.org/10.1088/1748-9326/ace375

Martinez, P., Blanco, M., & Castro-Campos, B. (2018). The Water–Energy–Food Nexus: A Fuzzy-Cognitive Mapping Approach to Support Nexus-Compliant Policies in Andalusia (Spain). Water, 10(5), 664. https://doi.org/10.3390/w10050664

Masia, S., Trabucco, A., Spano, D., Snyder, R. L., Sušnik, J., & Marras, S. (2021). A modelling platform for climate change impact on local and regional crop water requirements. Agricultural Water Management, 255(June). https://doi.org/10.1016/j.agwat.2021.107005

Matei, N. A., García-León, D., Dosio, A., Silva, F. B. e, Barranco, R., & Císcar Martínez, J. C. (2023). Regional impact of climate change on European tourism demand (pp. 1–40). Publications Office of the European Union. https://doi.org/10.2760/899611

Moccia, D., Salvadori, L., Ferrari, S., Carucci, A., & Pusceddu, A. (2020). Implementation of the EU ecological flow policy in Italy with a focus on Sardinia. Advances in Oceanography and Limnology, 11(1). https://doi.org/10.4081/aiol.2020.8781

Piani, C., Haerter, J. O., & Coppola, E. (2010). Statistical bias correction for daily precipitation in regional climate models over Europe. Theoretical and Applied Climatology, 99(1–2), 187–192. https://doi.org/10.1007/s00704-009-0134-9

Ramirez, C., Almulla, Y., Joyce, B., Huber-Lee, A., & Nerini, F. F. (2022). An assessment of strategies for sustainability priority challenges in Jordan using a water–energy–food Nexus approach. Discover Sustainability, 3(1), 23. https://doi.org/10.1007/s43621-022-00091-w

Regione Autonoma della Sardegna. (2022). PIANIFICAZIONE E GESTIONE DELLE RISORSE IDRICHE - Aggiornamento dei modelli idraulici del Piano Stralcio per l'Utilizzo delle Risorse Idriche della Sardegna (PSURI).

Regione Sardegna. (2025). Sardegna Turismo—Report sui dati dei movimenti turistici in Sardegna. https://osservatorio.sardegnaturismo.it/it/report

Rodríguez Díaz, J. A., Weatherhead, E. K., Knox, J. W., & Camacho, E. (2007). Climate change impacts on irrigation water requirements in the Guadalquivir river basin in Spain. Regional Environmental Change, 7(3), 149–159. https://doi.org/10.1007/s10113-007-0035-3

Serrat-Capdevila, A., B., J., & V., H. (2011). Decision Support Systems in Water Resources Planning and Management: Stakeholder Participation and the Sustainable Path to Science-Based Decision Making. In C. Jao (A c. Di), Efficient Decision Support Systems—Practice and Challenges From Current to Future. InTech. https://doi.org/10.5772/16897

Serrat-Capdevila, A., Browning-Aiken, A., Lansey, K., Finan, T., & Valdés, J. B. (2009). Increasing Social-Ecological Resilience by Placing Science at the Decision Table: The Role of the San Pedro Basin (Arizona) Decision-Support System Model. Ecology and Society, 14(1), art37. https://doi.org/10.5751/ES-02839-140137

Trabucco, A., Sušnik, J., Vamvakeridou-Lyroudia, L., Evans, B., Masia, S., Blanco, M., Roson, R., Sartori, M., Alexandri, E., Brouwer, F., Spano, D., Damiano, A., Virdis, A., Sistu, G., Pulino, D., Statzu, V., Madau, F., Strazzera, E., & Mereu, S. (2018). Water-Food-Energy Nexus under Climate Change in Sardinia. EWaS3 2018, 609. https://doi.org/10.3390/proceedings2110609

Van Bemmelen, C. W. T., Mann, M., De Ridder, M. P., Rutten, M. M., & Van De Giesen, N. C. (2016). Determining water reservoir characteristics with global elevation data. Geophysical Research Letters, 43(21). https://doi.org/10.1002/2016GL069816

Yates, D., Sieber, J., Purkey, D., & Huber-Lee, A. (2005). WEAP21—A Demand-, Priority-, and Preference-Driven Water Planning Model: Part 1: Model Characteristics. Water International, 30(4), 487–500. https://doi.org/10.1080/02508060508691893

Additional material

Table 16: List of CMIP6 climate models adopted for the study

CMIP6 Model
CNRM-ESM2-1
EC-Earth3-Veg
IPSL-CM6A-LR
MIROC6
MPI-ESM1-2-HR
NorESM2-MM*
UKESM1-0-LL*

Table 17: Evolution of crop distribution between 2004 and 2023 in the irrigation Consortium of Oristano (CBO).

Crop categories	**Surface 2004 (ha)**	**Surface 2014 (ha)**	**Surface 2023 (ha)**	**Crop categories**
Arable and fodder crops	7271	9969	12005	Arable and fodder crops
Rice	2456	2994	3473	Rice
Vegetables	2137	1276	1412	Vegetables

Fruit trees	1076	952	981	Fruit trees
Grapevine	434	50	129	Grapevine
Olive	315	106	259	Olive
Total	13689	15347	18259	Total

Chapter 6. General conclusions and final recommendations

This thesis shows that the gap between WEFE Nexus and IWRM studies and operational water management can be addressed with simple, scalable, and integrated modelling approaches across spatial and temporal scales. This tries to answer to some of the concerns of Biswas, (2004) and Allouche et al. (2015), who pointed out the vagueness of these frameworks, as well as their complexity to make them effectively operational in practical applications. Considering that identifying a single framework which integrates all the aspects of the Nexus is excessively difficult (Li et al., 2025; Purwanto et al., 2021), this thesis proposes an alternative approach. First, focus on those sectors which are the most responsible for water depletion in the Mediterranean, that is agriculture. Second, the combination of simplified tools that address different operating scales (temporal and spatial) of water management, and the evaluation of their effect on water availability. For these reasons, this thesis posed attention to those features that can strengthen the Water–Food interlinkages of the Nexus.

The development and adoption of user-friendly tools is crucial, as both the WEFE Nexus and IWRM involve a multidisciplinary range of actors with heterogeneous competencies, who require accessible and transparent solutions (Hamidov & Helming, 2020; McGrane et al., 2019; Mersha, 2021). Otherwise, even the most advanced models risk remaining confined to academic applications if their level of complexity is high. The tools and frameworks illustrated in this thesis are based on models which are designed to be:

- **open source**, therefore, accessible to everybody, anytime;
- **applicable**, since they can be immediately applied in the real-world context;
- **simple & scalable**, as they require minimal and easy-to-access input.

These characteristics are particularly useful in Mediterranean environments, due to lack of easily accessible and reliable data sources (Zubel & Apprioual, 2020). The tools presented in this work involved regional models that project the long-term water availabilities given the climate change scenarios, as well as devices that support real-time water allocations at the local scale. In this way, the combined use of these tools allowed the connections of the different operational scales of water management, that is, the spatial (regional versus farm-level) and temporal (real-time versus multi-year analysis).

Key findings and recommendations

The impact of climate change on irrigation demand can be overestimated

Climate change is expected to cause an increase in agricultural water demand, however, Chapter 2 shows that this growth remains uncertain if the effect of CO_2 on evapotranspiration is considered. Elevated CO_2 concentrations can reduce transpiration through partial stomatal closure, thereby moderating the increase of irrigation demand. This means that, without CO_2 effect, irrigation demand can increase by about 12-18% under RCP 8.5 by 2050; with CO_2 effect, instead, this increase remains lower than 8%. Differences are minor under RCP 2.6 (+7-12% without CO_2 effect, 0-10% with CO_2 effect). Since many global crop models do not account for the CO_2 effect, this may lead to potential overestimations of future irrigation demand. When this effect is incorporated into projections, a clearer picture of future irrigation demand trends can be obtained.

Trade-offs between model's simplicity and accuracy

ACQUAOUNT-Farm's performance, illustrated in Chapter 3, showed moderate accuracy in reproducing soil moisture dynamics ($R^2 \approx 0.65$, RMSE ≈ 0.022 m³ m⁻³, MAD ≈ 0.016 m³ m⁻³). Even though these metrics look modest, sensor-model's differences remain below sensor accuracy (0.03 $m^3\ m^{-3}$) up to four days in three out of four farms. This is already a satisfactory achievement, considering the minimal input requested by the users. Similarly, Chapter 4 highlighted the potentials of IOTA² algorithm to generate large-scale crop mapping across the entire Sardinia region. Results show an Overall Accuracy of around 0.6, given the 26 classes employed in the study. Despite refinement is needed, the map provides a first overview of current crop systems in the region, with the possibility of easily reproducing maps for multiple years.

These results highlight the inherent trade-off between model simplicity and accuracy: while performance may be lower than that of more complex approaches, the reduced operational burden can facilitate adoption and practical implementation by non-expert users.

The roles of real-time versus long-term models

This study highlights the different goals and effects of modelling approaches and scales of operation. For instance, a real-time model like ACQUAOUNT-Farm operates at the local scale, as it is designed to support daily irrigation scheduling for a single, specific farm. In contrast, ACQUAOUNT-DST is designed to capture regional dynamics of water availability, and the long-term effects of different management interventions. This primarily supports strategic decision-making, which requires information on the long-term effects on water resources to formulate informed policies. These tools can mutually reinforce each other when combined. In the case of Sardinia region, ACQUAOUNT-DST compares the gains generated by the introduction of digital irrigation scheduling (e.g., an extensive application of ACQUAOUNT-Farm) in relation to an extension of irrigated areas and transfers to transboundary catchments. Tools like ACQUAOUNT-DST can help institutions to move beyond the typical reactive approach, where interventions are implemented only during or after an emergency.

Communication across operational scales

This work highlights the role of farmers and regional water managers as the key actors in achieving integrated water resources management. The first are responsible for water use and depend on the second for its delivery across the network. If irrigation is not optimized (as highlighted in Chapters 3 and 5), the introduction of ACQUAOUNT-Farm can improve water use efficiency in agriculture. However, improvements at the farm level alone are not sufficient if not aligned with coordinated regional strategies. The application of ACQUAOUNT-DST shows that the gains given by irrigation efficiency (+10-25% of normal state episodes in the reservoir) risks being undermined if regional water authorities do not improve water infrastructure or plan measures that increase exploitation. For this reason, the outcomes of ACQUAOUNT-DST should support enhanced coordination between these actors, to ensure that local and regional strategies are coherent and mutually reinforcing.

Limitations of this study

Standardization versus customization: One of the limitations in operationalizing IWRM and WEFE Nexus concepts is the trade-off between standardization or customization of the framework. A standardized approach can be deployed across regions with minimal adaptation, but at the cost of lower reliability. In contrast, tailoring the framework to regional conditions produces more accurate results but sacrifices scalability and demands substantial calibration effort for each new context. For instance, a big effort of customization was necessary when shifting ACQUAOUNT-DST from Sardinian network-based water distribution to Tunisian irrigation, mainly dependent on private groundwater wells.

Data scarcity: data availability and reliability constituted a major limitation affecting the accuracy of results. For example, the data used to calibrate ACQUAOUNT-DST was primarily obtained from reports provided by regional or national authorities and few from field measurements (ISTAT, 2018; Regione Autonoma della Sardegna, 2022). However, inconsistencies were frequently observed between reports and direct measurements. As a result, the calibration process required the identification of a trade-off between these sources. Similarly, LPIS data (European Court of Auditors, 2016) employed in Chapter 4 was often insufficiently clear and reliable, due to the intrinsic heterogeneity of the crop parcels.

System connectivity: internet connection and sensor reliability represented a critical constraint for the implementation of the ACQUAOUNT-Farm model. The model was successfully tested in Tunisia, where internet coverage was adequate to ensure continuous and reliable data acquisition. However, similar conditions were not present in the other case studies (Jordan, Lebanon, Sardinia) within the ACQUAOUNT project. Many sites experienced limited connectivity, as well as technical issues with sensors, which significantly limited data collection, thus preventing effective testing and validation of the model in those contexts.

Future perspectives

The offline validation approach adopted in this study (i.e., comparing model outputs against farmers' actual irrigation practices) points toward a natural experimental extension: a field trial in which one portion of a crop field is irrigated following ACQUAOUNT-Farm recommendations (treatment) while the other follows traditional farmer practices (control), both monitored by the IoT system. Such a controlled design would allow a direct assessment of whether ACQUAOUNT-Farm generates measurable gains in water use efficiency, defined as water consumed per unit of final crop output.

The geographical scope of this work should be extended to additional Mediterranean regions, allowing ACQUAOUNT-Farm to be tested across more diverse cropping systems and agricultural contexts, while IOTA^2 to be evaluated over multiple years and regions, to assess how crop mapping quality varies under different agro-environmental conditions. Scaling up these tools across multiple pilots, however, requires a degree of integration that the current fragmented architecture does not support. A unified platform that connects all four tools would address this gap directly: IOTA^2 crop maps would feed irrigated area estimates into both SIMETAW and ACQUAOUNT-DST, while field-level outputs from ACQUAOUNT-Farm would be used to calibrate optimized and non-optimized water demand scenarios in ACQUAOUNT-DST, enabling a more precise long-term assessment of water resource dynamics.

To fully operationalize the WEFE Nexus perspective that frames this thesis, future work should extend the analysis to include the ecosystem dimension, specifically, the impact of agricultural water withdrawals on freshwater-dependent ecosystems. Such an extension would strengthen the Water–Food–Ecosystem interlinkages that current modelling frameworks tend to treat separately and would provide decision-makers with a more complete evidence base for designing water allocation policies that do not externalize environmental costs onto local ecosystems.

Final remarks

This thesis acknowledges the importance of integrated frameworks that account for the interconnections between water management and different sectors and operational scales. However, it proposes a shift in perspective: rather than attempting to address the entire complexity of the problem at once, it recommends breaking it down into smaller and more manageable components, focusing on those interactions that have the greatest impact on water resources. Given that agriculture remains the largest consumer of freshwater resources worldwide, this sector represents the most logical starting point.

This research proposes the combined use of simple models characterized by limited data requirements and actionable outputs that can be readily interpreted by farmers, water and irrigation managers, and policymakers. Greater simplicity translates into higher applicability and scalability in real-world contexts. At the same time, the combination of multiple models allows water management challenges to be examined from different perspectives, overcoming the traditional sectoral approach that often characterizes decision-making.

Integrated and cross-sectoral water resource management has been extensively studied in research, yet its implementation in practice remains limited. More than a decade after the emergence of the IWRM and WEFE Nexus frameworks, the absence of a widely accepted and operational framework suggests that the challenge may be too complex to be addressed through a single approach. While many researchers continue to emphasize the need for studies that incorporate all WEFE components simultaneously, this thesis argues that such ambition may limit practical implementation. IWRM and the WEFE Nexus should not remain primarily intellectual exercises for researchers. To effectively contribute to the long-term sustainability of water resources, their principles must be translated into practical, accessible, and scalable solutions that can be applied in real-world decision-making processes.

References

Allouche, J., Middleton, C., & Gyawali, D. (2015). *Technical Veil, Hidden Politics: Interrogating the Power Linkages behind the Nexus*. *8*(1), 610–626.

Biswas, A. K. (2004). Integrated Water Resources Management: A Reassessment: A Water Forum Contribution. *Water International*, *29*(2), 248–256. https://doi.org/10.1080/02508060408691775

European Court of Auditors (A c. Di). (2016). *The Land Parcel Identification System: A useful tool to determine the eligibility of agricultural land - but its management could be further improved; Special report No 25, 2016*. Publications Office. https://doi.org/10.2865/19472

Grigg, N. S. (2024). Framework and Function of Integrated Water Resources Management in Support of Sustainable Development. *Sustainability*, *16*(13), 5441. https://doi.org/10.3390/su16135441

Hamidov, A., & Helming, K. (2020). Sustainability Considerations in Water–Energy–Food Nexus Research in Irrigated Agriculture. *Sustainability*, *12*(15), 6274. https://doi.org/10.3390/su12156274

IPCC. (2023). *IPCC, 2023: Summary for Policymakers. In: Climate Change 2023: Synthesis Report. Contribution of Working Groups I, II and III to the Sixth Assessment Report of the Intergovernmental Panel on Climate Change*. https://www.unep.org/resources/report/climate-change-2023-synthesis-report

ISTAT. (2018). *IstatData—Superfici agricole in Sardegna* [Dataset]. https://esploradati.istat.it/databrowser/#/it/dw/categories/IT1,Z1000AGR,1.0/AGR_CRP/DCSP_COLTIVAZIONI

Li, W., Ward, P. J., & Van Wesenbeeck, L. (2025). A critical review of quantifying water-energy-food nexus interactions. *Renewable and Sustainable Energy Reviews*, *211*, 115280. https://doi.org/10.1016/j.rser.2024.115280

McGrane, S. J., Acuto, M., Artioli, F., Chen, P., Comber, R., Cottee, J., Farr-Wharton, G., Green, N., Helfgott, A., Larcom, S., McCann, J. A., O'Reilly, P., Salmoral, G., Scott, M., Todman, L. C., Van Gevelt, T., & Yan, X. (2019). Scaling the nexus: Towards integrated frameworks for analysing water, energy and food. *The Geographical Journal*, *185*(4), 419–431. https://doi.org/10.1111/geoj.12256

MedECC. (2020). *Current situation and risks for the future First Mediterranean Assessment Report* (p. 632). https://zenodo.org/record/4768833

Mersha, A. N. (2021). *Integrated Water Resources Management: A Systems Perspective of Water Governance and Hydrological Conditions: Integrated Water Resources Management* (1ª ed.). CRC Press. https://doi.org/10.1201/9781003231035

Purwanto, A., Sušnik, J., Suryadi, F. X., & De Fraiture, C. (2021). Water-Energy-Food Nexus: Critical Review, Practical Applications, and Prospects for Future Research. *Sustainability*, *13*(4), 1919. https://doi.org/10.3390/su13041919

Regione Autonoma della Sardegna. (2022). *PIANIFICAZIONE E GESTIONE DELLE RISORSE IDRICHE - Aggiornamento dei modelli idraulici del Piano Stralcio per l'Utilizzo delle Risorse Idriche della Sardegna (PSURI)*.

Zubel, K., & Apprioual, A. (2020). *Agriculture and Food Security in Climate Sensitive Areas in the Mediterranean*. IEMed. https://www.iemed.org/publication/agriculture-and-food-security-in-climate-sensitive-areas-in-the-mediterranean/